CHALMERS
UNIVERSITY OF TECHNOLOGY

Sea state estimation using response data from a container vessel

An investigation of the reliability of a ship-as-a-wave-buoy

Master's thesis in Naval Architecture and Ocean Engineering

ANDREAS BÅGFELDT

Department of Mechanics and Maritime Sciences
CHALMERS UNIVERSITY OF TECHNOLOGY
Gothenburg, Sweden 2018

Master's thesis 2018:91

Sea state estimation using response data from a container vessel

An investigation of the reliability of a ship-as-a-wave-buoy

Andreas Bågfeldt

CHALMERS
UNIVERSITY OF TECHNOLOGY

Department of Mechanics and Maritime Sciences
Division of Marine Technology
Chalmers University of Technology
Gothenburg, Sweden 2018

Sea state estimation using data from a container vessel
An investigation of the reliability of a ship-as-a-wave-buoy
Andreas Bågfeldt

Examiner/Supervisor 1: Ulrik Dam Nielsen, Associate Professor, Technical University of Denmark
Examiner/Supervisor 2: Wengang Mao, Associate Professor, Chalmers University of Technology
External Examiner: Jesper Dietz, A.P. Møller-Mærsk

Master's Thesis 2018:91
Department of Mechanics and Maritime Sciences
Division of Marine Technology
Chalmers University of Technology
SE-412 96 Gothenburg
Telephone (+46) 31 772 1000

Cover: A container vessel operating in severe weather condition. Photo taken by officer in charge on Atlantic Companion. Used with permission.

Typeset in LaTeX
Printed by Chalmers Reproservice
Gothenburg, Sweden 2018

Sea state estimation using response data from a container vessel
An investigation of the reliability of a ship-as-a-wave-buoy
Andreas Bågfeldt
Department of Mechanics and Maritime Sciences
Chalmers University of Technology

Abstract

In the strive of introducing autonomy in to the shipping industry there is a need of fast and reliable sea state estimation procedures which can capture wave parameters. Based on recent research by U. D. Nielsen proposing a brute force approach to estimate the sea state estimation, this thesis will evaluate the approach by using full scale measured data along with simulated vessel motions. By using 8100 timeseries of motions the procedure will be evaluated based on the reliability and level of uncertainty of the estimation. The results indicates that the proposed procedure is promising even though it does not work as a fully general approach and is still in the need of modifications for each vessel. The research has also shown promising results regarding the transformation from encounter to absolute domain taking the Doppler effect in to account. The conclusion drawn is that the proposed procedure is promising and that future validation and fine tuning is needed using a wider approach with numerous different vessel types including full scale measured motion data, before it can be used in real applications on board vessels.

Keywords: Sea state estimation, Brute force, Wave buoy analogy, Vessel response spectrum, Wave spectrum, Spectrum transformation, Simulated wave induced vessel motions

Acknowledgements

I would like to start to thank my main supervisor and examiner Ulrik Dam Nielsen at Technical University of Denmark whom always took the time to support me in my work and prioritized my learning from the project as well as always staying enthusiastic and positive about my findings even though it was contradictory to his own results in the same research area. I am very grateful for the flexibility in the supervising role and enabled lots of online meetings due to different geographical locations as well the fact that he used a lot of his leisure to answer questions and ensuring my project ran smoothly. Without him, this project would never be possible.

I would also like to thank my secondary supervisor Wengang Mao at Chalmers University of Technology for his support and that he took the time to act as both a supervisor and examiner in my Master's thesis. Further, I also want to give my gratitude towards Poul Andersen at Technical University of Denmark for taking the initiative on the Nordic Five Tech consortium which enabled me to carry out this thesis in collaboration with both Technical University of Denmark and Chalmers University of Technology.

I would like to send my gratitude to DNV GL for supplying me with vessel specific information and data which laid the foundation for this thesis. Further, I am very thankful for the great generosity of Henrik Karle and AdMare Ship Management AB in Gothenburg for granting me access to their office which acted as my work base during this thesis as well as supplying me with lots of coffee over this 6 months.

Finally, I which to send my best gratitude towards my family who have always supported my choices in life and encourage me along the way and they are one main factor that I now finish my Master's degree. Further, I would like to thank all of my friends, both new and old, for making my journey up to this point so much easier. Last but certainly not least, I would like to send my biggest and warmest thank you towards my girlfriend whom has motivated and pushed me in tough times, acted as partner to discuss with and finally she has made me smile every day of this thesis work. Thank you!

Andreas Bågfeldt, Gothenburg, June 2018

Table of Contents

List of Figures

List of Tables

This page is intentionally left blank.

Nomenclature

Abbrevations

CTH	Chalmers University of Technology
DP	Dynamic Positioning
DSS	Decision Support System
DTU	Technical University of Denmark
FFT	Fast Fourier Transformation
ITTC	International Towing Tank Conference
RAO	Response Amplitude Operator
SSE	Sea State Estimation
TEU	Twenty-foot Equivalent Unit

Nomenclature

β	Final heading estimate
β_0	First heading estimate in [0 180] deg.
β_2	Second heading estimate in [0 360] deg.
χ	Relative wave heading
$\Im$	Indicates the *imaginary* part of a complex value
ω	Wave frequency
ω_0	Absolute wave frequency
ω_e	Encounter wave frequency
$\overline{X}$	Complex conjugate of the transfer function
Φ	Transfer function
ϕ	Roll
$\Re$	Indicates the *real* part of a complex value
θ	Pitch
φ	Yaw

ζ	Wave elevation
E	Directional wave spectrum
g	Acceleration of gravity
H_s	Significant wave height
R	Motion response spectrum
S	Response spectrum
S	Wave spectrum
T_0	Modal period, also known as T_p
T_m	Mean period
T_p	Mean peak period
T_z	Mean zero-upcrossing period
U	Forward speed
X	Complex-valued transfer function
z	Heave

1

Introduction

1.1 Background

Nowadays high focus is on autonomous transportation were the automotive industry making big headlines and progress in the strive of replacing the humans as the responsible driver and utilize computers as decision maker. The same research is ongoing in the maritime area were the vessels are transforming to a more autonomy structure, minimizing the amount of monitoring needed by the crew. This trend of minimize crews and maximize the level of autonomy on the vessels are expected to stay on a high development level in the future (Ludvigsen and Sørensen, 2016). Fully autonomous vessels are not yet ready for commercial introduction, even though full-size tests are carried out by early adapters, e.g. MV Yara Birkendal (Wikipedia, 2018b). Institutions have stated that the maritime sector will have a big increase in autonomy over the next years and in 20 years reach a fully autonomy deep ocean vessel fleet (plc, 2016) while others only states that the maritime sector is not yet fully autonomous and have a long way to go until it can compete with the automotive industry, however with the right focus, it will be reality in the near future (Rylander and Man, 2016).

According to the Lighthouse study (Rylander and Man, 2016), one of the main area of improvements needed before a higher level of autonomy can be reached is to further develop the technologies and software used to phase out the crew onboard. The technology available today is not as good as an officer on watch and until that is reality, the crew can not be replaced with computers since it would imply a degrading of the security and safety of the maritime operations. One of the motivations for introducing autonomy into vessels is the safety and eliminating the risk of human errors, together with economic benefits, hence it would be contradictory to urge an implementation of the unmanned vessels before the available products can fully replace today's tasks with the same safety and security standards. For this reason, the available technology is mostly used as decision support systems (DSS) for the crew on board the vessels by presenting the most probable case while still relying on the crew to interpret the information and make the correct decision for the acting situation.

One of the areas were autonomy is of interest is in the strive of decreasing the crew on board which in turn implies that the possibility to do sea state estimations (SSE) must be enabled. Until today, thorough research has been conducted in the topic with promising results (Nielsen et al., 2018). Sea state estimation focuses on the operational aspect of the interaction between the vessel and the appearing waves and with captured data make an estimate of the future sea state by assuming that the sea state is steady over time and area. There are multiple areas that could make use of the sea state estimation, such as but not

limited to safety of the crew, cargo and passengers, fuel performance, hull girder structure, dynamic positioning (DP), safe operations including shore-vessel, air-vessel, vessel-vessel, offshore structure-vessel. Prior work has mostly focused on the wave buoy analogy with the frequency domain approach, while on later years, more resources have been allocated to the time domain approach (Nielsen et al., 2018). In the beginning, the research mostly focused on a, position wise, stationary structure since this was the natural approach with the data available at the moment together with the demand from the offshore industry etc., this have now shifted to also include the effect of forwards speed.

Recently, a new method of implementation of the wave buoy analogy have been proposed by Brodtkorb et al. (2018) that focused on DP vessels, hence no forward speed was included in the research, however very promising results could be found during full scale tests. To make the procedure more usable, research was carried out on including the forward speed as well as short-crested waves while the original procedure only taking long crested waves in to account (Nielsen et al., 2018). It should be urged that this procedure is favorable due to its direct spectral approach that enable very high computational efficiency. At this stage, the sea state estimations are only reliable for a short time in future and can therefore be used in a limited amount of applications. By increasing the computational efficiency, the procedure could be used as a starting guess in more complex procedures than the proposed method and by that increasing the total computational efficiency.

The procedure proposed by Nielsen et al. (2018) is interpreting the vessel as a wave buoy, which is widely used for coastal sea state estimation. By introducing the wave buoy analogy for sailing vessels, it is possible to cover areas were today's wave buoys are not present. Today's application of the sea state estimation is divided into two areas; real time and post-processing. The usage of real time information is used in operational aspects, such as cargohandling between different vessels or vessel to platform. Furthermore, it is used to evaluate the routes in a post process were fuel consumption can be evaluated etc.

In the future, sea state estimation could be used for route optimization and increasing of safety by re-routing to avoid areas with severe weathers. Such decisions are today carried out by man-work on board the vessels and before an autonomy fleet can be reality, these decisions must be transferred to computers instead of humans. With this as a starting point, it can be of big interest both in a research and commercial perspective to enable high precision SSE and in the future use this to decrease the crew as well as the operations onboard the vessels.

1.2 Purpose of Project

The purpose of this Master's thesis is to implement, validate and verify the proposed procedure for sea state estimation given by Nielsen, Brodtkorb, and Sørensen in the paper "A brute-force spectral approach for wave estimation using measured vessel responses" (Nielsen et al., 2018). It will be done using full scale data from an in-service container vessel and its corresponding motion and responses. The area of research is a highly relevant topic both in matter of education, as it is closely related to ship operations, and commercial, since numerous operational benefits can be the consequence of a well functional sea state estimation procedure resulting in both economical gains and the environment onboard the vessel for crew, passengers and cargo. The Master's thesis is carried out as part of the joint master degree Maritime Engineering in the consortium Nordic Five Tech which implies

studies at two member universities in the Nordic countries. The specific track is within Ship Operations and the first year was carried out at Chalmers University of Technology (CTH) while the second year is carried out at Technical University of Denmark (DTU) and will result in a Master's degree from both member universities (Andersen, 2015).

1.3 Scope of Work

The work will start with a thorough literature study based on the research paper by Nielsen et al. (2018) including relevant citations to the paper. In the same process, external literature will be studied to find alternative ways of conducting the sea state estimation and get a good overview of what methods that are available at the moment. The project is focused on working with a specific procedure by Nielsen et al. (2018) and will be the main objective, to add strength in the research. Other available theories will be compared and discussed to get a well-established position compared to the competition.

An in-house MATLAB®-script implementing the sea state estimation procedure (Nielsen et al., 2018) will be used as a starting point, implying that the scripts do not have to be developed from scratch. The focus will be to modify the script to suit the data given for the vessel under investigation and with the use of the data, verify and validate the estimation procedure. To make it as similar to a profession approach, the focus will be on the data handling and sorting as well as modification of already existing programs in effort to mimic the fact that programs are rarely written from scratch and that data is most often not modified to fit the application in mind. The verification and validating will be carried out by the use of available wave data from wave radar and simulations.

In the later stage of the project, once the proposed procedure is implemented in a stable MATLAB®-script, the procedure will be evaluated to what level it could be implemented in a PYTHON®-program and investigate possible gains of using an alternative language instead of MATLAB®.

The vessel used in this project is a 2800 TEU DNV GL-classed vessel that has been equipped with sensors and measurement equipment during a period of time (Storhaug and Heggelund, 2008). The vessel regularly operates on a route between northern Europe and Canada and data collected over a 2-year period is available for this work. The available vessels main particulars are displayed in Appendix A.

In the project, vessel motions is simulated using general wave elevation theory as a reference point. The simulated motions for the vessel are based on the transfer functions available. By introducing simulated motions, it is possible to ensure the accuracy of the data, eliminating sources of error due to wrongly installed measurements equipment or defect equipment etc.

In the first part of the Master's thesis, it could be concluded that the interaction between the vessel motion data and the transfer functions retrieved from DNV GL was faulty and could not, without further investigation, be used in the sea state estimation. A deviation from the original intentions for the thesis was needed. The focus shifted to exclusively including the simulated data in the validation and verification process, which enabled a higher level of accuracy of the data. The shift of focus is further introduced in Section 3.5 while Section 3.3 regards the problem from the measured data.

1.3.1 Objectives

Based on the background and purpose of this Master's thesis project, a number of objectives are stated and will be the basis of the carried out work.

1. Implement and verify the procedure proposed by Nielsen et al. (2018) by using the in-service data given by DNV GL for a 2800 TEU container vessel.
2. Enable simulated vessel motions as a reference point ensuring correct sea state estimation result without the inference of external error sources.
3. Compare results with other available sea state estimation data from sources such as wave radar, satellite measurements or wave buoy passings.
4. Create an user friendly program that can be used for the estimation procedure written in MATLAB®and if possible a secondary program written in PYTHON®.
5. Thorough literature study of available techniques and procedures for sea state estimation
6. Sorting and modification of given vessel data to suit the procedure mentioned in Nielsen et al. (2018)

1.3.2 Deliverables

The following products will be delivered to the Technical University of Denmark and Chalmers University of Technology in the end of the project:

1. Administration oriented
   (a) Planning report
   (b) Final report along with a presentation at each university
   (c) Disputation report (Only for CTH)
2. Result oriented
   (a) Documentation of the performance of the sea state estimation according to Nielsen et al. (2018) using the in-service data given by DNV GL for a 2800 TEU container vessel.
   (b) User friendly MATLAB®-program that can be used for the estimation procedure and if possible, a secondary program developed in PYTHON®will be delivered
   (c) Propose future work

1.3.3 Limitations

This Master's thesis will *not* focus on:

1. the data collecting procedure, including the measurement systems and transfer of data
2. the quality of the collected data compared to the real wave parameters

1.4 Report Structure

The report follows a general structure, i.e. Introduction, Theory, Method, Results and Conclusion. To start, the main theory is explained, including other relevant procedure that is not be used in this project but is part of a literature study in an effort to explain what is available on the market. A detailed methodology chapter is presented since the work has mainly focused on retrieving results and improving them to achieve sufficient accuracy and these are of big importance when introducing the learning objectives and knowledge gain from the project. The work consists of numerous interim results indicating different errors in the procedure and these results is not presented, instead, a concise selection of results is presented in the Results chapter of the report. Finally, a conclusion chapter is presented including a thorough discussion as well as future work.

1.5 Ethical Statement

It is of importance to ensure that all work is evaluated in terms of ethics and sustainability, both for how the work is carried out but also what is to be investigated. The area of research does not have a big ethics impact, anyhow, the outcome of the work could affect the maritime market in accordance with the Sustainable Development Goals by United Nations (United Nations General Assembly, 2015). The united nations have stated that over the next 15 years, all the member states should work for improving the global climate which the outcome of this thesis could be a part of, since it can improve the optimization of the routes. One other aspect is that the outcome could improve the working conditions onboard the vessel since severe weather conditions could be avoided.

This Master's thesis will ensure that no unnecessary resources is used in terms of paper, computational power etc. No confidential information will be included in the report, meaning that for example the vessel name will not be included. General research ethics will apply for this Master's thesis, for example that all sources of information will be presented.

This page is intentionally left blank.

2

Theory

2.1 Sea State Estimation

Sea state estimation is a practice were the waves on the sea is estimated using available measurements together with mathematical procedures. Historically, statistical information from fixed wave buoys have been used as input to the calculations to estimate how the sea will behave. It has been pointed out by Nielsen (2017b) that this information includes a big level of uncertainty compared to the undergoing sea state since it relies on statistical information and not real-time information. Furthermore, the performance of the vessels is highly depending on the encountered waves and this can not be retrieved from statistical data hence it would be hard to build a reliable DSS with this information. Instead it can be realized that a vessel with correctly equipped measurement devices could be used as a real time, sailing wave buoy. Thus, in the past, numerous of researches in the field have been carried out focusing on different sub-areas and interesting results regarding full-scale vessel data, including the forward speed, have been exploited. (Nielsen, 2017b)

2.2 Wave Buoy Analogy

Most of today's available and used procedures for sea state estimation can be categorized into two different areas; frequency domain and time domain. This Master's thesis will only focus on the frequency domain approach and therefore is the only theory that will be covered.

2.2.1 Frequency Domain

According to Nielsen (2017b), marine structures and vessels are often equipped with sensors that constantly measure global motions. Such as heave, pitch and vertical acceleration etc. which in the correct combination can represent a classic wave buoy. It should be noted that the geometry of a vessel is more complicated than a simple wave buoy however with the correct information about the vessel, it can be accounted for. By using a mathematical model including information about the vessel, such as transfer function, the sea state can be estimated according to the flowchart in Fig. 2.1.

When applying the wave buoy analogy assumptions are made which are widely accepted and used to enable the calculations. In non-severe waves it is assumed that the relation between the waves and the 6 degrees of freedoms are linear (these are surge, x, sway, y,

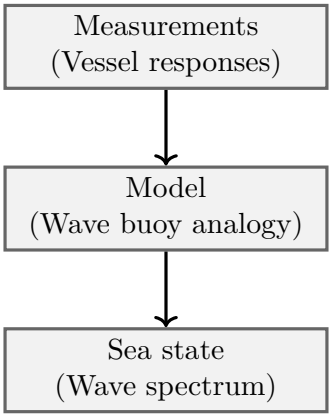

Figure 2.1: A Principle view of how the sea state estimation is carried out by using the wave buoy analogy. The measurements are retrieved in real time (at least close to real time) while the mathematical model is stationary and available at all time. Using the model and the measurement together results in the sea state estimation. Reproduced from Nielsen et al. (2016).

heave, z, roll, ϕ, pitch, θ, yaw, φ, which are defined in Fig. 2.2). This implies that the vessel motions are proportional to the waves. By using superposition of regular waves, it is possible to mimic an irregular wave system and still carry out the sea state estimation. Assuming a linear relation between the waves and the motion, makes it possible to build transfer functions, also known as response amplitude operators (RAO), that implicitly describes how the motion of the sea level is transferred into vessel motions.(Nielsen, 2017b)

To consider the sea state estimation in the frequency domain additional assumptions are needed as stated on page 353 in Nielsen (2017b):

> "the ocean waves and associated responses represent ergodic random processes (e.g. Ochi (1990)), so that stationary, in a stochastic sense, applies within a certain period of response records at each estimation sequence."

Furthermore, the second assumption defines that the speed and heading relative to the waves are constant over the measurement. If so, it is possible to process the data using

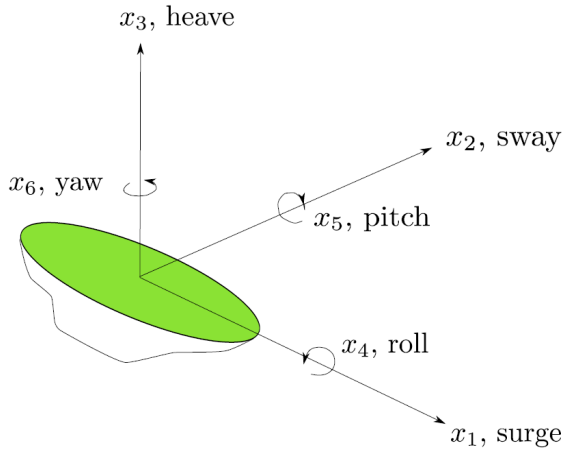

Figure 2.2: Definition of the 6 degrees of freedom of a vessel. (Bingham, 2017)

Fast Fourier Transformation (FFT) or multivariate auto-regressive procedures Nielsen (2005, 2006), such as the WAFO®- toolbox function `dat2spec` (WAFO-group, 2017). Commonly, the used model in the sea state estimation compares the measured spectral energy distribution with the theoretical one (Nielsen, 2017b). As described in Section 2.2.1, when the response spectrum is available in the frequency domain, it is possible to calculate the response spectrum in the frequency domain using transfer functions. This is illustrated with Fig. 2.3.

A more fundamental description on what the named procedures for transforming the wave elevation from time domain to frequency-domain are given in Fig. 2.4. There it can be seen how random ocean wave can be subdivided in to different regular sinusoidal waves. Depending on the energy and the period of these waves, the wave spectrum can be built in the frequency domain.

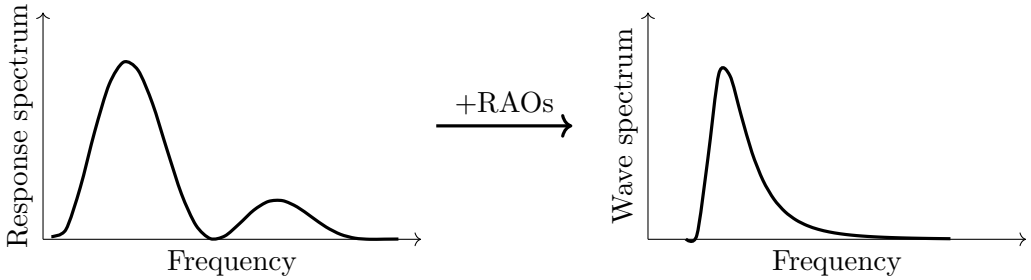

Figure 2.3: Principle view of the wave buoy procedure using the responses in the frequency domain. Reproduced from Nielsen et al. (2016).

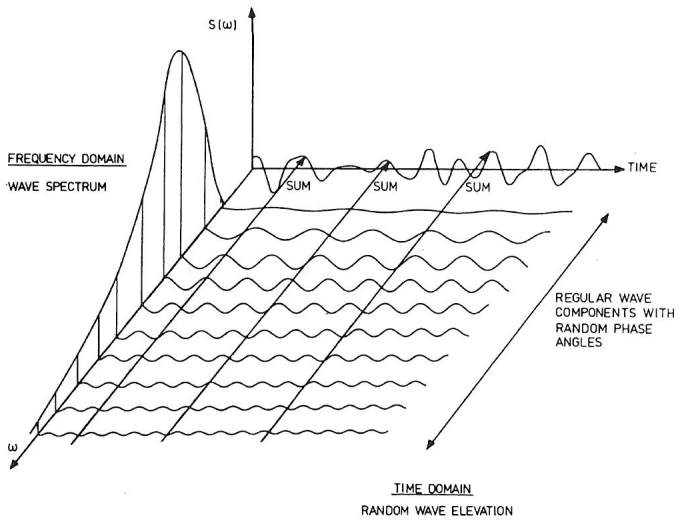

Figure 2.4: A schematic description of how a irregular wave system can be built based on regular sinusoidal waves and how the time domain relates to the frequency domain. (Faltinsen, 1993)

Spectral Energy Distribution

An important feature of the frequency domain approach is that the energy is conserved when translating the responses from the time domain in to the frequency domain. It is done by building up the spectral energy distribution. These spectral energy distributions can be used as a wave spectrum estimation by doing a comparison of the measured data and the theoretical onee explained here. For a set of the 6 ship responses the complex-valued transfer functions, $X_i(\omega_e, \chi)$ and $X_j(\omega_e, \chi)$ which correspond to the i-th and j-th responses, are known and can be related to the response spectra, $S_{ij}(\omega_e)$, and the directional wave spectrum, $E(\omega_e, \chi)$ according to Eq. (2.1) where ω_e is the encounter wave frequency and χ is the relative wave heading which is defined according to Fig. 2.5. The over-line indicates the complex conjugate.

$$S_{ij}(\omega_e) = \int_{-\pi}^{\pi} X_i(\omega_e, \chi)\overline{X_j(\omega_e, \chi)}E(\omega_e, \chi)\, d\chi \tag{2.1}$$

It is important to be aware of the triple-valued function governed by the speed of advance can be a problem in following seas were the encounter frequency could correspond to three different wave frequencies, also known as the Doppler effect which is further explained in Section 2.3. This problem has been correctly incorporated by Iseki and Ohtsu (2000) and results in Eq. (2.2) where U is the forward speed of the vessel, g is the gravity acceleration.(Nielsen, 2017b)

$$\omega_e = \omega_0 - \omega_0^2\psi, \qquad \psi = \frac{U}{g}\cos\chi \tag{2.2}$$

In Eq. (2.1), the left side represent ocean data while the right side is governed by mathematical expression and thus a error minimization problem can be formulated to estimate the wave parameters correctly. The minimization problem is expressed as Eq. (2.3) where $||\cdot||$ represent the L_2 norm. The wave spectrum, that is expressed in $\mathbf{f}(\mathbf{x})$ and the response spectrum in the vector $\mathbf{b}$ and the matrix $\mathbf{A}$, is built on elements from the transfer functions. (Nielsen, 2006)

$$\epsilon^2(\mathbf{x}) \equiv ||\mathbf{A}\mathbf{f}(\mathbf{x}) - \mathbf{b}||^2 \tag{2.3}$$

The problem described with the Eq. (2.3) can be approached in numerous ways, two main approaches are based on *Bayesian modelling* **or** *parametric modelling*. The parametric modelling assumes a directional wave spectrum that can be modeled by e.g. JONSWAP or Bretschneider spectres (see Sections 2.6 and 2.7) or similar wave spectrum. The Bayesian

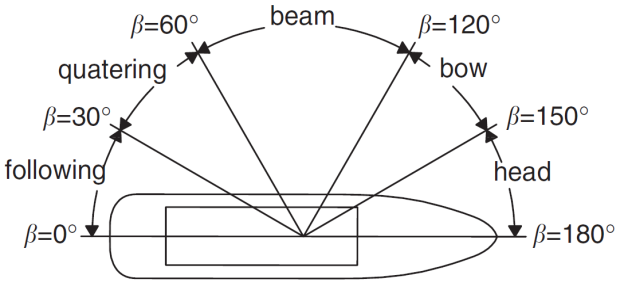

Figure 2.5: Definition of the encounter wave angle β, in cases were the encounter wave angle is represented by χ it follows the same definition as β. (Nielsen, 2006)

modelling focus on finding the components of a frequency-directional wave spectrum. Over the years, reports with promising results have been published using both models and with or without vessel speed (e.g. Iseki and Ohtsu (2000); Iseki et al. (2001); Nielsen (2006); Pascoal and Soares (2008); Tannuri et al. (2003); Pascoal et al. (2007); Simos et al. (2007)). It is noted that these two approaches are not necessarily competitors and could work in symbiosis to complement each other since they both have advantages and disadvantages, which have been discussed in Nielsen et al. (2013) and Nielsen and Stredulinsky (2012)

Spectral Moments

A recent study (Montazeri et al., 2016b) proposed a sea state estimation approach based on the spectral moments of the wave spectrum. This procedure is a continuation on the technique were the right and left sides of Eq. (2.1) are integrated over the frequency, resulting in Eq. (2.4) where l and h correspond to the lower and higher limits.

$$\int_{\omega_e,l}^{\omega_e,h} S_{ij}(\omega_e)\, d\omega_e = \int_{\omega,l}^{\omega,h} \int_{-\pi}^{\pi} X_i(\omega,\chi)\overline{X_j(\omega,\chi)}E(\omega,\chi)\, d\chi\, d\omega \tag{2.4}$$

The procedure makes two estimations, one for the wind sea and one for the swell which are super-positioned for the total spectrum, see Fig. 2.6. Each of the two components follows a general unidirectional spectrum defined by Eq. (2.5) Boukhanovsky and Soares (2009). In the equation, $\alpha, \beta, \gamma, \sigma, \omega_p, r, n$ are the fitting parameters which, together with a spreading function, D, are optimized for minimizing the error between the left and right side in Eq. (2.4).

$$S(\omega) = \alpha g^2 \omega^{-r} \exp(-\beta\omega^{-n})\gamma^{\exp\frac{-(\frac{\omega}{\omega_p}-1)^2}{2\sigma^2}} \tag{2.5}$$

The directional spectrum is thereafter computed according to Eq. (2.6) with the condition that the spreading function as $\int_{-\pi}^{\pi} D(\chi|\omega)\, d\chi$ where χ correspond to the wave direction.

$$E(\omega,\chi) = S_{\text{wave}}(\omega)D(\chi|\omega) \tag{2.6}$$

The procedure focusing on the spectral moments and the corresponding energy have the advantage that no transformation between wave- and encounter wave frequency is needed. The total energy in the two spectrums must be the same together with the fact that the following sea problem will not appear.(Nielsen, 2017b)

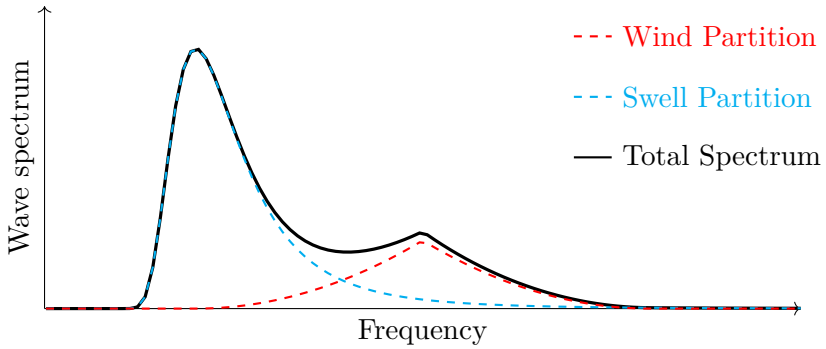

Figure 2.6: Principle view of the swell and wind component together with the total frequency spectrum. Reproduced based on (Montazeri et al., 2016b).

Summary

The frequency domain approach to the problem of sea state estimation is widely used and verified. However, the procedure is not optimal due to the reasons which is listed below, without any particular order (Nielsen, 2017b):

- It gives a reasonable estimation result(Nielsen (2006); Nielsen and Stredulinsky (2012); Nielsen et al. (2013); Montazeri et al. (2016a)) however it is very dependent on the transfer functions used.
- It is very dependent on the ship responses and that these are taken in stationary condition i.e. same speed, wave heading and sea state
- To perform the estimate, a time interval is needed as basis, as a consequence the estimate will in fact be based on "old" information and not real-time

2.3 Brute-Force Spectral Approach

In the following section the theory of a specific brute-force approach proposed by Nielsen et al. (2018) will be explained in detail since this is what the main work of this Master's thesis will focus on. Parts of the theory will be repeated from Section 2.1 to ensure that all theory for the main work is gathered in one place.

The theory regards wave induced ship motions due to irregular short-crested waves in the frequency domain. The main assumption is that the responses are linear to the waves, which is defined with the vessel speed, U, and the relative heading to the waves $\chi \in [0, 360[$ deg. were $\chi = 180$ deg. corresponds to head seas, as described in Fig. 2.5. The relationship between the encounter wave frequency, which is represented by the frequency observed on a moving reference frame along with the vessel, and the absolute wave frequency, which is represented by a fixed reference frame in space without any advance speed, is described by the Doppler effect in Eq. (2.7) which also can be seen in Eq. (2.2). The Doppler effect is of importance due to the 1-3 mapping problem, were in following sea 1 encounter frequency could be mapped to 3 different absolute frequencies, see Fig. 2.7, and the solution imply that it is very straight forward. In theory it is, however the practical implementation is not, anyhow it is possible and will be explained thorough later in the paper. (Nielsen et al., 2018)

$$\omega_e = \omega_0 - \omega_0^2 \psi, \qquad \psi = \frac{U}{g} \cos \chi \tag{2.7}$$

2.3.1 Fundamental Equations

The analyze is performed in the frequency domain were it is assumed that the sea state is stationary and the linear relationship between short-crested waves and ship motions can be formulated as Eq. (2.8) where R_{ij} is the complex-valued cross spectrum of the motions heave, roll and pitch. X_i represent the complex-valued transfer functions while $\overline{X}$ represent the complex conjugate of the transfer functions. S_e is the wave spectrum ordinate in the encounter frequency domain and is obtained by the product between E, which is the point

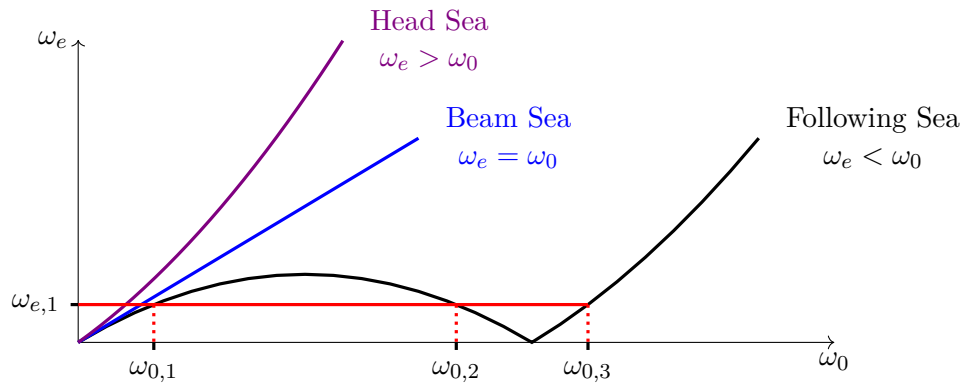

Figure 2.7: The Doppler effect indicating that in following seas, one encounter frequency can correspond to three absolute frequency which the red line indicate, while in beam- and head seas it is a 1 to 1 relation.

spectrum, and φ, which is a directional spreading function, in Eq. (2.9). following that, Eq. (2.8) can be rewritten as Eq. (2.10) (Nielsen et al., 2018)

$$R_{ij}(\omega_e) = \int X_i(\omega_e, \mu + \chi)\overline{X_j(\omega_e, \mu + \chi)}S_e(\omega_e, \mu)\, d\mu \tag{2.8}$$

$$S_e(\omega_e, \mu) = E(\omega_e)\varphi(\mu) \tag{2.9}$$

$$R_{ij}(\omega_e) = E(\omega_e) \int X_i(\omega_e, \mu + \chi)\overline{X_j(\omega_e, \mu + \chi)}\varphi(\mu)\, d\mu \tag{2.10}$$

The spreading function is defined according to Bhattacharyya (1978) as seen in Eq. (2.11) where Γ is the Gamma function (Wikipedia, 2018a), s is the spreading parameter and K is determined by fulfilling the following statement, $\int_{\mu_2}^{\mu_2} \varphi(\mu)\, d\mu \equiv 1$.

$$\varphi(\mu) = A(s) \times \cos^{2s}\left(\frac{\mu}{2}\right), \qquad A(s) = K \cdot \frac{2^{2s-1}\Gamma^2(s+1)}{\pi\Gamma(2s+1)} \tag{2.11}$$

The information about the encounter angle, χ, can sometimes be hard to determine by only taking one motion in to consideration since a vessel can often be assumed to be symmetric around the center line and sometimes even around mid-ship section, e.g. if the waves are encountered from 160 deg. or 200 deg. which is evenly spread around head seas (i.e. 180 deg.). By introducing the cross spectra, using the cross power spectral density function, e.g. `cpsd` in MATLAB®, it is possible to retrieve information about the angle since the transfer functions imaginary part is not symmetric. As shown by Brodtkorb et al. (2018) in Fig. 2.8 the cross spectrum is real valued while $i \equiv j$, otherwise it is a complex valued function where the off-diagonals are complex conjugate pairs, i.e. $\Im(R_{ij}) = -\Im(R_{ji})$, and by calculating the phase and modulus of these it is possible to retrieve the encounter angle which will be further explained later. It should be noted that from any three motions, it is possible to calculate six independent power spectra along with three phase spectra.

Eq. (2.10) could be solved directly in the complex valued domain, however to enhance the computational stability, it is chosen to introduce the six power spectra and excluding the phase for a later stage in the process, as a consequence the governing equations in the estimation process can be seen in Eq. (2.12) where the motion component pairs are given

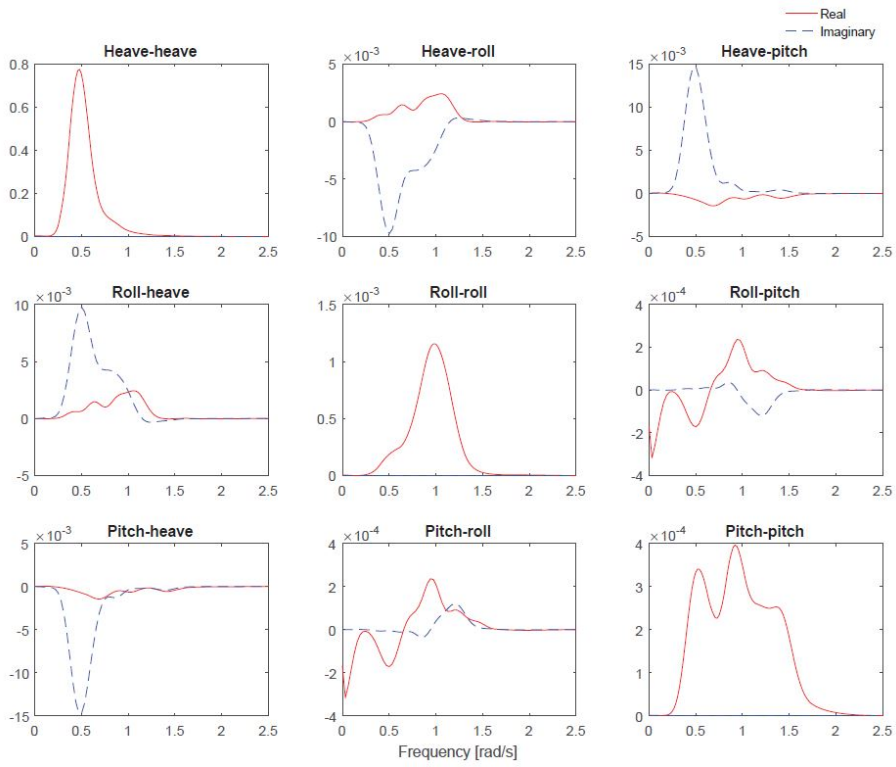

Figure 2.8: Cross spectrum calculated for a vessel regarding heave, roll and pitch using matlab function `cpsd`. Brodtkorb et al. (2018)

as (z,z), (ϕ,ϕ), (θ,θ), (z,ϕ), (z,θ), (ϕ,θ).

$$|R_{ij}(\omega_e)| = E(\omega_e) \int \left| X_i(\omega_e, \mu+\chi)\overline{X_j(\omega_e, \mu+\chi)} \right| \varphi(\mu)\, d\mu \tag{2.12}$$

where the left side is obtained through measurements while the right side is calculated by using known transfer functions together with information about the wave energy spectrum.

Be aware of the fact that Eq. (2.12) is stated in the encounter-frequency domain while the transfer functions are not and it will be necessary to make a shift between the two domains. In the case of following seas, it is needed to consider all 3 encounter frequencies simultaneous and by introducing the different mapping accordingly, $\{\omega_e \rightleftharpoons \omega_{01}\}$ for head seas and $\{\omega_e \rightleftharpoons \omega_{01}, \omega_{02}, \omega_{03}\}$ for following seas (Nielsen, 2017a). Including this formulation into Eq. (2.12) makes it possible to arrive at the final version of the governing equations as follows in Eq. (2.13) where the first line of the equation is always considered while the second line is only occurring in the case of following seas.

$$\begin{aligned} |R_{ij}(\omega_e)| = E(\omega_e) &\int |\Phi_{ij}(\omega_{01}, \mu+\chi)|^2 \varphi(\mu)\, d\mu \\ &+ E(\omega_e) \int \left[|\Phi_{ij}(\omega_{02}, \mu+\chi)|^2 + |\Phi_{ij}(\omega_{03}, \mu+\chi)|^2 \right] \varphi(\mu)\, d\mu \end{aligned} \tag{2.13}$$

where $|\Phi_{ij}(\omega_{0k}, \mu+\chi)|^2 = \left| X_i(\omega_e, \mu+\chi)\overline{X_j(\omega_e, \mu+\chi)} \right|$. Calculating the absolute frequency according to the Doppler effect in Eq. (2.7) gives the following frequencies for head- and following- seas respectively.

For head seas:

$$\omega_{01} = \frac{1 - \sqrt{1 - 4\psi\omega_e}}{2\psi}, \quad \text{all } \omega_e \tag{2.14}$$

For following seas:

$$\omega_{01} = \frac{1 - \sqrt{1 - 4\psi\omega_e}}{2\psi}, \quad \omega_e < \frac{1}{4\psi} \tag{2.15}$$

$$\omega_{02} = \frac{1 + \sqrt{1 - 4\psi\omega_e}}{2\psi}, \quad \omega_e < \frac{1}{4\psi} \tag{2.16}$$

$$\omega_{03} = \frac{1 + \sqrt{1 + 4\psi\omega_e}}{2\psi}, \quad \text{all } \omega_e \tag{2.17}$$

2.3.2 Stepwise Estimation

The estimation procedure is divided into two parts, firstly an initial estimation based on the brute force approach that does not take the actual true heading in to account and a later, post processing process estimating the actual wave heading. Therefore, it is only of interest to include headings $\chi = [0\ 180]$ deg. since the rest is represented by its symmetry around the centerline. These two steps will be explained further in detail below.

Brute-force Solution

The brute-force solution focus on directly solving the linear equation in Eq. (2.13) by using the proposed scheme by Brodtkorb et al. (2018) seen in Eqs. (2.18) to (2.20) that can be solved for any set of motions. It is of importance to know that Eq. (2.20) is calculated according to the conditions mentioned for Eq. (2.13) based on following seas versus head seas.

$$\tilde{R}_{ij} = R_{ij}(\omega_e) - \hat{R}_{ij} \tag{2.18}$$

$$\hat{E}_{ij}(k) = \hat{E}_{ij}(k) + h\tilde{R}_{ij} \tag{2.19}$$

$$\hat{R}_{ij} = \hat{E}_{ij}(k) \int \sum_{m=1}^{3} \left|\Phi_{ij}(\omega_{0m}, \mu + \chi_k)\right|^2 \varphi(\mu)\, d\mu \tag{2.20}$$

The actual implementation of the procedure can be seen in the pseudo script in Algorithm 1 where the following are of importance.

- **Discretization**. The wave directions are discretized in to N_χ while the encounter frequencies are discretized into N_{ω_e}. Due to the fact that the wave directions are not known from the start, it is necessary to loop over all directions hence the following statement:

$$\tilde{\chi}(k) = [0\ 180] \text{ deg.}, \qquad k = 1 : N_\chi \tag{2.21}$$

- **Initialization**. The procedure is initialized by assigning the wave spectrum and the response spectrum as zero, $\hat{E}_{ij} = 0$ and $\hat{R}_{ij} = 0$. Then when the difference between the measured response and the estimated response is calculated, it will give a value big enough to initiate the script.

- **Doppler effect**. The absolute frequency is a function of the encounter frequency which will be calculated using the function $f(\omega_e|\chi, U)$ which implements the Doppler effect expressed in Eqs. (2.14) to (2.17).
- **Updates**. The parameter $\tilde{R}_{ij}$ is used to improve the estimate by adjusting $\hat{E}_{ij}$ based on $\tilde{R}_{ij}$ and a factor $h > 0$. This is done until a threshold value is reached, i.e. $\tilde{R}_{ij} \leq \epsilon$ where $\epsilon > 0$.

Algorithm 1 Pseudo script for wave spectrum estimation

```
for (i, j) = {(z, z), (φ, φ),(θ, θ), (z, φ), (z, θ), (φ, θ)} do
  for k = 1 : Nχ do
    Ê_ij(k) = zeros(1, N_ωe)
    R̂_ij = zeros(1, N_ωe)
    R̃_ij = R_ij(ω_e)
    ω_0 = f(ω_e|χ, U)
    while |R̃_ij| > ε do
      R̃_ij = R_ij(ω_e) − R̂_ij
      Ê_ij(k) = Ê_ij(k) + h R̃_ij
      R̂_ij = Ê_ij(k) ∫ Σ_{m=1}^{3} |Φ_ij(ω_0m, μ + χ_k)|^2 φ(μ) dμ
    end while
  end for N_χ
end for i
```

The output of the procedure is a matrix of dimension $6 \times (N_\chi \cdot N_{\omega_e})$ and will appear as Eq. (2.22) when the used motions are heave, pitch and roll. In Eq. (2.22), each component represent a row vector including all encounter frequencies.

$$\bar{E} = \begin{bmatrix} \hat{E}_{zz}(1,\omega_e) & \hat{E}_{zz}(2,\omega_e) & \dots & \hat{E}_{zz}(N_\chi,\omega_e) \\ \hat{E}_{\phi\phi}(1,\omega_e) & \hat{E}_{\phi\phi}(2,\omega_e) & \dots & \hat{E}_{\phi\phi}(N_\chi,\omega_e) \\ \hat{E}_{\theta\theta}(1,\omega_e) & \hat{E}_{\theta\theta}(2,\omega_e) & \dots & \hat{E}_{\theta\theta}(N_\chi,\omega_e) \\ \hat{E}_{z\phi}(1,\omega_e) & \hat{E}_{z\phi}(2,\omega_e) & \dots & \hat{E}_{z\phi}(N_\chi,\omega_e) \\ \hat{E}_{z\theta}(1,\omega_e) & \hat{E}_{z\theta}(2,\omega_e) & \dots & \hat{E}_{z\theta}(N_\chi,\omega_e) \\ \hat{E}_{\phi\theta}(1,\omega_e) & \hat{E}_{\phi\theta}(2,\omega_e) & \dots & \hat{E}_{\phi\theta}(N_\chi,\omega_e) \end{bmatrix} \tag{2.22}$$

The brute force solution is now reached and gives, not one but six, sub-solution to the wave estimation problem. The rest of the procedure is post-processing of the solution to go from 6 solutions that are in the encounter wave spectra and only includes relative headings in the span $\chi \in [0\ 180]$ deg. to a final solution for one wave estimation in the absolute frequency domain and the true relative heading.

Increment Size

Recent studies by H. Brodtkorb et al. (2018) propose that the increment size, h, in Eq. (2.19) should be response dependent to achieve the best possible result in the sea state estimation process. The proposed relation follows Eq. (2.23).

$$h_{ij} < \frac{2}{\max_\omega \left(\max_\chi \left| X_i(\omega,\chi)\overline{X_j(\omega,\chi)} \right| \right)}, \qquad ij = \{zz, \phi\phi, \theta\theta, z\phi, z\theta, \phi\theta\} \tag{2.23}$$

Post-Processing

It is known that the wave spectrum in Eq. (2.22) is in the encounter frequency domain and the interest is for the wave spectrum in the absolute domain. To do this conversion, it is possible to use the relationship that energy is preserved between the two domains which can be represented by the significant wave height, H_s. Doing this conversion Eq. (2.24) can be obtained were each component represents the component at the same position in Eq. (2.22).

$$\bar{H} = \begin{bmatrix} \hat{H}_{s,zz}(1,\omega_e) & \hat{H}_{s,zz}(2,\omega_e) & \dots & \hat{H}_{s,zz}(N_\chi,\omega_e) \\ \hat{H}_{s,\phi\phi}(1,\omega_e) & \hat{H}_{s,\phi\phi}(2,\omega_e) & \dots & \hat{H}_{s,\phi\phi}(N_\chi,\omega_e) \\ \hat{H}_{s,\theta\theta}(1,\omega_e) & \hat{H}_{s,\theta\theta}(2,\omega_e) & \dots & \hat{H}_{s,\theta\theta}(N_\chi,\omega_e) \\ \hat{H}_{s,z\phi}(1,\omega_e) & \hat{H}_{s,z\phi}(2,\omega_e) & \dots & \hat{H}_{s,z\phi}(N_\chi,\omega_e) \\ \hat{H}_{s,z\theta}(1,\omega_e) & \hat{H}_{s,z\theta}(2,\omega_e) & \dots & \hat{H}_{s,z\theta}(N_\chi,\omega_e) \\ \hat{H}_{s,\phi\theta}(1,\omega_e) & \hat{H}_{s,\phi\theta}(2,\omega_e) & \dots & \hat{H}_{s,\phi\theta}(N_\chi,\omega_e) \end{bmatrix} \tag{2.24}$$

To obtain the "correct" wave estimate, one value has to be chosen among all the values in Eq. (2.24). In the perfect case, one of the columns in the matrix will obtain the same values, that are non-zero values, and these values represents the actual significant wave height. This column will also indicate the relative wave heading estimation. In reality, this will most surly not be the case and therefore a different approach is needed to find out the best estimate. The proposed solution by Nielsen et al. (2018) is to choose the column with the smallest variation of the significant wave height. This column will include 6 different values for the significant wave height and the final estimate is calculated as the average value of these six values. For example in the case of using the motion heave, pitch and roll the formula is described in Eq. (2.25) were the average value is obtained for the heading with the least variation of significant wave height which correspond to χ_K.

$$\begin{aligned} \hat{E}_{final}(\chi_K,\omega_e) = \frac{1}{6}\Big(&\hat{E}_{zz}(\chi_K,\omega_e) + \hat{E}_{\phi\phi}(\chi_K,\omega_e) + \hat{E}_{\theta\theta}(\chi_K,\omega_e) \\ &+ \hat{E}_{z\phi}(\chi_K,\omega_e) + \hat{E}_{z\theta}(\chi_K,\omega_e) + \hat{E}_{\phi\theta}(\chi_K,\omega_e)\Big) \end{aligned} \tag{2.25}$$

Until this stage, the wave headings considered are only in the spectra $\chi \in [0, 180]$ and are not necessarily the actual wave heading since it could be its symmetry part around the center-line. The information about the real wave heading can be found in the imaginary parts of the off-diagonal in the cross spectrum shown in Fig. 2.8 since the information about the phase shift is given by this parameter. Based on the fundamental equation in Eq. (2.10), and in a similar way as done with Eq. (2.12), three new equations can be formulated according to Eq. (2.26) with the motion components (i, j) as (z, ϕ), (z, θ) and (ϕ, θ). It is noted that, similar to the case in Eq. (2.13), the problem of following seas should be approached and solved in a similar way using the Doppler effect described in Eqs. (2.14) to (2.17).

$$\Im[R_{ij}(\omega_e)] = E(\omega_e) \int \Im\left[X_i(\omega_e, \mu+\chi)\overline{X_j(\omega_e, \mu+\chi}\right] \varphi(\mu)\, d\mu \tag{2.26}$$

The implementation is similar as the one for the wave spectrum in Algorithm 1 with the difference that it is solved for the wave heading instead of the point wave spectrum. Practically, it implies that the calculations applies for a discretized set of headings, $\tilde{\chi}_k$, were

$k = 1, 2, \ldots, N$ on the full circle $\chi \in [0, 360[$ instead of only for the half circle $\chi \in [0, 180]$. For each heading, the right side of Eq. (2.26) is calculated with the use of the estimated spectrum given in Eq. (2.25). It can then be subtracted from the left side of Eq. (2.26) which gives an error, ϵ_k^2, for each heading. The final wave heading estimate is calculated using a minimizing equation of the least square using the L_2 norm according to Eq. (2.27) were the right side of Eq. (2.26) has been written as $f(\tilde{\chi}_k)$.

$$\min_{\tilde{\chi}_k} \epsilon_k^2 \equiv \min ||\Im[R_{ij}(\omega_e)] - f(\tilde{\chi}_k)||^2 \tag{2.27}$$

To summarize, the procedure consist of four main steps as follows:

1. With basis in Eq. (2.22) calculate the significant wave height through the area of the moment to obtain Eq. (2.24).
2. Detect the columns were the standard deviation of the significant wave height, $\overline{H}_s$, is the lowest.
3. Use these corresponding wave spectrums were the standard deviation of the significant wave height is the lowest to calculate one average wave spectrum according to Eq. (2.25).
4. By using the obtained optimum wave spectrum in a minimizing problem, as seen in Eq. (2.27), between the right- and left side of Eq. (2.26) is used to find the optimum wave heading.

Absolute Domain

The transfer from encounter domain to absolute domain comes with difficulties, especially in the case of following seas where it is impossible to find one unique solution. In this Master's thesis it is needed to transform to absolute domain to obtain the periods, mean period, zero-upcrossing period and peak period, of the wave spectrum. A thorough research has been carried out in the area by Nielsen (2017a) were a practical engineering solution have been proposed for the non-unique problem of following seas. This solution can be sufficient for this Master's thesis and its applications. In principle, the solution looks like Eq. (2.28), were g is the mapping function described in Nielsen (2017a) which transform the estimated wave spectrum to the absolute domain.

$$E(\omega_0) = g(\hat{E}_{final}(\omega_e)|\tilde{\chi}_k, U) \tag{2.28}$$

2.4 Transfer Functions

It is possible to generate the transfer functions in numerous ways, e.g. through 2-D strip theory, panel methods, fully 3-D methods as well as closed form functions. The later has been proposed by Jensen et al. (2004) with proven good results. Here the focus is not on the transfer functions itself but rather the usage of them and for this reason it is chosen to use well established procedures to generate the functions. Therefore, the DNV GL software Sesam will be used due to its widely acceptance and simplicity while still providing good results (DNV, 1993). Sesam makes use of a 2-D strip theory developed by Salvesen et al. (1970) were it is assumed that the exiting forces for the 6 degrees of freedom/motions are

linear, i.e. that the vessel motions are linear to the waves. This assumption of a linear relationship is well established and accepted however it should be known that it is only valid for waves up to a certain level which afterwards tend to be non-linear however for the big range of waves it is indeed valid.

2.5 Sea State Parameters

The wave system can be described by the appearance of the wave spectrum itself anyhow, to do so for a wide set of wave spectrums are inefficient, along with the fact that a wave spectrum itself does not give the reader much information unless its compared with other spectrums, i.e. many figures would be needed to do this. The solution is instead to let the wave spectrum be represented by a set of sea state parameters that are widely used in marine engineering applications. These parameters are significant wave height ,H_s, peak period ,$\bar{T}_p$, zero-upcrossing period ,$\bar{T}_z$, mean period ,T_m. The significant wave height represents the average value of the highest third of measurement over time. Peak period describes the period corresponding to the highest level of energy in the wave spectrum, also known as the modal period, T_0. Zero-upcrossing period represent the average period between two successive up- or downward zero crossing periods. Nielsen (2010)

As described in Sections 2.2.1 and 2.3, the analysis of the waves is made in the frequency domain, meaning that the wave parameters have to be calculated based on the frequency domain wave spectrum which can be done using Eqs. (2.29) to (2.33). Note that the procedure of calculating these parameters are the same in both the encounter frequency domain and the absolute frequency domain.

First, the n-th order spectral moments are defined according to Eq. (2.29) where $S(\omega)$ is the wave spectrum in frequency domain, either encounter or absolute.

$$m_n = \int_0^\infty \omega^n S(\omega)\, d\omega \qquad \text{(n=0,1,2,...)} \tag{2.29}$$

The key parameters can be calculated accordingly:

$$T_m = 2\pi \frac{m_0}{m_1} \tag{2.30}$$

$$\bar{T}_z = 2\pi \sqrt{\frac{m_0}{m_2}} \tag{2.31}$$

$$\bar{T}_p = \frac{2\pi}{\omega_p}, \qquad \omega_p = \arg\max(S_\omega) \tag{2.32}$$

$$H_s = 4 \cdot \sqrt{m_0} \tag{2.33}$$

2.6 Bretschneider Spectrum

Based on the key parameters of the wave spectrum, it is possible to re-create a parametric wave spectrum. The International Towing Tank Conference (ITTC) has decided that the Bretschneider spectrum (Bretschneider, 1959) is the best available parameterized wave

spectrum to describe how the ocean waves act and is described by Eqs. (2.34) to (2.36). Therefore, the Bretschneider spectrum is adopted as the standard spectrum Nielsen (2010).

$$S_B(\omega) = \frac{A}{\omega^5} \exp\left(\frac{-B}{\omega^4}\right) \tag{2.34}$$

$$A = \frac{H_s^2}{4\pi} \left(\frac{2\pi}{T_z}\right)^4 \tag{2.35}$$

$$B = \frac{1}{\pi} \left(\frac{2\pi}{T_z}\right)^4 \tag{2.36}$$

2.7 JONSWAP Spectrum

In certain cases, usually in coastal areas, the ITTC proposed Bretschneider spectrum fails to represent the waves in correct way due to the fact that the waves are not fully developed. Therefore, the Joint North Sea Wave Project (JONSWAP) made a modification of the Bretschneider spectrum (the North Sea is a area were waves are not fully developed). The JONSWAP spectrum is defined according to (Nielsen, 2010):

$$S_J(\omega) = 0.658 \cdot C \cdot S_B(\omega) \tag{2.37}$$

$$C = 3.3^J \tag{2.38}$$

$$J = \exp\left[\frac{-1}{2\gamma^2}\left(\frac{\omega T_0}{2\pi} - 1\right)^2\right] \tag{2.39}$$

$$\gamma = 0.07 \quad \text{for} \quad \omega \leq \frac{2\pi}{T_0} \tag{2.40}$$

$$\gamma = 0.09 \quad \text{for} \quad \omega > \frac{2\pi}{T_0} \tag{2.41}$$

3

Methods

The work performed in this project focuses on the theory described in Section 2.3 which mostly follows the proposed procedure by Nielsen et al. (2018). The starting point in this Master's thesis is an in-house implementation written with a certain, different, vessel in mind. Therefore, the in-house implementation needs to be modified to a more general form to suit different vessel types and sizes. In the following sections, the working method will be described including the format of the input data and how the program can be improved.

3.1 Input Format

In the MATLAB®programs, important data, such as the vessel motions and the transfer functions are needed. The vessel motions can either be simulated or real measured values over time from an in service vessel. The important is that it is organized according to Table 3.1 where the time is in seconds. The actual motions can be any of the 6 possible motions but as a starting point, heave, roll and pitch will be used where heave is in meters while roll and pitch are in degrees. The main reason for choosing these three motions over sway, yaw and surge is that these motions had transfer functions available. For heave, roll and pitch, there is closed form expressions for the transfer functions that could be further used to validate the information. In reality, any of the six motions could be used as long as there is available motions and transfer functions. According to Nielsen et al. (2018) it is possible to include other responses such as vertical bending moment as long as there is transfer functions available. It is important to ensure that at least one of the motions include the information about the symmetry planes, meaning it can identify if the waves are encountered from port or starboard side, which is included in the roll transfer function.

Table 3.1: Schematic structure of the vessel motions data that is to be used in the MATLAB®programs.

Time (s)	Heave (m)	Roll (deg.)	Pitch (deg.)
t_1	z_1	ϕ_1	θ_1
t_2	z_2	ϕ_2	θ_2
t_3	z_3	ϕ_3	θ_3
$\vdots$	$\vdots$	$\vdots$	$\vdots$
t_N	z_N	ϕ_N	θ_N

The transfer functions should correspond to the chosen motions, e.g. if heave, roll and pitch are chosen as the motions under investigation, then the corresponding transfer functions should be used in the same unit. The transfer functions can be calculated with suitable software, as mentioned in Section 2.4. The transfer functions are case dependent, which implies that they are dependent on loading condition, vessel speed and heading. To enable an investigation at different vessel speeds, a numerous of transfer functions needs to be calculated corresponding to each condition and each case has to follow the structure described in Table 3.2 were it should be an even increment step size of the heading $\chi \in [0\ 360[$ and the structure should start with following seas.

For the purpose of verifying the results in the program, it is also good practice to include the actual wave elevation since it will be possible to calculate the real wave spectrum over the period and by that extract the wave characteristics. This information should be on a similar format as the motions, more specifically according to Table 3.3. Depending on what information that is available, the wave elevation could also be exchanged for the actual wave spectrum, directional wave spectrum or the wave spectrum characteristics.

Table 3.2: Schematic structure of the vessel transfer functions that is to be used in the MATLAB®programs, in this example, the heading step size is 10 degrees but could be any value.

Frequency	Heave		Roll		Pitch	
0 deg.	0 deg.	0 deg.	0 deg.	0 deg.	0 deg.	0 deg.
ω_1	$\Re(z_1)$	$\Im(z_1)$	$\Re(\phi_1)$	$\Im(\phi_1)$	$\Re(\theta_1)$	$\Im(\theta_1)$
ω_2	$\Re(z_2)$	$\Im(z_2)$	$\Re(\phi_2)$	$\Im(\phi_2)$	$\Re(\theta_2)$	$\Im(\theta_2)$
ω_3	$\Re(z_3)$	$\Im(z_3)$	$\Re(\phi_3)$	$\Im(\phi_3)$	$\Re(\theta_3)$	$\Im(\theta_3)$
$\vdots$	$\vdots$	$\vdots$	$\vdots$	$\vdots$	$\vdots$	$\vdots$
ω_N	$\Re(z_N)$	$\Im(z_N)$	$\Re(\phi_N)$	$\Im(\phi_N)$	$\Re(\theta_N)$	$\Im(\theta_N)$
10 deg.	10 deg.	10 deg.	10 deg.	10 deg.	10 deg.	10 deg.
ω_1	$\Re(z_1)$	$\Im(z_1)$	$\Re(\phi_1)$	$\Im(\phi_1)$	$\Re(\theta_1)$	$\Im(\theta_1)$
ω_2	$\Re(z_2)$	$\Im(z_2)$	$\Re(\phi_2)$	$\Im(\phi_2)$	$\Re(\theta_2)$	$\Im(\theta_2)$
ω_3	$\Re(z_3)$	$\Im(z_3)$	$\Re(\phi_3)$	$\Im(\phi_3)$	$\Re(\theta_3)$	$\Im(\theta_3)$
$\vdots$	$\vdots$	$\vdots$	$\vdots$	$\vdots$	$\vdots$	$\vdots$
ω_N	$\Re(z_N)$	$\Im(z_N)$	$\Re(\phi_N)$	$\Im(\phi_N)$	$\Re(\theta_N)$	$\Im(\theta_N)$
$\vdots$	$\vdots$	$\vdots$	$\vdots$	$\vdots$	$\vdots$	$\vdots$
$\vdots$	$\vdots$	$\vdots$	$\vdots$	$\vdots$	$\vdots$	$\vdots$
350 deg.	350 deg.	350 deg.	350 deg.	350 deg.	350 deg.	350 deg.
ω_1	$\Re(z_1)$	$\Im(z_1)$	$\Re(\phi_1)$	$\Im(\phi_1)$	$\Re(\theta_1)$	$\Im(\theta_1)$
ω_2	$\Re(z_2)$	$\Im(z_2)$	$\Re(\phi_2)$	$\Im(\phi_2)$	$\Re(\theta_2)$	$\Im(\theta_2)$
ω_3	$\Re(z_3)$	$\Im(z_3)$	$\Re(\phi_3)$	$\Im(\phi_3)$	$\Re(\theta_3)$	$\Im(\theta_3)$
$\vdots$	$\vdots$	$\vdots$	$\vdots$	$\vdots$	$\vdots$	$\vdots$
ω_N	$\Re(z_N)$	$\Im(z_N)$	$\Re(\phi_N)$	$\Im(\phi_N)$	$\Re(\theta_N)$	$\Im(\theta_N)$

Table 3.3: Schematic structure of the wave elevation data that is to be used in the MATLAB®programs.

Time (s)	Wave elevation (m)
t_1	ζ_1
t_2	ζ_2
t_3	ζ_3
$\vdots$	$\vdots$
t_N	ζ_N

3.2 Output Format

From the calculations made in the MATLAB®programs, it is possible to retrieve large amounts of information however only a few of them are of interest, while the others have the function of indicating the accuracy of the estimation. The main target of the procedure is to describe the wave parameters which implies values of the significant wave height, periods and the encounter angle etc. of the waves in the absolute domain. As described in Section 2.3 the estimation procedure is carried out in steps were it firstly focus on the encounter frequency domain and calculates the wave parameters in the vessels moving frame of reference. Even the estimation in the encounter frequency domain is divided into two parts, firstly calculating the significant wave height and the encounter wave angle based on the absolute values of the transfer functions. Two examples of the results is shown in Fig. 3.1 were the heading estimate is chosen at the placement where the variance is the lowest. The heading estimation is $\beta_0 \in [0\ 180]$ deg..

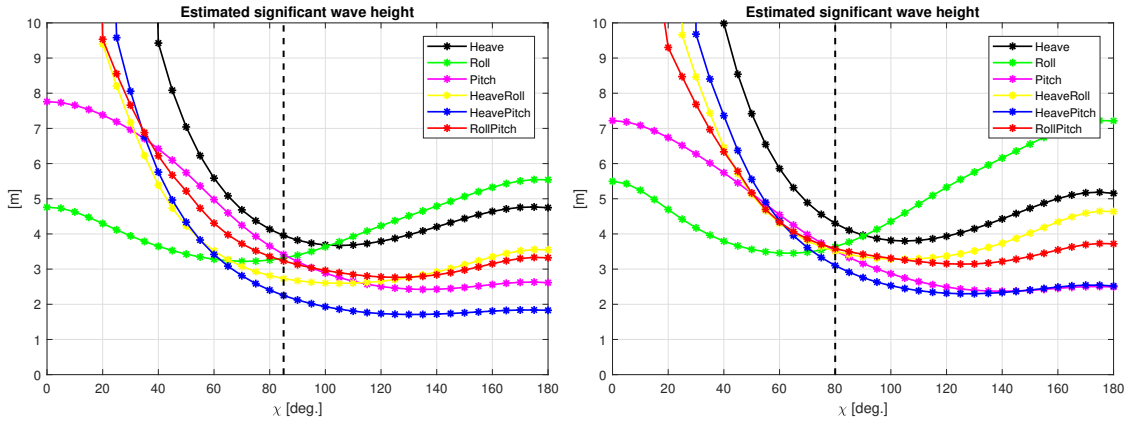

(a) Estimated angle is 85 deg. and the true angle is 90 deg.

(b) Estimated angle is 80 deg. and the true angle is 270 deg which is the symmetry angle to 90 deg.

Figure 3.1: The calculated estimation of the wave spectrum based on only the absolute values of the transfer functions, i.e. only considering the spectra of $\chi \in [0\ 180]$ deg.. β_0 is chosen based on the angle where the lowest variation occurs which is indicated by the vertical dotted line, the significant wave height is taken as the average value of the responses at the same angle.

The information retrieved from the first estimate, which can be seen in Fig. 3.1, is not enough since it only indicates the heading on the spectrum of $\chi \in [0\ 180]$ and the intention is to calculate on the full compass, $\chi \in [0\ 360[$ deg. To do so, the imaginary parts of the transfer functions must be included in the estimation. Two examples of the results of this practice is shown in Fig. 3.2 were the actual wave heading estimate is found were the blue line, named 'Total', takes its minimum value. This secondary heading estimate is $\beta_2 \in [0\ 360[$ deg.

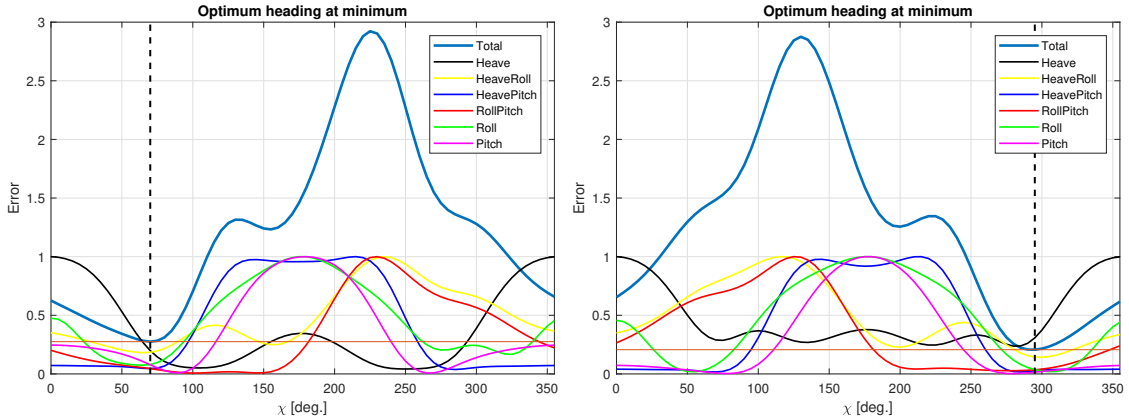

(a) Estimated angle is 70 deg. and the true angle is 90 deg.

(b) Estimated angle is 285 deg. and the true angle is 270 deg.

Figure 3.2: The second estimated heading β_2, based on the imaginary parts of the transfer functions, i.e. considering the whole spectra of $\chi \in [0\ 360[$ deg., the approach follows Eq. (2.27) and gives the heading as the position where the 'Total' line takes the minimum value which is indicated with the vertical dotted line.

The generated information about the wave is in the encounter wave domain and must be transformed in to the absolute domain which is carried out by using the information about the wave spectrum itself. By using the information about the wave angle and the vessel speed it is possible to know the characteristics to calculate the absolute domain spectrum by introducing the Doppler effect. After doing so, all the information wanted is estimated, which implies values on the significant wave height, the wave encounter angle and the periods.

3.3 Measured Values

In cooperation with DNV GL, vessel specific (for reference, see Table A.1) data were provided for the project which included the motions of the vessel, the transfer functions for heave, roll and pitch along with the directional wave spectrum measured with the system Miros Wavex (Mir, 2011). The information gathered from the vessel was firstly re-structured according to the format described in Section 3.1. Transfer functions were only available for certain vessel speeds and in a first stage, motion time periods were chosen so the speed of the vessel at the time of measurement were of the same speed of the available transfer functions. It requires extensive work to first find time periods where the heading and speed was fairly constant and then transform the data into the correct structure and then run the estimation procedure.

It was rapidly realized that the procedure did not estimate the wave parameters correctly since the output of the script could indicate a significant wave height of 10 meters when the correct result should be 0.5 meters. This sort of results was recurring and without any clear trend or reason.

The first step in the process of finding the error source was to investigate the transfer functions since these are highly important and without correct transfer function, it will be impossible to estimate the wave parameters. By turning the procedure around, it is possible to check how well the transfer functions performs. Instead of looking at the motions and trying to predict the wave parameters, the information given can be used to re-generate the motions and thereby compare the actual motions with the motions calculated by using the wave spectra information.

The result of the described procedure, to investigate how well the transfer functions performs compared to the reality, can be seen in Fig. 3.3. In Fig. 3.3a it is possible to see the measured wave spectrum together with a parametric wave-spectrum according to Bretschneider theory described in Section 2.6 using the wave parameters given from the

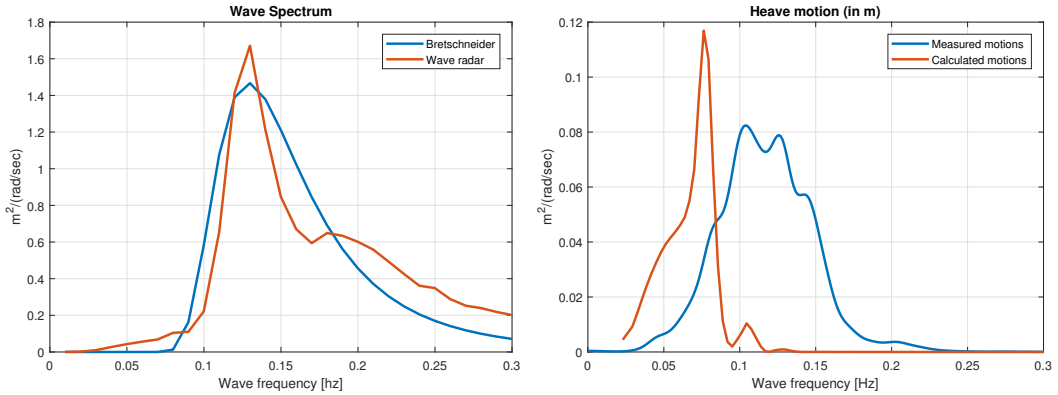

(a) Comparison of the wave spectrum and a Bretschneider wave spectrum with the same wave parameters.

(b) Comparison of the heave motions based on measured values and calculated based on the transfer function.

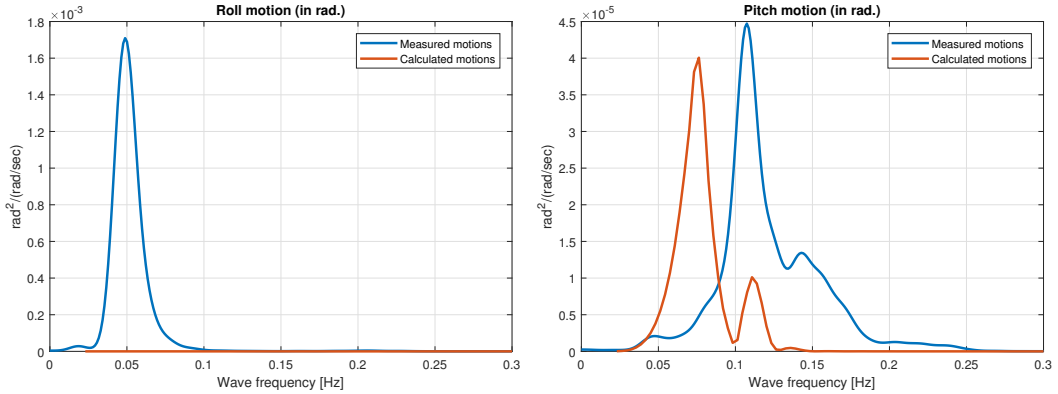

(c) Comparison of the roll motion based on measured values and calculated based on the transfer function.

(d) Comparison of the pitch motion based on measured values and calculated based on the transfer function.

Figure 3.3: Re-generated vessel motions based on the transfer functions in combination of the directional wave spectrum.

vessel data. The comparison shows a good correlation which means that the given wave parameters describes the wave oceans in a fairly good way, indicating that the data of the wave spectrum is correct. In Figs. 3.3b to 3.3d the comparison between the measured motions and the re-calculated motions using the transfer functions can be seen and it is clear that there is a differences between the two response spectrums for each motion. This indicates that either the measured motions and/or the transfer functions are faulty. In an effort to trace if the error originated in the transfer functions or in the measured responses, one more comparison was done with a new set of transfer functions received from DNV GL with similar errors as shown in Fig. 3.3.

3.4 Choosing Transfer Functions

With the results pointing out that the transfer functions might not be fully correct when using them together with the measured vessel motions, and at this moment, there are two sets of transfer functions available which none of them are working well with the motions data. DNV GL offered to re-calculate the transfer functions. Without any promised improvements since it could in the end be the measured vessel motions that are faulty and if so, it does not matter how detailed the transfer functions are. Instead, it was chosen to investigate the two sets of transfer functions and continue the research using the transfer functions that are most likely to be correct. This could be done by introducing closed form expressions of the transfer functions. It is possible to generate transfer functions based on main particulars of the vessel according to the theory given by Jensen et al. (2004). The procedure is outlined in Appendix B. The importance is the comparison between the two sets of transfer functions with the closed form expression transfer functions. In Figs. 3.4 and 3.5 the comparisons can be seen. It is clear that both sets of transfer functions performs somewhat well against the closed form expressions, especially for heave and pitch motions. The roll motion transfer functions from Sesam deviate more from the closed form expressions than the ones retrieved directly from DNV GL that correlate well with the closed form expressions. It can also be seen a higher deviation of the transfer functions for heave and pitch retrieved directly from DNV GL than the ones from Sesam. With this information only, it is hard to make a well-informed decision upon which of the two sets of transfer functions that should be further used since the transfer functions shown in the figures are both accurate but in different areas. The fact that the later transfer functions, obtained directly from DNV GL, are more detailed with both more speeds, headings and frequencies, it is decided that the best option would be to go forward with the later transfer functions, the ones received directly from DNV GL, also shown in Fig. 3.5, will be used in the rest of the project work.

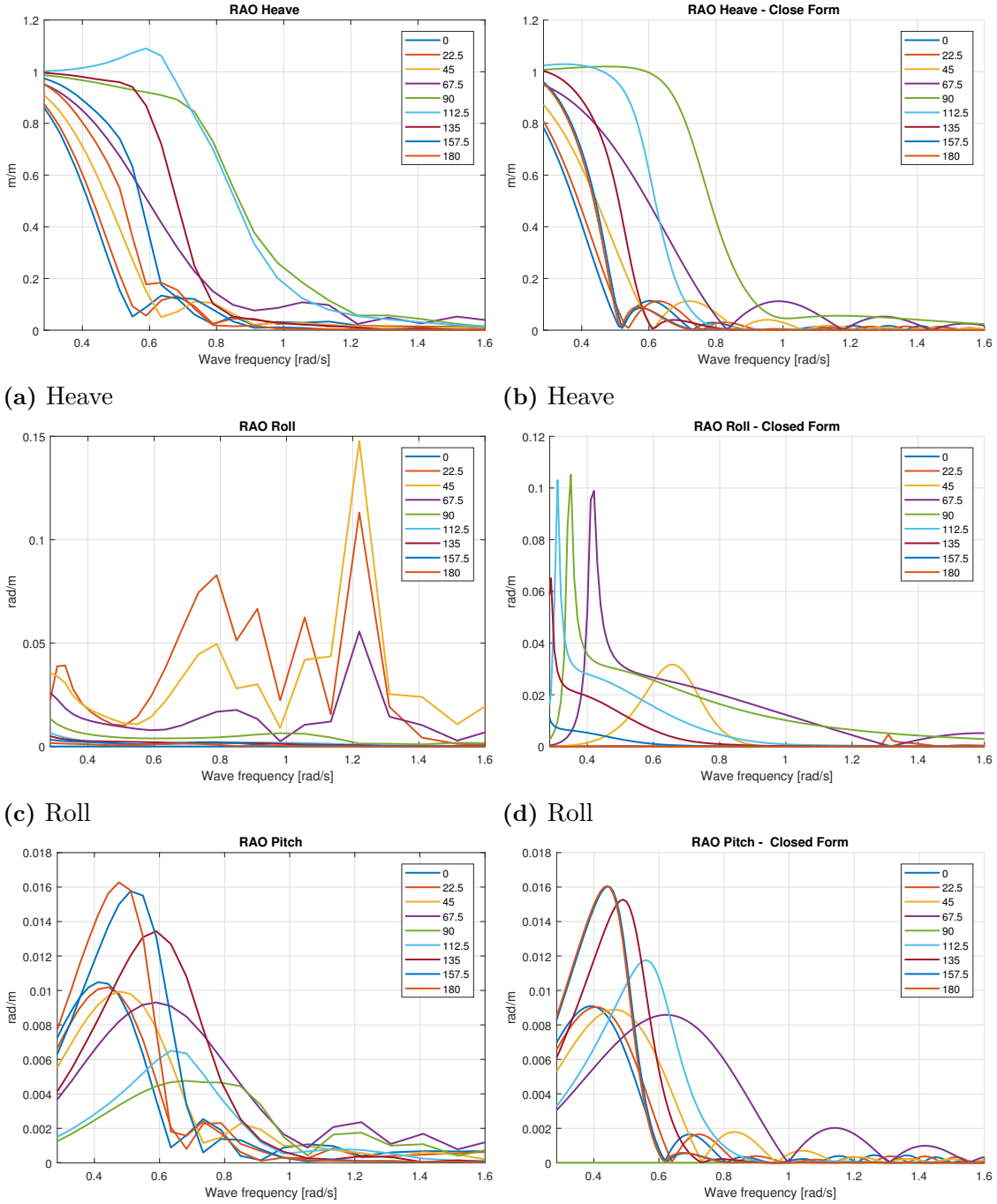

(a) Heave **(b)** Heave

(c) Roll **(d)** Roll

(e) Pitch **(f)** Pitch

Figure 3.4: Comparison between the transfer functions obtained from the software Sesam with transfer functions calculated based on the closed form expressions by Jensen et al. (2004). On the left side is the software calculated functions, on the right side is the closed form expressions functions.

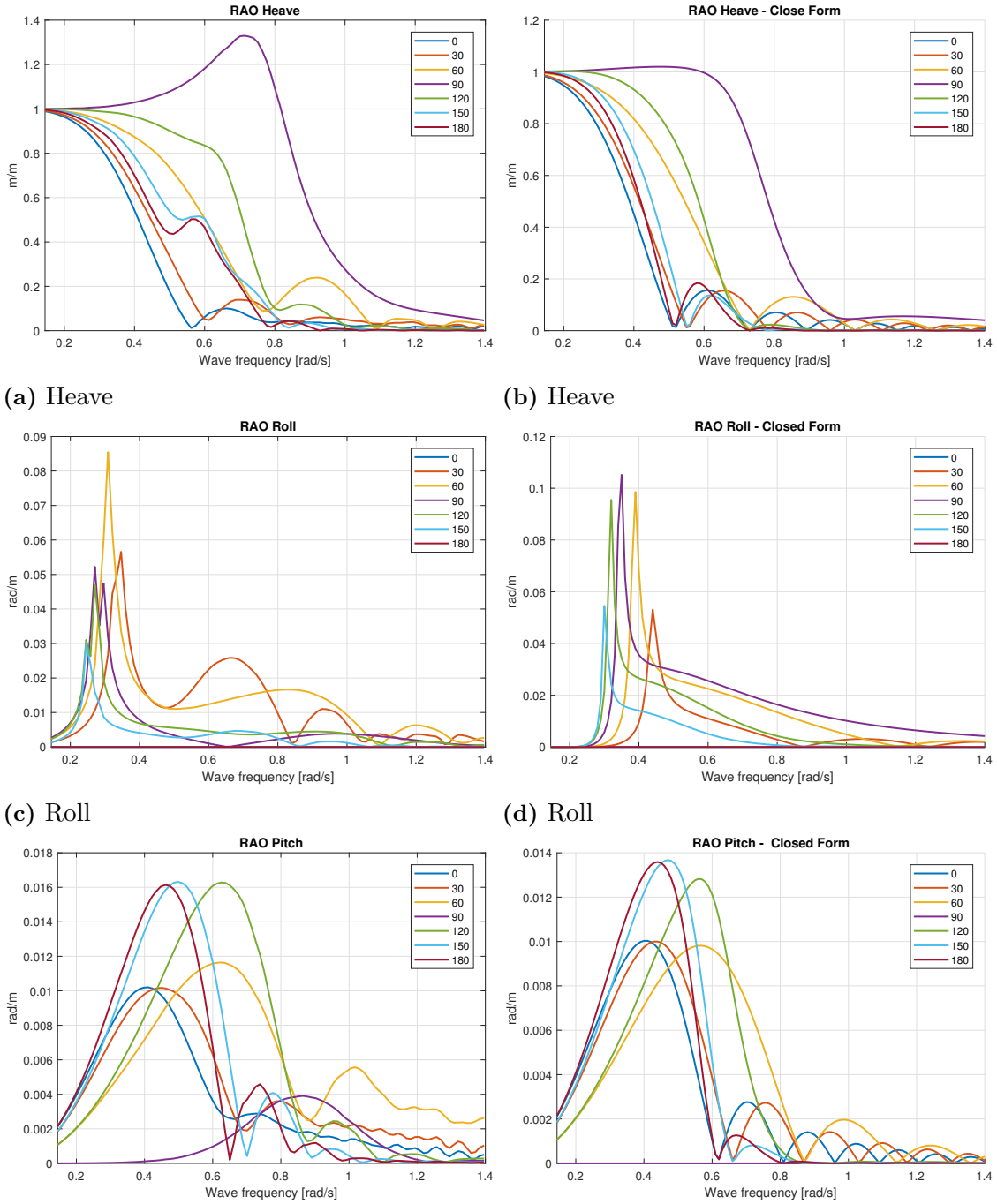

(a) Heave **(b)** Heave

(c) Roll **(d)** Roll

(e) Pitch **(f)** Pitch

Figure 3.5: Comparison between the transfer functions obtained directly from DNV GL with transfer functions calculated based on the closed form expressions by Jensen et al. (2004). On the left side is the software calculated functions, on the right side is the closed form expressions functions.

3.5 Simulated Motions

Based on the problems described in Section 3.3, that it is uncertain exactly where the error is introduced since none of the two transfer functions can estimate the wave spectrum correctly together with the fact that the vessel motion data is measured by outside companies and that it is 10 years old data makes it a bit uncertain how much this data can be trusted. It can originate from numerous sources of error along the way that in the end affects the results so much that the outcome is not satisfactory. Therefore, it is decided to generate data though computer simulations using the chosen vessel transfer functions. In that way it is possible to completely control all variables and make sure that the data itself is correct. In the following list, the advantages and disadvantages of using own generated data over the measured data is presented:

Advantages

- It is possible to control all parameters of the waves
- It is possible to generate a wide set of time histories enabling big data analysis
- The correctness of the transfer functions becomes a no-problem since the transfer functions are used to generate the data
- Noise canceling can be enabled
- Quick feedback loop

Disadvantages

- The evaluation of the brute force approach proposed by Nielsen et al. (2018) is not made on real, measured, data.

By first generating a random wave elevation based on the theory that ocean waves can be described by a finite amount of sinusoidal waves added together creating a fully developed wave system similar to whats shown in Fig. 2.4. The result of this is shown in the top of Fig. 3.6. Once the wave elevation is generated, it is possible, using Eq. (2.8), to calculate each of the responses at each time step of the time series. The motion output is then according to the three lowest plots in Fig. 3.6.

Each time series is decided to be the length of 30 minutes i.e. 1800 seconds with a sampling rate of 5 hertz, giving 9000 measurement points per time series. As mentioned, this is a computational quick process and thereby enabling big data analysis, based on that, it was decided to generate time series corresponding to the following inputs:

- $\mathbf{H_s}$: from 2 meter to 6 meters in steps of one meter
- $\mathbf{T_p}$: from 10 s to 12 s in steps of 1 second
- $\boldsymbol{\chi}$: from 0 deg. to 350 deg. in steps of 10 deg.
- **Speed**: 10.7 knots, 16.0 knots, 21.3 knots, based on the speeds of the available transfer functions
- **No**: 5 time series per set up

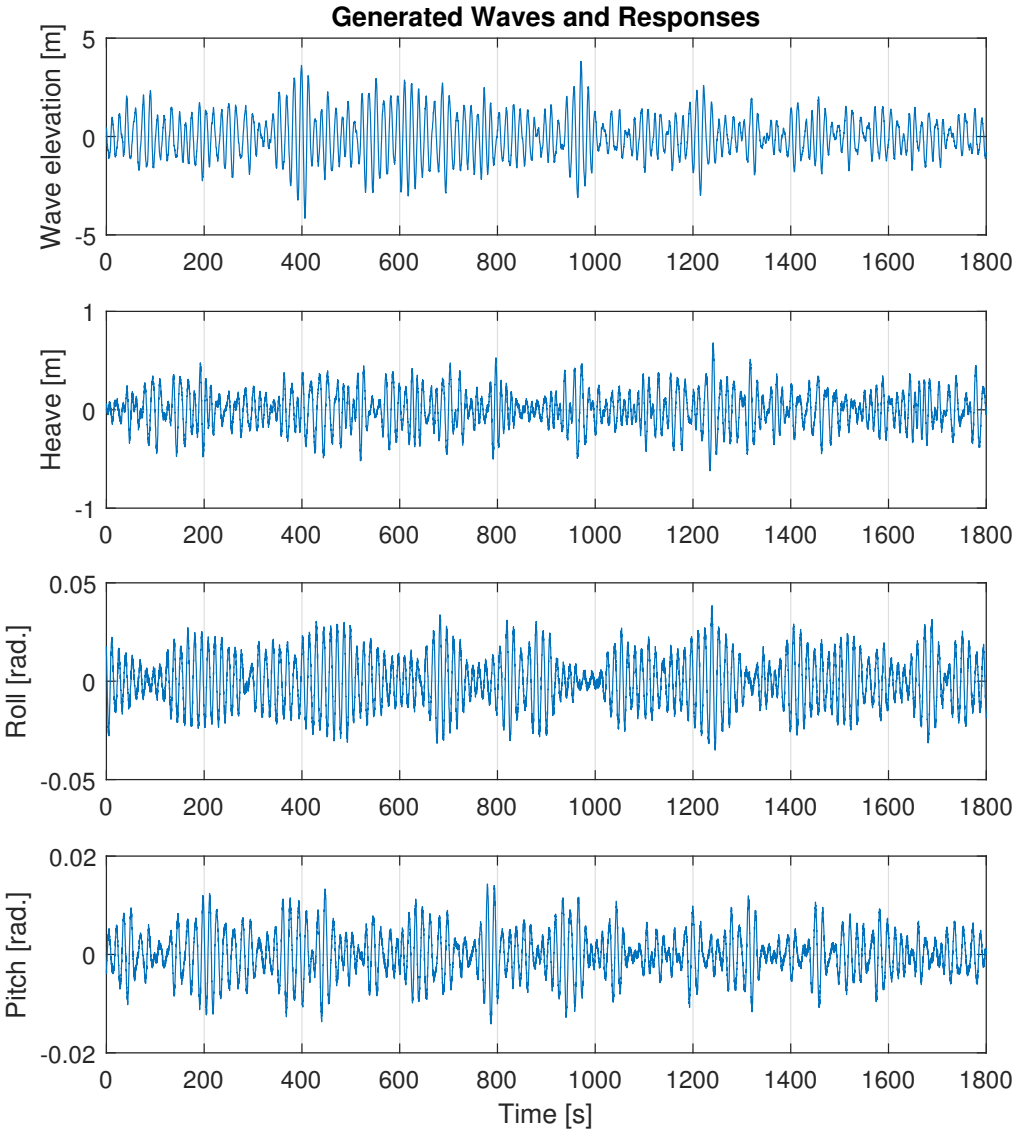

Figure 3.6: Simulated vessel motions together with the wave elevation. The top plot is the wave elevation in meters over a half hour period, second plot is the heave motion in meters over the same half hour period, third and fourth plot is the roll and pitch motion respectively in radians over the same half hour period.

In total, this set up of the time series generation creates 8100 unique time series of 30 minutes each which all can be used in the analysis of the sea state estimation which correspond to almost half a year of open seas operations. It is important to point out that the wave elevation is a random process which also indicates that the resulting value of the wave parameters will not be exactly the same as the input, however over time it will tend to converge towards the input value.

In Fig. 3.7 the simulated motions from one of the generated time series is shown. The procedure has been the same as for Fig. 3.3 were the motions are re-calculated using the

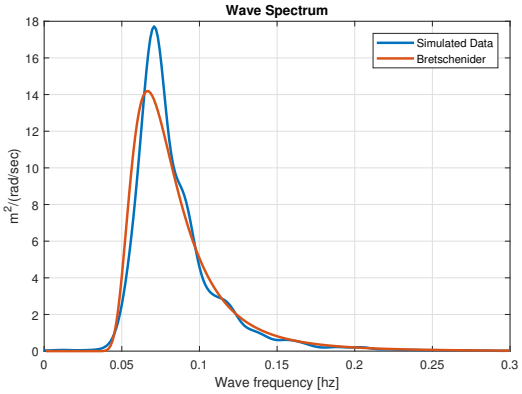

(a) Comparison of the simulated wave spectrum and a Bretschneider wave spectrum with the same wave parameters.

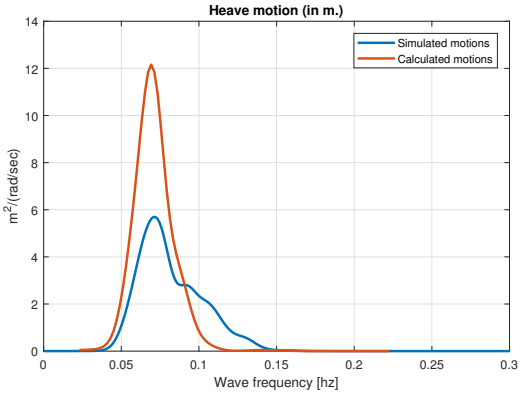

(b) Comparison of the heave motions based on simulated values and calculated based on the transfer function.

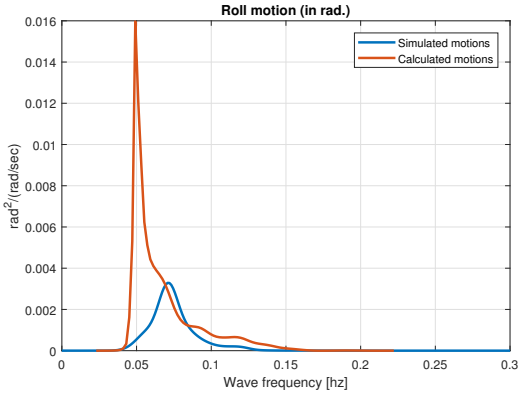

(c) Comparison of the roll motion based on simulated values and calculated based on the transfer function.

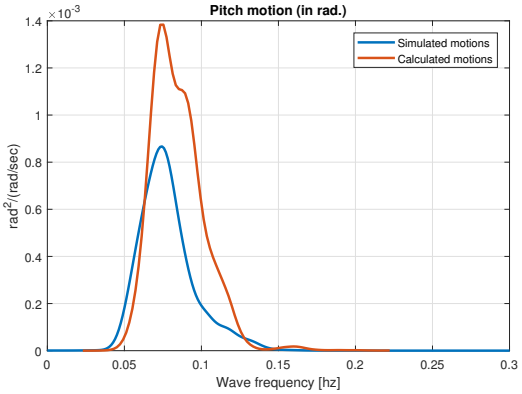

(d) Comparison of the pitch motion based on simulated values and calculated based on the transfer function.

Figure 3.7: Re-generated vessel motions based on the transfer functions in combination with the simulated wave spectrum.

wave spectrum and the transfer functions for the specific case. Thereby it is possible to identify how well the transfer functions work with the simulated data. In this case, and in general, the simulated data and the calculated data using transfer functions correlate well, and according to theory, it should, since the actual motions are generated using the present transfer functions. In the best case, the simulated motions and the calculated motions should be identical. However, noise is added to the simulated data to imitate real data and therefore it will not be identical. It should be close to each other, which is presented in Fig. 3.7. The biggest deviation can be seen in Fig. 3.7c were a peak is present, this can be explained by the transfer functions that have a peak at exactly 0.05 Hz. However, in reality this will not occur since it is at such a small band width and will only occur if the waves are all at 0.05 Hz. The peak in the transfer function could be occurring if the added damping from viscous effect is to low. A sample of closed form expression transfer functions with different added damping can be seen in Fig. 3.8 which indicates that the transfer functions might have been generated based on wrong input values on the viscous damping. With a higher added damping in the roll transfer function, the peak

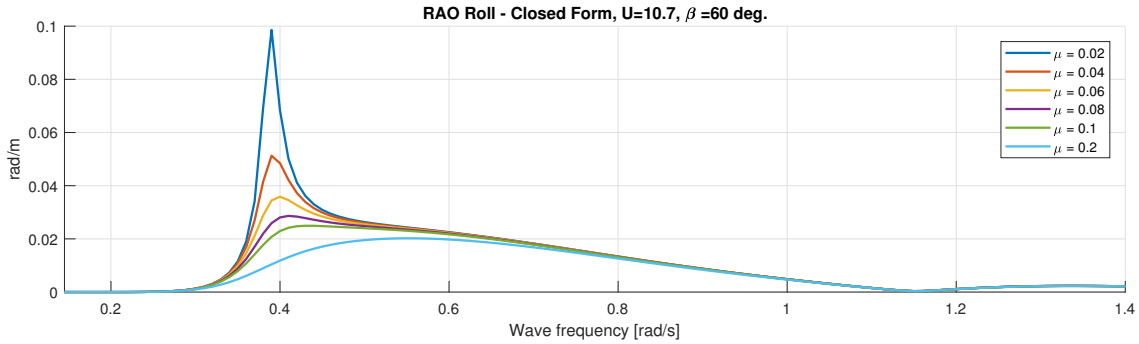

Figure 3.8: The effect of different added damping on the roll transferfunctions based on the theory by Jensen et al. (2004). μ is the percentage of the critical damping that is added to imitate the viscous effects. The speed, U, and heading angle, β, is the same as for the ones used in Fig. 3.7.

in the roll response spectrum, see Fig. 3.7c, could most probably be avoided and a more representative response spectrum would be the result.

3.6 Faulty Results

Knowing that the time series simulations are correct, based on the transfer functions in use, enables the sea state estimation procedure to continue. At the earlier stage when the estimation procedure did not work, it was not known were the error source originated. However, with own simulated data, there is no outside error source and all the values can be chosen along an own scheme. Furthermore, it is not dependent on the vessels actual routes and the apparent weather at that time.

It was realized once again that the procedure was not successful in predicting the sea state in an accurate manner. It was now possible to ensure that the error originated from the procedure itself. It became clear that all parameters deviated in numerous of the cases, even though it was realized that the periods could not, by any means, be estimated correctly if the wave heading estimate is incorrect since it is an important factor in the transformation. Even in cases were the wave heading was correct, the periods most often resulted in values far from the true value. It was decided that both the height estimate and the wave heading estimate should be re-worked to increase the correctness. In Table 3.4 the errors of the heading estimate in the 8100 time series simulations can be seen.

Table 3.4: The heading estimate errors per speed using the original estimation procedure. Mean absolute value represent the mean value of the absolute errors, meaning that the sign is not included. Correctly chosen heading represent the amount of times the best available heading between the β_0 and β_2 is chosen.

Speed [knots]:	**Mean absolute error [deg.]:**	**Standard deviation of the error:**	**Correctly chosen heading [%]:**
10.7	14.6	12.3	66.9
16.0	21.9	24.8	54.6
21.3	25.9	22.0	37.9

Table 3.5: The significant wave height estimate errors per speed using the original estimation procedure. Mean absolute value represent the mean value of the absolute errors, meaning that the sign is not included.

Speed [knots]:	**Mean absolute error [m.]:**	**Standard deviation of the error:**
10.7	1.14	2.25
16.0	6.52	13.20
21.3	4.23	10.27

Similarly, the error of the significant wave height is shown in Table 3.5 for the same set of time series used in Table 3.4.

It can be concluded that the errors are fairly big in general and that the error increase as speeds increases. In fact, the significant wave height is calculated based on the heading estimation and therefore it can also be stated that the error in the significant wave height can be traced to the error in the wave heading estimation.

3.7 Improvements

The faulty results shown in Table 3.5 indicates that something has to be done to achieve more accurate results. It can be done in different ways, (1) the estimation procedure is re-worked from the beginning, generating a new theory based estimation procedure that would give more promising results, or (2) the procedure is fine-tuned based on the information at hand.

Based on the knowledge of the author of this thesis and the time in the project, it was not practically possible to start over trying to find a new estimation procedure even though it could possibly give better results. The more efficient strategy in this case is to use what is available and fine tune the procedure based on this specific vessel. From a general estimation procedure point of view, it is not optimal to tune the program since it will lead to sub-optimized programs for each vessel however it is still the most practical at this moment.

3.7.1 Heading Estimate

The first, most essential, estimated parameter is the wave heading which will be re-worked in a first instance. At the stage of estimating the wave heading only a few parameters are known:

- Vessel speed U
- β_0 (the first heading estimate based on the absolute value of the transfer function)
- β_2 (the second heading estimate based on the imaginary part of the transfer function)

Therefore, an evaluating process had to be established using only this information in an effort to optimize the selection, decreasing both the mean error and the standard deviation. Most important, increasing the "correctly" chosen estimate between β_0 and β_2

since the estimates accuracy is hard to increase without changing the estimation procedure fundamentally.

By investigating the error between the "true" heading and β_0 and β_2 respectively, it is possible to search for trends based on either the β_0 or β_2. It became clear that for certain values of either of the two β, one or the other estimate is preferred over the other and it was consistently throughout most of the data. Rules started to form in the format of "if the speed is X and β_0 is Y then use the value of β_2 for the final heading estimate" since it enabled the possibility to choose the best possible heading estimate. It was realized that rules could be generated into infinity to gain ~0.1% extra accuracy hence guidelines had to be created which follows:

1. Maximum 5 rules per vessel speed
2. Either β_0, β_2 or the mean value of them both.

Following these guidelines ensures that the rules will stay simple and easy to adopt and update for other vessels and importantly "good enough" relative to the time spent on developing them. The resulting rules can be seen Algorithm 2 which applies for the specific vessel in this project. It should be noted that in reality, it would be necessary to add one more dimension were the speed can vary more than between three specific speeds, meaning that the rules would need to be developed for example according to "**If** $U \in$ [8 12] knots **then** ...". Transfer functions only were available for three speeds in this project so it became impossible to develop that sort of rules.

β_0 only covers the spectra [0 180] deg. which then must be compensated for in the cases of choosing β_0 as the final heading estimate, this is done by investigating the value of β_2. If β_2 is above 180, then the symmetry part of β_0 is chosen, otherwise it is kept as the originally estimate value. The outcome of implementing these rules can be seen in Table 3.6 which can be compared to the values shown in Table 3.4.

Table 3.6: The improved heading estimate errors per speed using the developed rules in Algorithm 2. Mean absolute value represent the mean value of the absolute errors, meaning that the sign is not included. Correctly chosen heading represent the amount of times the best available heading between the β_0 and β_2 is chosen. Values in parenthesis are the results without the rules applied.

Speed [knots]:	**Mean absolute error [deg.]:**	**Standard deviation of the error:**	**Correctly chosen heading [%]:**
10.7	7.6 (14.6)	10.4 (12.3)	78.1 (66.9)
16.0	12.7 (21.9)	25.1 (24.8)	86.9 (54.6)
21.3	7.5 (25.9)	14.9 (22.0)	93.4 (37.9)

Algorithm 2 Improved process of finding the best estimated heading. U is the speed in knots, β_x is the heading in degrees relative to the waves.

```
if U=10.7 then
  if β0 ∈ [50 105] then
    β = β0
  else if β0 ∈ [110 145] then
    β = (β0 + β2)/2
  else
    β = β2
  end if
else if U=16.0 then
  if β2 ∈ [340 20] then
    β = β2
  else if β0 ≥ 120 then
    β = β2
  else if β0 = 0 then
    β = β0
  else
    β = β0
  end if
else if U=21.3 then
  if β0 > 110 then
    β = β2
  else if β0 ≤ 40 then
    β = β2
  else
    β = β0
  end if
end if
if β = β0 then
  if β2 > 180 then
    β = 180 + (180 − β)
  end if
end if
```

3.7.2 Significant Wave Height

Using a similar approach as for the wave heading estimate, the significant wave height are to be optimized. The originally proposed procedure estimates the significant wave height with significant large errors, especially for vessel speeds of 16.0 and 21.3 knots were the error is not unusually deviating 10 meters, which is not acceptable, see Table 3.5 for reference. The values in Table 3.5 are based on the wave heading without the rules applied, which naturally lower the accuracy of the significant wave height estimate due to the theory described in Eq. (2.25) where the mean value of all 6 responses are chosen at the heading estimate. It could be discussed how big impact the heading estimate has on the significant wave height and it has been shown by unpublished result that the improved wave heading estimate is not enough to lower the error level to an acceptable level and therefore effort

has to be put on improving the estimate. To do so, the only known parameters to be used are:

- Vessel speed, U
- Final heading estimate, β

It could easily be found responses that were very untrustworthy for certain headings while other responses turned out to predict the resulting significant wave height very well. Theoretical, there are 63 different combinations of the 6 responses, anyhow only 57 of these will be considered since using only one response could be risky in matter of standard deviation since there is nothing "damping" extreme cases. Thereby, general rules are established accordingly for the response selection:

1. Maximum of 5 rules per vessel speed
2. Minimum combination of 2 responses
3. A certain response can only be used once, which means no scaling factor nor weight
4. The average value of the chosen responses

Rule number 3 is included to limit the number of possible combinations, It would theoretically be an infinite amount of combinations that could give a better estimate, however it is a matter of practically possible and results that are "good enough". The resulting rules can be seen in Algorithm 3. Since the significant wave height is estimated using the absolute values of the transfer functions, it is only possible to make use of heading estimates on [0 180] deg. Therefore, in the cases where the estimate is higher than 180 deg., it has to be recalculated for its symmetry part around the centerline, see Fig. 2.5.

Using the rules established in Algorithm 3 the improvements of the significant wave height estimate is good for this specific vessel. It is not a general approach, however, it is actually a vessel specific approach. A summary of the resulting errors can be seen in Table 3.7 and the difference from not using these rules are significant. In all speed cases, the values are more than halved and in extreme cases, the new value is lowered with over 83% compared to the originally value. Two things should be noted, (1) there is yet no information of the distribution on the error along different heading estimates and (2) in reality, one more parameter should be added to the rules were the speed can take values apart from these three pre-defined speeds.

Table 3.7: The improved significant wave height estimate errors per speed using the developed rules in Algorithm 3. Mean absolute value represent the mean value of the absolute errors, meaning that the sign is not included. Value in parenthesis is the result without the rules applied.

Speed [knots]:	**Mean absolute error [m.]:**	**Standard deviation of the error:**
10.7	0.45 (1.14)	0.59 (2.25)
16.0	2.62 (6.52)	4.62 (13.20)
21.3	1.30 (4.23)	1.71 (10.27)

Algorithm 3 The process of choosing the best suitable combinations of responses to calculate the significant wave height. The following abbreviations are used: H = Heave, R = Roll, P = Pitch, HR = Heave-Roll, HP = Heave-Pitch, RP = Roll-Pitch

if $\beta_2 > 180$ **then**
  $\beta = 180 + (180 - \beta)$
end if
if U=10.7 **then**
  if $\beta \in [0\ 40]$ **then**
    Use R + P
  else if $\beta \in [45\ 80]$ **then**
    Use R + HR + HP
  else if $\beta \in [85\ 100]$ **then**
    Use R + P + HP
  else if $\beta \in [105\ 125]$ **then**
    Use R + P
  else if $\beta \in [130\ 180]$ **then**
    Use H + P + HP
  end if
else if U=16.0 **then**
  if $\beta \in [0\ 20]$ **then**
    Use R + P
  else if $\beta \in [25\ 95]$ **then**
    Use HR + HP + RP
  else if $\beta \in [100\ 115]$ **then**
    Use P + RP
  else if $\beta \in [120\ 150]$ **then**
    Use R + P
  else if $\beta \in [155\ 180]$ **then**
    Use P + HP
  end if
else if U=21.3 **then**
  if $\beta \in [0\ 40]$ **then**
    Use R + P
  else if $\beta \in [45\ 75]$ **then**
    Use HP + RP
  else if $\beta \in [80\ 100]$ **then**
    Use P + HR + HP
  else if $\beta \in [105\ 180]$ **then**
    Use P + HP
  end if
end if

3.8 Periods

In parallel to this project, the main supervisor of this project has been informed that parts of the estimation procedure were most certain faulty for the specific vessel in mind which lead to suggested improvements. In a newly submitted paper (Nielsen, 2018) based on the original findings in this project, a new and improved, procedure of the transformation

between the encounter domain to the absolute domain has been presented. It treats the problem of estimating the periods in following seas, since the following seas was the cases were faulty results were present.

The main approach by Nielsen (2018) is to make use of a parameterized wave spectrum, such as the Bretschneider spectrum or the JONSWAP spectrum described in Sections 2.6 and 2.7. The aim is to fit a general parameterized wave spectrum to the measured values in terms of peak period and significant wave height and from this fitting, make use of the general parameters such as the mean period and the zero-upcrossing period eliminating values that are far off the true value.

In theory, this procedure relies on the peak period and the significant wave height that has been shown to have relatively high accuracy. The downside is that it assumes a standard wave spectrum and there are cases when the reality does not follow the parameterized spectrums. In a general approach this should increase the accuracy.

In the estimating procedure, the spectrum generation is carried out for all cases where the estimated heading is lower than 90 deg. or higher than 270 deg., indicating a following sea cases. Then based on these results, the transformation between the two domains is carried out

4

Results

The main results of the sea state estimation procedure proposed by Nielsen et al. (2018) are the wave parameters; significant wave height, H_s, peak period, $\bar{T}_p$, mean period, T_m, zero-upcrossing period, $\bar{T}_z$, and wave heading, β. The estimation results can either be presented in the encounter domain or the absolute domain depending on what application the estimation is intended for. Furthermore, the transformation between different domains are somewhat cumbersome and can in certain cases introduce errors in the estimate. The Doppler effect as well as the fact that the heading estimate is *very* important for the periods to be correctly transformed from one domain to the other. Therefore, the estimates both before and after the transformation will be presented ensuring the best coverage possible.

The results will be presented sorted by parameters were encounter- and absolute domain will be side by side for each speed cases; 10.7, 16.0 and 21.3 knots. The results will be presented in the same order as it was calculated, starting with heading estimate, significant wave height and then all the periods.

In Fig. 4.1, the mean heading estimate for each true heading is presented together with the standard deviation. The green line represents the "correct" estimation which is the goal of the procedure. In Fig. 4.2 the mean error of the estimated significant wave height is presented, where the error definition is calculated according to Eq. (4.1), meaning that a negative error indicates that the estimated value is higher than the true value. In Chapter 3, the interim results were calculated using the absolute value of the error, in this section it is decided to use the true error meaning that the sign of the error is included. The peak period is presented in Fig. 4.3, the zero-upcrossing period in Fig. 4.4 and mean period in Fig. 4.5. Note that all sub-figures in the same figure have the same y-axis limits.

$$\text{Error} = \text{True Value} - \text{Estimated Value} \tag{4.1}$$

The results shown in this chapter are selection of data indicating the errors for different speeds of the different 5 main wave parameters. A wider selection of results are presented in Appendix C.

4.1 Wave Heading Estimate

The resulting heading estimate using the created rules in Algorithm 2 performs well. It is possible to distinguish trend in Fig. 4.1 that the higher the speed is, the lower the accuracy of the estimate is. The figures indicates that the highest accuracy is found in head seas, 180 deg., and in following seas, meaning close to 0 or 360 deg. The same trend can not be seen in Table 4.1 since it takes the whole mean value, and as seen in e.g. Fig. 4.1b the procedure underestimate the heading in the spectra 0-180 deg. while overestimating the heading in the spectra 180-360 deg. which in turn eliminates each other creating a very low mean error. Thereby, it can be of better interest to investigate the absolute mean error that is presented in Table 4.2.

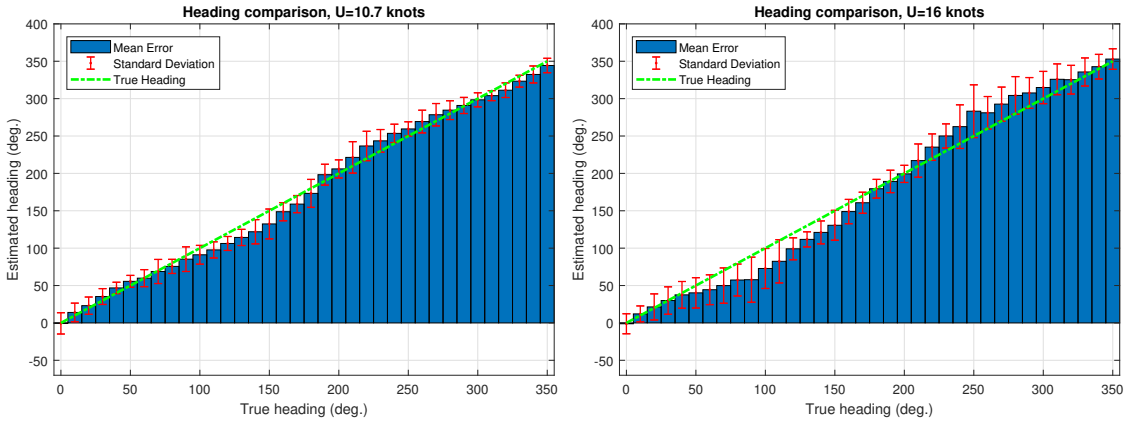

(a) Speed 10.7 knots

(b) Speed 16.0 knots

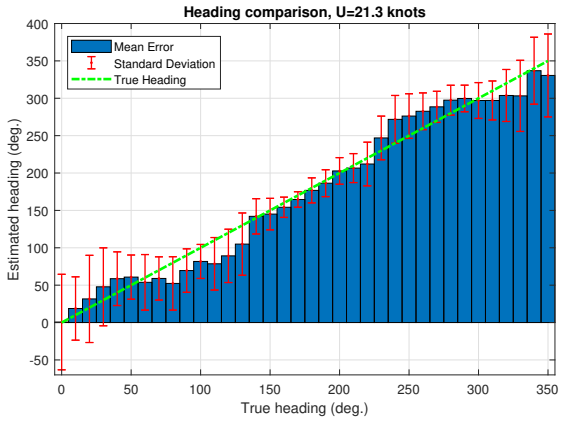

(c) Speed 21.3 knots

Figure 4.1: Comparison of the estimated heading with the true heading, the blue bar represent the mean value of the heading estimate, the red line represent the standard deviation of each heading estimate and the green dotted line represent the optimal case where the estimated heading is the same as the true heading.

Table 4.1: Summarized results for the heading estimate including the mean error for all "true" headings and the standard deviation for the same spectra. The results are divided in to the three different speeds, further, the mean error for all three vessel speeds i presented in the row named "All".

Speed [knots]:	**Mean error [deg.]:**	**Standard deviation of the error:**
10.7	1.57	20.79
16.0	0.66	26.23
21.3	1.95	37.48
All	1.39	28.99

Table 4.2: Summarized results for the heading estimate including the absolute mean error for all "true" headings and the standard deviation for the same spectra. The results are divided in to the three different speeds, further, the mean error for all three vessel speeds i presented in the row named "All".

Speed [knots]:	**Mean error [deg.]:**	**Standard deviation of the error:**
10.7	12.15	16.95
16.0	18.26	18.84
21.3	23.70	29.10
All	18.02	22.75

4.2 Significant Wave Height

In Fig. 4.2 the significant wave height estimate can be seen, including both encounter- and absolute domain, and according to theory, these two domains should not differ significant and that is the case. The results vary quite a lot between different speeds and headings. For the lower speeds is the estimate very accurate while the middle speed tends to deviate from the true value more, especially in the following-/beam- seas cases while the head sea cases estimates the waves with high accuracy. Beam seas is defined as waves encountered from either 90 deg. or 270 deg. according to Fig. 2.5. The highest speed tends to have a low mean error of the estimate, anyhow, the standard deviation is much higher than for the 10.7 knot case, indicating that the results fluctuates more and are a bit less reliable.

Table 4.3: Summarized results for the significant wave height estimate including the mean error for all headings and the standard deviation for the same spectra. The results are divided in to the three different speeds, further, the mean error for all three vessel speeds i presented in the row named "All".

Speed [knots]:	**Mean error [m.]:**	**Standard deviation of the error:**
Encounter Domain		
10.7	-0.18	0.72
16.0	-2.31	4.78
21.3	-0.67	2.04
All	-1.05	3.16
Absolute Domain		
10.7	-0.17	0.71
16.0	-2.61	5.43
21.3	-0.62	2.26
All	-1.13	3.58

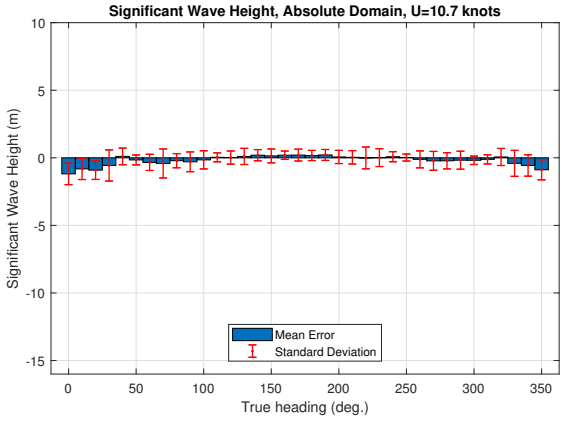

(a) Absolute domain, speed 10.7 knots

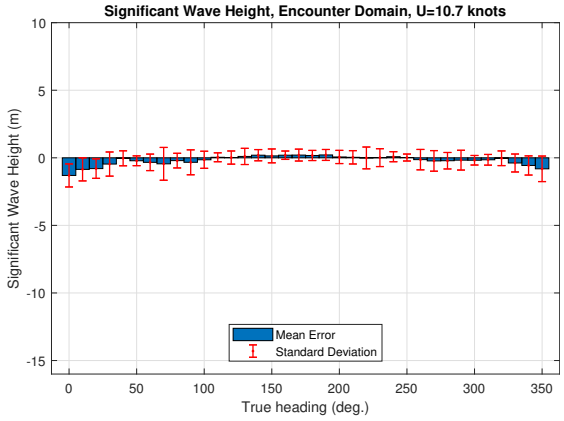

(b) Encounter domain, speed 10.7 knots

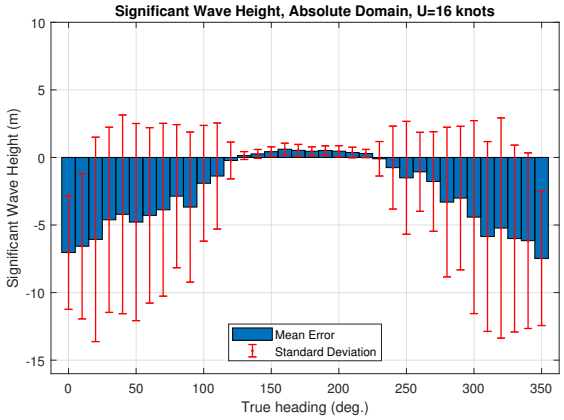

(c) Absolute domain, speed 16.0 knots

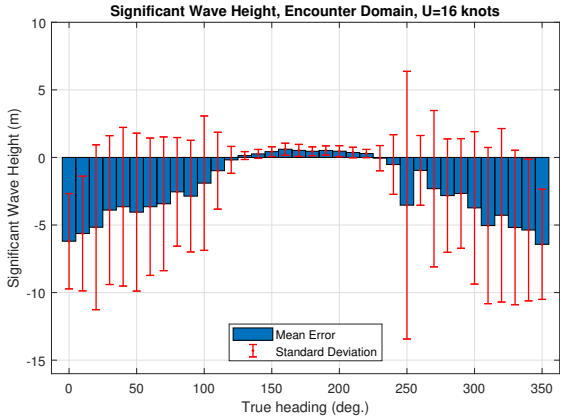

(d) Encounter domain, speed 16.0 knots

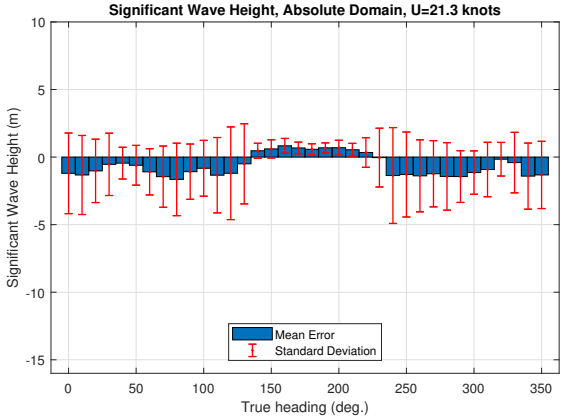

(e) Absolute domain, speed 21.3 knots

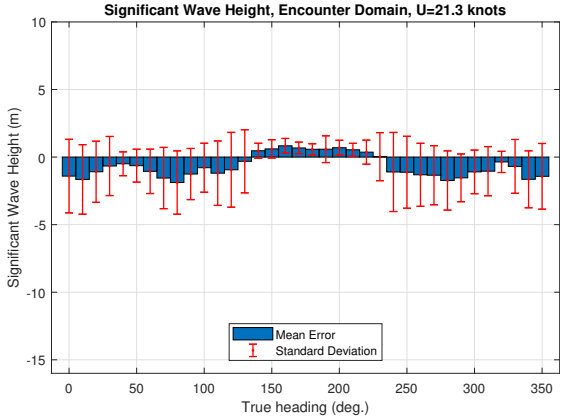

(f) Encounter domain, speed 21.3 knots

Figure 4.2: Comparison of the estimated significant wave height with the true significant wave height. To the left, the absolute domain comparison is displayed while on the right side the encounter domain comparison is shown. The blue bars represent the mean error between the true and estimated height for each true heading and the red line represent the standard deviation of the error values. Be aware that the comparison does not include any information about the true significant wave height, i.e. it only shows the error values.

4.3 Peak Period

The error of the estimated peak period is shown in Fig. 4.3 which shows a similar behavior regarding the accuracy as the results for the significant wave height. Firstly, it can be seen a decrease of the accuracy in the following sea cases and secondly, the accuracy is higher for the lower speeds compared to the higher speeds. The absolute domain results are the first presented results which is highly dependent on the transformation from encounter- to absolute domain and the procedure in fact improves the estimation even though it is one of the more challenging steps in the whole procedure.

Table 4.4: Summarized results for the peak period estimate including the mean error for all headings and the standard deviation for the same spectra.The results are divided in to the three different speeds, further, the mean error for all three vessel speeds i presented in the row named "All".

Speed [knots]:	**Mean error [s.]:**	**Standard deviation of the error:**
Encounter Domain		
10.7	0.52	1.55
16.0	1.99	2.81
21.3	2.26	5.00
All	1.59	3.51
Absolute Domain		
10.7	0.13	1.70
16.0	1.14	2.93
21.3	-0.83	5.62
All	0.15	3.87

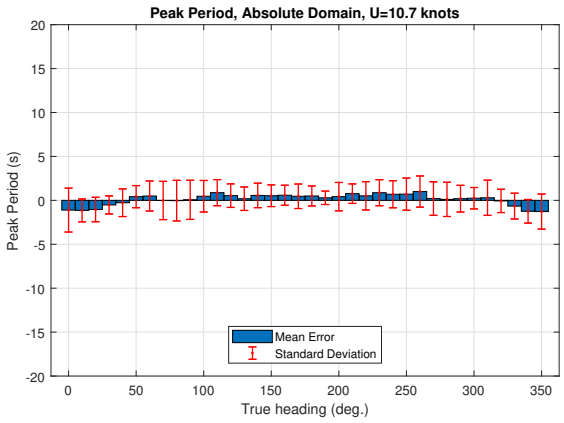

(a) Absolute domain, speed 10.7 knots

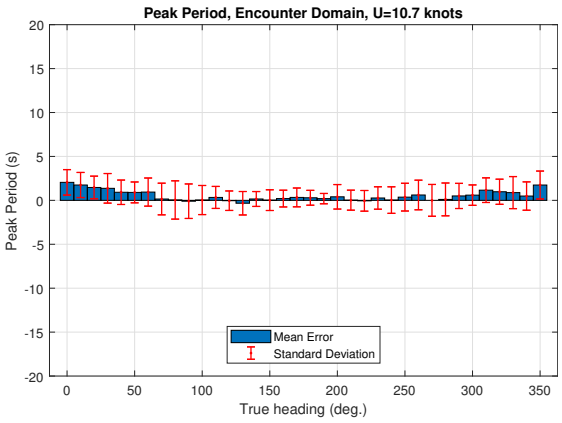

(b) Encounter domain, speed 10.7 knots

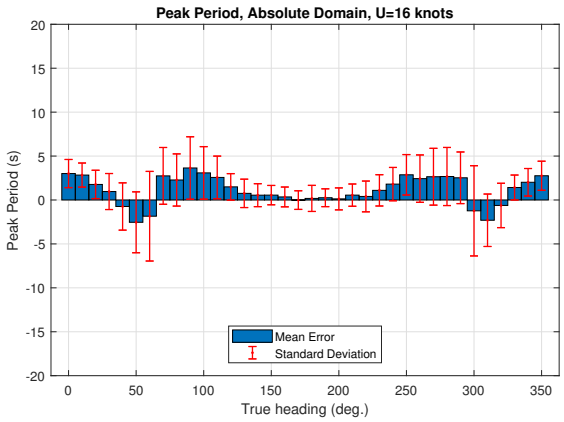

(c) Absolute domain, speed 16.0 knots

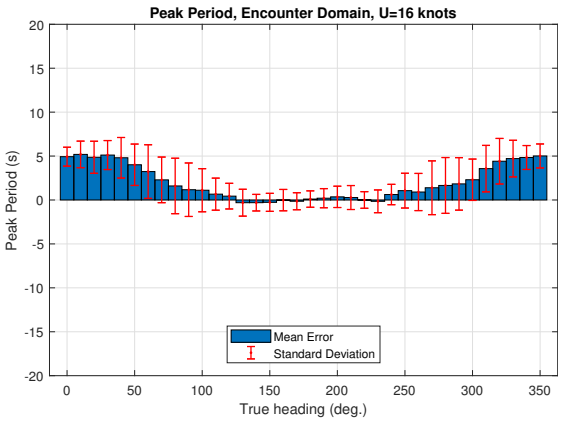

(d) Encounter domain, speed 16.0 knots

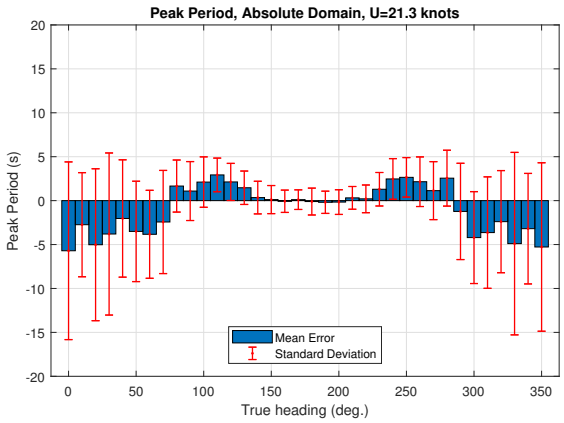

(e) Absolute domain, speed 21.3 knots

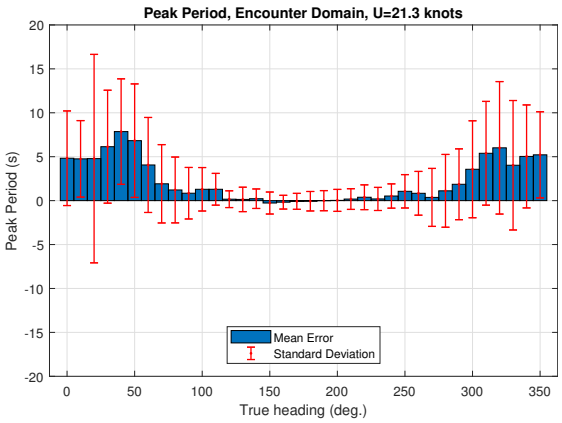

(f) Encounter domain, speed 21.3 knots

Figure 4.3: Comparison of the estimated peak period with the true peak period. To the left, the absolute domain comparison is displayed while on the right side the encounter domain comparison is shown. The blue bars represent the mean error between the true and estimated period for each true heading and the red line represent the standard deviation of the error values. The comparison does not include any information about the true peak period, it only shows the error values.

4.4 Zero-upcrossing Period

The results of the zero-upcrossing period is given in Fig. 4.4 and Table 4.5 which shows that the transformation between the two domains is performing well since it rapidly improves the results and lowering the mean error with roughly 70% for all speeds. The real improvements can be found in the headings [90 270] which can be explained by the improved estimation procedure proposed by Nielsen (2018). Furthermore, a very big deviation can be seen for the encounter domain in the following sea cases where the estimated T_z is roughly the double size of the true value.

Table 4.5: Summarized results for the zero-upcrossing period estimate including the mean error for all headings and the standard deviation for the same spectra. The results are divided in to the three different speeds, further, the mean error for all three vessel speeds i presented in the row named "All".

Speed [knots]:	**Mean error [s.]:**	**Standard deviation of the error:**
Encounter Domain		
10.7	5.84	2.74
16.0	5.74	3.50
21.3	4.90	3.13
All	5.50	3.16
Absolute Domain		
10.7	1.61	2.48
16.0	1.88	1.74
21.3	1.17	2.06
All	1.56	2.14

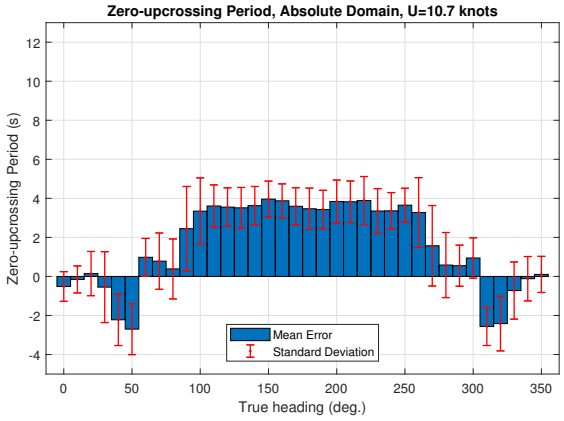

(a) Absolute domain, speed 10.7 knots

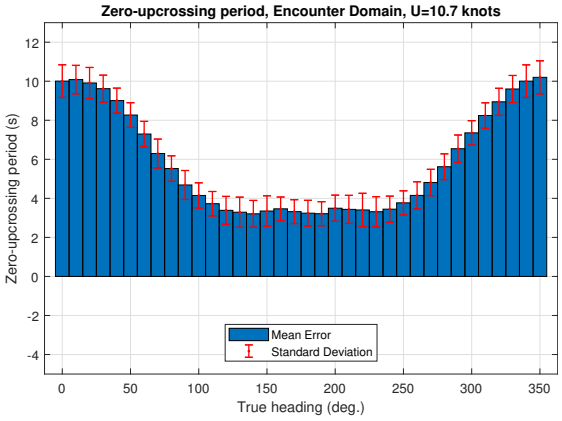

(b) Encounter domain, speed 10.7 knots

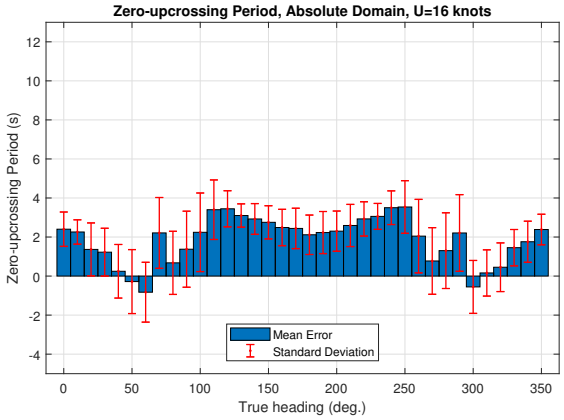

(c) Absolute domain, speed 16.0 knots

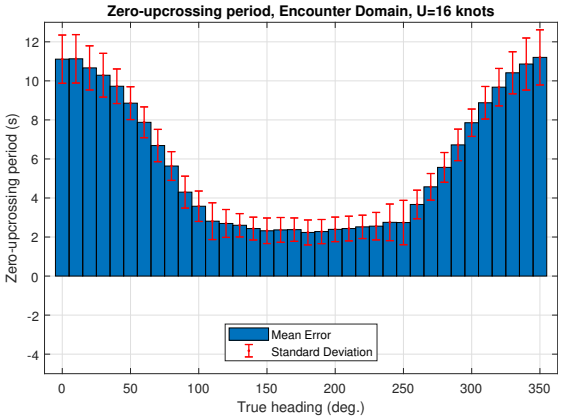

(d) Encounter domain, speed 16.0 knots

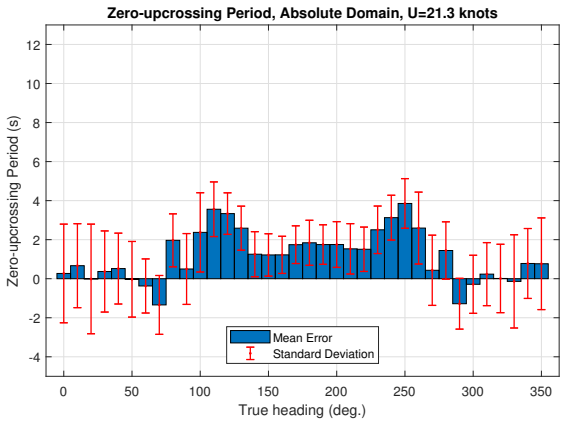

(e) Absolute domain, speed 21.3 knots

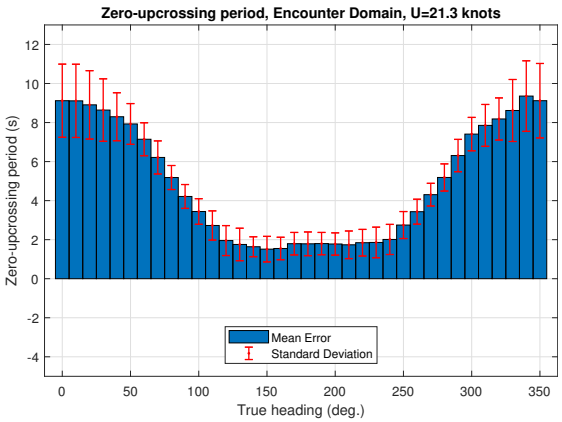

(f) Encounter domain, speed 21.3 knots

Figure 4.4: Comparison of the estimated zero-upcrossing period with the true peak period. To the left, the absolute domain comparison is displayed while on the right side the encounter domain comparison is shown. The blue bars represent the mean error between the true and estimated period for each true heading and the red line represent the standard deviation of the error values. Be aware that the comparison does not include any information about the true zero-upcrossing period, i.e. it only shows the error values.

4.5 Mean Period

The resulting mean period estimations seen in Fig. 4.5 and Table 4.6 is acting very similar to the zero-upcrossing period in Fig. 4.4 and Table 4.5 but with other values.

The error in encounter domain of the mean period in following seas is even higher than the zero upcrossing period in the same set up by comparing e.g. Figs. 4.4d and 4.5d.

Table 4.6: Summarized results for the mean period estimate including the mean error for all headings and the standard deviation for the same spectra. The results are divided in to the three different speeds, further, the mean error for all three vessel speeds i presented in the row named "All".

Speed [knots]:	**Mean error [s.]:**	**Standard deviation of the error:**
Encounter Domain		
10.7	4.50	2.58
16.0	5.69	5.02
21.3	5.85	6.10
All	5.34	4.83
Absolute Domain		
10.7	0.98	1.80
16.0	1.42	1.60
21.3	0.47	2.70
All	0.96	2.12

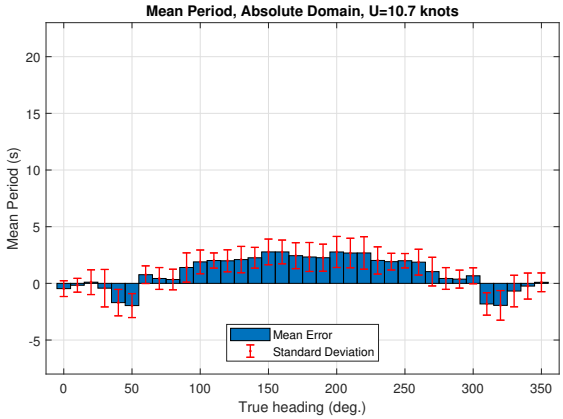

(a) Absolute domain, speed 10.7 knots

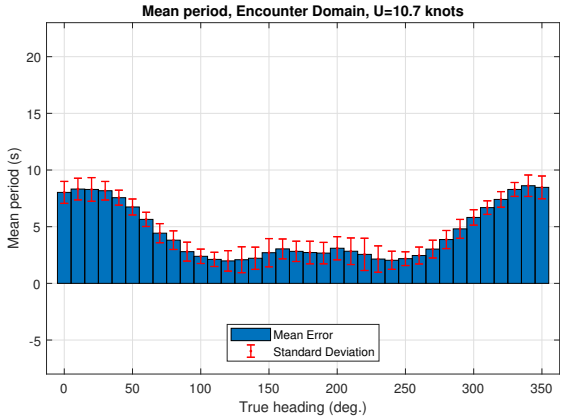

(b) Encounter domain, speed 10.7 knots

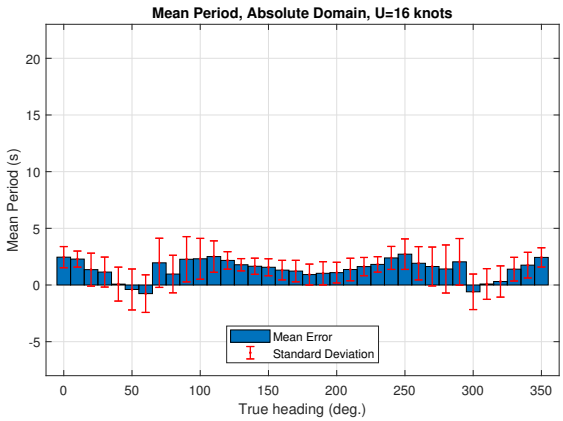

(c) Absolute domain, speed 16.0 knots

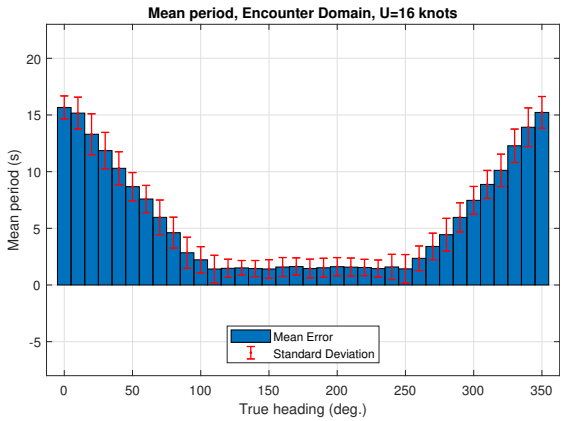

(d) Encounter domain, speed 16.0 knots

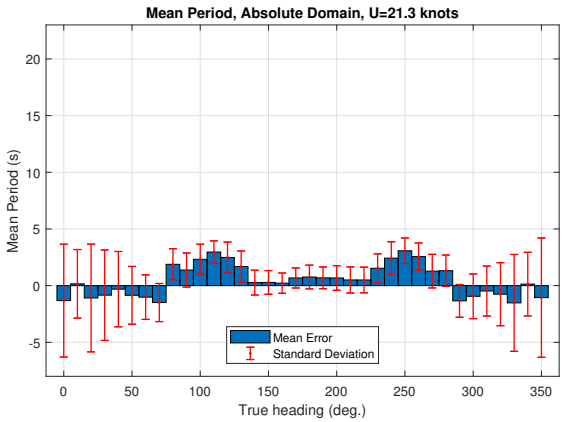

(e) Absolute domain, speed 21.3 knots

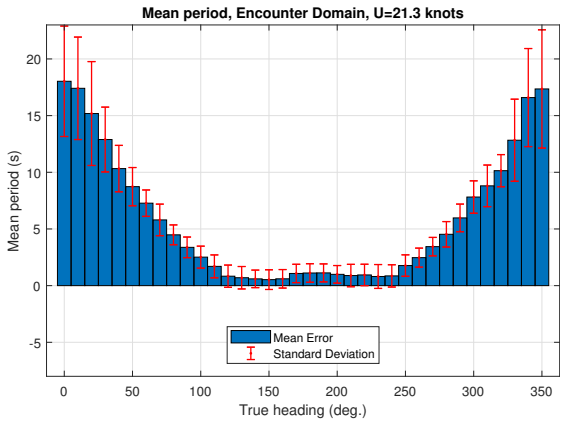

(f) Encounter domain, speed 21.3 knots

Figure 4.5: Comparison of the estimated mean period with the true peak period. To the left, the absolute domain comparison is displayed while on the right side the encounter domain comparison is shown. The blue bars represent the mean error between the true and estimated period for each true heading and the red line represent the standard deviation of the error values. Be aware that the comparison does not include any information about the true mean period, i.e. it only shows the error values.

This page is intentionally left blank.

5

Discussion

5.1 Captured Data

The main aim of this Master's thesis was to implement, verify and validate the sea state estimation procedure proposed by Nielsen et al. (2018) by the use of real, measured, vessel data from an in service container vessel operating regularly between north Europe and North America. The data from the vessel were made available from DNV GL and have been used in numerous researches, e.g. Storhaug and Heggelund (2008); Mao et al. (2010, 2012), however not on the exact same application as the sea state estimation but rather structural assessment such as vibrations and bending moments. Based on the fact that the vessel's data had been used numerous times before by research institutions, it seemed obvious that the captured data was reliable and that the start of the Master's thesis would mostly focus on re-structuring the available data to fit the pre-written MATLAB®programs, and partly get an insight on how the MATLAB®scripts was structured and built. Unfortunately it was realized, as reported in Chapter 3, that either the captured vessel data, the transfer functions or the sea state estimation was faulty. The faultiness was seen when applying the whole procedure on the data since it did not meet the expected results. It was not a matter of being close to the intended values, rather quite far from a satisfying result. Even though obstacles did appear early on, the aim was to implement the vessel data and the data itself was measured constantly over a 2-year period, indicating that there was a lot of available data.

At first, a thorough attempt to find captures that performed well with the procedure, which was a time-consuming practice since it needed much manual work. It had to be made sure that the capture was stationary in relation to speed, heading and sea state. It had to be ensured that the capture was on the open seas where the fully developed waves was occurring. Further, the time series motions was controlled for faulty periods and that there was transfer functions available for the speed. Then it could be determined whether the time series generated any satisfying results.

After ~100 different time series had been controlled accordingly, only very few of these showed any realistic results, it was realized that something was not correct. The captured data had been used before with good results which indicated that the data itself should be reliable. The transfer functions on the other hand had not been used widely before since vessel motion transfer functions are not used when the focus is on structural matters. Based on that, the transfer functions was investigated by the use of closed form expressions were a big deviation could be seen between the closed form expression transfer functions and the ones from Sesam, see Fig. 3.4. A new set of transfer functions was made available from DNV GL that hopefully could improve the results from the procedure. These new

transfer functions appeared to be a bit different from the original ones hence a similar test procedure was carried out with these new transfer functions without satisfying results.

With the known information at the moment decision were to be made which implied that the focus on the Master's thesis shifted slightly. One option was to put focus on the measured data and spend effort on trying to find a few cases which could generate good results using the procedure. That option could, if fortunate, give good insights on real measure data. However, there were no real guarantees in using the measured data since it was carried out by a third party and neither the author of this Master's thesis nor any of the supervisors was involved in capturing the data. Hence, it could be a troublesome work without any results in the end.

The other option was to discard the measured motions of the vessel and by simple means generate data sets based on the transfer functions itself. This option was desirable in numerous aspects, and to mention a few: the data could be controlled to 100%, it was easy to generate a wide set of time periods quick. Furthermore, the importance the transfer function was reduced since the same transfer functions were used to calculate the sea state as used when motions where generated, eliminating the problem of defected transfer functions compared to the present motions. Finally, it was of great purpose that by simulating own data, it was possible to go forward in the sea state estimation process and start to look at the outcome of reliable results.

Based on the discussion above together with the information in Chapter 3, it was decided to continue the project with own, simulated data, since it enabled a reasonable chance to carry out the project and meet the intended objectives instead to shifting focus of big data handling.

5.2 Simulated Data

Shifting focus to simulated data which was easier to control than the captured full-scale data, the anticipation was that the procedure would work smoothly and directly generate useful results. After all, very promising results have been published by Nielsen et al. (2018) using the same procedure as this Masters thesis applied on full scale data. At first, the results were promising, however, over time it came clear that the outcome was unreliable and the results was not to be trusted. The original procedure indicated that the secondary wave heading estimate, β_2, using the imaginary parts of the transfer functions, made the best estimate in all cases and after the first iteration, this statement was challenged since the secondary wave heading estimate, β_2, was the best choice in roughly 50% of the cases. Therefore, it was decided, as reported in Chapter 3, to generate 8100 different time series, each corresponding to 30 minutes of sea operations. These 8100 time periods was then used with the estimation procedure and the output could be statistically evaluated and the result is presented in Table 3.4, which only verified the first thoughts that the secondary heading estimate would not be the best estimate in all cases. By investigating the trends of the two wave heading estimates, β_0 and β_2, it was possible to build up simple rules that improved the wave heading drastically. These rules were developed for the specific vessel in and could most surly not be applied to another vessel without modifications. This has not been investigated yet and could be of future interest to look in to how general these rules could be made and if it is possible to find a compromise between level of accuracy and generalization.

In a similar manner, it was assumed in the estimation procedure proposed by Nielsen et al. (2018) that all responses were equally valid for every heading estimate and should be included in the significant wave height estimation. This assumption was not necessarily true in all cases and especially as shown in Chapter 3 that the significant wave height estimate using that approach was not accurate enough. Using the same 8100 time series, all 6 responses together with all possible combinations of them were evaluated based on the heading estimate as described in Chapter 3 which lead to increased level of accuracy of the estimate.

During the process, it was realized that the mean period and the zero-upcrossing period fluctuated and were in numerous cases unreliable. Therefore, it was decided to use a parameterized wave spectrum to lower the fluctuation of the values meaning that the parameterized wave spectrum was more controlled and behaved in a more accurate manner. This choice removed parts of the captured information and relied on statistics of how the waves behaved. It was not optimal but have been proven in this Master's thesis that it gave a more accurate and consistent estimate than using the information form the estimated wave spectrum.

When introducing the simulated data, it was possible to use a statistical approach when evaluating the procedure and nevertheless in the improvements since the data could be controlled in every way giving a wide set of data covering the whole operational aspect. Simulated data is not the same as measured data which was experienced in this Master's thesis work were the real life measured data came with a lot of uncertainties.

5.3 Results

The final results presented in this report indicated that the procedure proposed by Nielsen et al. (2018) is promising since it enabled a good estimate on especially the heading estimate and the significant wave height. The results showed that the error of the wave heading estimate was low, and was decreased even further for lower vessel speeds. Having an absolute mean error of just above 10 deg. for a speed of 11 knots is to be consider as successful, especially since the step size of the estimation was set to 5 deg. It was possible to identify a higher deviation from the true value when speed was increased, however it should be noted that today it is very rare that vessels travel with speeds of 20 knots due to the economic gain of slow steaming. The intention was to have a procedure that estimated the sea state well in higher speeds as well. Today the most urgent is to find a procedure that applies for lower speeds which would result in a wider audience that could benefit from the sea state estimation.

The results indicating that the encounter frequency periods, especially the zero-upcrossing and the mean period, is unreliable and this is something that has to be further investigated before it can be stated as 100% reliable. It is important to keep in mind the order of interest in between the different wave parameters. In the intended application, as an on board system helping the crew in operational aspects or enable autonomous operations, the important parameters is the wave heading and the wave heights since these are the ones with big consequences in either structural damages or cargo loss while the periods are not of the same importance. The periods are not unimportant, however if 2 out of the three (wave heading, significant wave height and period) can be chosen, the most probable answer would be wave heading and height.

With the results presented in this report it is possible to state that the first aspect of the procedure which is the significant wave height and the wave heading is satisfying while the periods, and also the transformation is a still unsure to what extent it can be relied on. The wave height and heading is not affected by the unreliable transformation however the periods are. The peak periods in this report are estimated in a satisfying manner and also transformed in to the absolute domain with reliable results. The two other period estimates are not satisfying in the encounter domain while it is much better in the absolute domain. It is not determined where this error occurs since the absolute domain is somewhat based on the values in the encounter domain. It could be that the modification using the parameterized wave spectrum enables this change, apart from that it is not possible to find a logical reason for the deviation. Therefore it is something that must be further elaborated on.

It would be very interesting, in a commercial aspect, to investigate how well the rules developed based on simulated data performs on full scale data. If the same rules are valid for full scale data then it would for example be possible to generate these rules before the system is installed on board a vessel which would enable the use of the procedure in reality without the need of full scale data in the vessel specific modification process.

During this Master's thesis, parallel research have been carried out at DTU regarding the proposed sea state estimation technique by Nielsen et al. (2018). Indications have been presented that the increment size, h, in Eq. (2.19) can have a significant impact on the results. This was not known in the early stages of this Master's thesis and have therefore not been possible to incorporate in the results presented but it would be of very high interest to further investigate the impact of the increment size.

5.4 Limitations

In the beginning of this Master's thesis, objectives were defined which can be found in Section 1.3.1 and these were the aim for the final product. Anyhow, these objectives had to be revised due to numerous, unexpected, obstacles during the process. The decision of continue the project with simulated data was taken in project week 10 out of 24 i.e. a lot of time was spent on trouble shooting both the MATLAB®programs which implemented the proposed sea state estimation procedure but also the data itself. When the decision was taken to use simulated data, there were new obstacles in faulty results. Altogether, it limited the project from most of the objectives. Writing a PYTHON®program that would have implemented the procedure was impossible to have time for. Furthermore, the objectives regarding full scale data had to be changed for simulated data instead. Anyhow, the learning outcome of the project is very high even though the intended objectives was not full filled. Instead of the originally proposed objectives a thorough troubleshooting has been carried out which is important itself, but also by introducing the captured data in this troubleshooting process made it very realistic compared to the professional careers. In real projects it is unusual that all data is verified and all procedure is modified for the specific data etc. which implies that in all project, much time is spent on trouble shooting.

Further, it is important to mention that the results achieved in this project is only valid for the specific vessel and the simulated data. To draw more general conclusions about the proposed procedure by Nielsen et al. (2018) a wider set of vessels would be needed in the investigation together with measured vessel data instead of simulated data since

even if you add noise to the simulated data it is hard, and unrealistic, to mimic the ocean waves and the interaction with the vessel in a correct way. The reality is always more complicated due to different loading conditions, wind and current loads, assumptions etc. together with the operational parameter based on the crews' choices.

5.5 Ethical Aspects

The discussion about the ethical aspect of improving the sea state estimation in the long time-horizon is of importance. A reliable sea state estimation could improve the working conditions on board a vessel by optimizing the routes and avoiding severe weather conditions. Anyhow, by achieving a high accuracy of the estimate, it can enable more autonomous operations meaning that personnel on board could be loosing their employment. The affect of introducing autonomous systems in the maritime market is not yet fully known and therefore this Master's thesis will not further make any comments more than the fact that there is a demand for well working SSE procedures.

This page is intentionally left blank.

6

Conclusion

6.1 Results

The aim of the present research was to examine how well the brute force sea state estimation procedure proposed by Nielsen et al. (2018) performs on full-scale measured motion data from an in-service container vessel. The study showed that the received measured data from a 2800-TEU container vessel was most surly defected since the measurements were not consistent. After a thorough troubleshooting session, it could be concluded that the present transfer functions were most certainly correct even though it did not correlate exactly to the closed form expression transfer functions. Based on that finding, it could also be concluded that the measured motion data or wave data was defected. Simulated waves and motions based on the present transferfunctions were used to overcome the problem of erroneous data.

The simulated data enabled a big data analysis of which it is possible to draw the conclusion that the general approach proposed by Nielsen et al. (2018) is not accurate for this vessel. It has been shown that the estimate of the wave encounter angle is deviating from the true value which implicit indicates that the other wave parameter estimates are faulty since the wave parameters are calculated with basis in the wave encounter angle.

It can be concluded that the procedure proposed by Nielsen et al. (2018) can be improved drastically by the use of statistics on a big set of time series. By using the knowledge from 8100 time series it is possible to achieve a accuracy for the wave heading estimate that can be seen as sufficient for the operational aspect of the sea state estimation. Furthermore, it can be seen that the significant wave height estimate can be improved and reach a satisfying level of accuracy by using the knowledge from these 8100 time series and based on those develop vessel specific rules.

Finally, the accuracy of the estimation of the peak period has been shown to be relatively high while the accuracy for the mean period and zero-upcrossing period is deviating more from the true value. Based ion this, it can not be verified that the procedure estimates the periods correct and will have to be further investigated.

To summarize, the proposed procedure for sea state estimation using a brute force approach by Nielsen et al. (2018) have showed promising results on certain parameters for simulated data when vessel specific rules are applied. The complete procedure can not be fully confirmed by this study neither can it be rejected meaning that further studies will be needed before a proper and fair conclusion can be drawn regarding its accuracy.

6.2 Future Work

To continue develop the sea state estimation procedures used in this thesis that was originally proposed by Nielsen et al. (2018) future work is needed. These points will be explained in short:

- **More ships:** Include a bigger variety of vessels. This report has shown that the procedure has to be modified for the vessel under investigation, therefore a wider verity of vessels has to be investigated for possible general rules.
- **Measured data:** Include real life measured data from in service vessels to verify that the procedure works even for non-simulated data.
- **Open source software:** Develop an open source software that has implemented the procedure so it can be used in the reality. Also take in to account the operational aspects such as real-time information on a vessel.
- **Periods:** Verify the period estimates, especially the mean- and zero-upcrossing periods.
- **Linking simulations with measured data:** Investigate if the rules generated with basis on the simulated data also is applicable for measured data.

Bibliography

Poul Andersen. Programme structure - nordic master in maritime engineering. `http://www.nor-mar-eng.org/education/programme_structure`, Aug 2015. [Online; accessed 7-February-2018].

Rameswar Bhattacharyya. *Dynamics of marine vehicles*. John Wiley & Sons Inc, 1978.

Harry B Bingham. *Supplemental Lecture Note for: "Wave Loads on Ships and Offshore Structures" - Course no. 41222*. Technical University of Denmark, Section of Coastal, Structural and Maritime Engineering, November 2017.

AV Boukhanovsky and C Guedes Soares. Modelling of multipeaked directional wave spectra. *Applied Ocean Research*, 31(2):132–141, 2009.

Charles L Bretschneider. Wave variability and wave spectra for wind-generated gravity waves. Technical report, CORPS OF ENGINEERS WASHINGTON DC BEACH EROSION BOARD, 1959.

Astrid H Brodtkorb, Ulrik D Nielsen, and Asgeir J Sørensen. Sea state estimation using vessel response in dynamic positioning. *Applied Ocean Research*, 70:76–86, 2018.

Waveship user's manual. DNV, Det Norske Veritas Seasam AS, Høvik Norway, 1 edition, October 1993. Report No.: 93-7080.

Odd Faltinsen. *Sea loads on ships and offshore structures*, volume 1. Cambridge university press, 1993.

Astrid H. Brodtkorb, Ulrik D. Nielsen, and Asgeir J. Sørensen. Online wave estimation using vessel motion measurements. *IFAC-PapersOnLine*, 2018. ISSN 2405-8963.

Toshio Iseki and Kohei Ohtsu. Bayesian estimation of directional wave spectra based on ship motions. *Control Engineering Practice*, 8(2):215–219, 2000.

Toshio Iseki, Daisuke Terada, et al. Bayesian estimation of directional wave spectra for ship guidance system. In *The Eleventh International Offshore and Polar Engineering Conference*. International Society of Offshore and Polar Engineers, 2001.

Jørgen Juncher Jensen, Alaa E Mansour, and Anders Smærup Olsen. Estimation of ship motions using closed-form expressions. *Ocean Engineering*, 31(1):61–85, 2004.

Martin Ludvigsen and Asgeir J. Sørensen. Towards integrated autonomous underwater operations for ocean mapping and monitoring. *Annual Reviews in Control*, 42:145 – 157, 2016. ISSN 1367-5788. doi: https://doi.org/10.1016/j.arcontrol.2016.09.013.

Wengang Mao, Zhiyuan Li, Thomas Galtier, Jonas W Ringsberg, and Igor Rychlik. Estimation of wave loading induced fatigue accumulation and extreme response of

a container ship in severe seas. In *ASME 2010 29th International Conference on Ocean, Offshore and Arctic Engineering*, pages 133–141. American Society of Mechanical Engineers, 2010.

Wengang Mao, Zhiyuan Li, Jonas W Ringsberg, and Igor Rychlik. Application of a ship-routing fatigue model to case studies of 2800 teu and 4400 teu container vessels. *Proceedings of the Institution of Mechanical Engineers, Part M: Journal of Engineering for the Maritime Environment*, 226(3):222–234, 2012.

Wavex 5 technical handbooks, volume 1 of 4. Miros, 1 edition, October 2011. Report No.: PR-002/TH/001.

Najmeh Montazeri, Ulrik Dam Nielsen, and Jørgen Juncher Jensen. Estimation of wind sea and swell using shipboard measurements–a refined parametric modelling approach. *Applied Ocean Research*, 54:73–86, 2016a.

Najmeh Montazeri, Ulrik Dam Nielsen, and Jørgen Juncher Jensen. *Estimation of waves and ship responses using onboard measurements*. DTU Mechanical Engineering, 2016b.

Ulrik D Nielsen. Transformation of a wave energy spectrum from encounter to absolute domain when observing from an advancing ship. *Applied Ocean Research*, 69:160–172, 2017a.

Ulrik D Nielsen. A refining technique for ship motion-based sea state estimation. In *Proc. 6th WMTC*, Shanghai, China, 2018.

Ulrik D Nielsen and David C Stredulinsky. Sea state estimation from an advancing ship–a comparative study using sea trial data. *Applied Ocean Research*, 34:33–44, 2012.

Ulrik D Nielsen, Ingrid Marie V Andersen, and Jos Koning. Comparisons of means for estimating sea states from an advancing large container ship. *Proceedings of 12th PRADS*, 2013.

Ulrik D Nielsen, Roberto Galeazzi, and Astrid H Brodtkorb. Evaluation of shipboard wave estimation techniques through model-scale experiments. In *OCEANS 2016-Shanghai*, pages 1–8. IEEE, 2016.

Ulrik D Nielsen, Astrid H Brodtkorb, and Asgeir J Sørensen. A brute-force spectral approach for wave estimation using measured vessel motions. *Marine Structures*, 60: 101–121, 2018.

Ulrik Dam Nielsen. Estimation of directional wave spectra from measured ship responses. *Maritime Transportation and Exploitation of Ocean and Coastal Resources*, pages 1103–1112, 2005.

Ulrik Dam Nielsen. Estimations of on-site directional wave spectra from measured ship responses. *Marine Structures*, 19(1):33–69, 2006.

Ulrik Dam Nielsen. *Ship Operations - Engineering Analyses and Guidance, Course material*. Technical University of Denmark, Section of Coastal, Structural and Maritime Engineering, January 2010.

Ulrik Dam Nielsen. A concise account of techniques available for shipboard sea state estimation. *Ocean Engineering*, 129:352–362, 2017b.

Michel K Ochi. *Applied probability and stochastic processes: In Engineering and Physical Sciences*, volume 226. Wiley-Interscience, 1990.

R Pascoal and C Guedes Soares. Non-parametric wave spectral estimation using vessel motions. *Applied Ocean Research*, 30(1):46–53, 2008.

R Pascoal, C Guedes Soares, and AJ Sørensen. Ocean wave spectral estimation using vessel wave frequency motions. *Journal of Offshore Mechanics and Arctic Engineering*, 129(2):90–96, 2007.

Rolls-Royce plc. Autonomous ships - the next step. `http://www.rolls-royce.com/~/media/Files/R/Rolls-Royce/documents/customers/marine/ship-intel/rr-ship-intel-aawa-8pg.pdf`, 2016. [Online; accessed 6-February-2018].

Robert Rylander and Yemao Man. Autonomous safety on vessels - an international overview and trends within the transport sector. Technical report, Lighthouse, 2016.

Nils Salvesen, EO Tuck, and Odd Faltinsen. Ship motions and sea loads. *Trans. SNAME*, 78(8):250–287, 1970.

Alexandre N Simos, João V Sparano, Eduardo A Tannuri, Vinícius LF Matos, et al. Directional wave spectrum estimation based on a vessel 1st order motions: field results. In *The Seventeenth International Offshore and Polar Engineering Conference*. International Society of Offshore and Polar Engineers, 2007.

G Storhaug and SE Heggelund. Measurements of wave induced vibrations and fatigue loading onboard two container vessels operating in harsh wave environment. *Transactions of RINA, Design & Operation of Container Vessels, London*, 2008.

Eduardo A Tannuri, Joao V Sparano, Alexandre N Simos, and José J Da Cruz. Estimating directional wave spectrum based on stationary ship motion measurements. *Applied Ocean Research*, 25(5):243–261, 2003.

United Nations General Assembly. resolution 70/1, transforming our world: the 2030 agenda for sustainable development , a/res/70/1. `http://www.un.org/ga/search/view_doc.asp?symbol=A/RES/70/1&Lang=E`, September 2015. [Online Accessed: 29 May 2018].

WAFO-group. *WAFO - A Matlab Toolbox for Analysis of Random Waves and Loads - A Tutorial*. Math. Stat., Center for Math. Sci., Lund Univ., Lund, Sweden, 2017.

Wikipedia. Gamma function — wikipedia, the free encyclopedia. `https://en.wikipedia.org/w/index.php?title=Gamma_function&oldid=826893339`, 2018a. [Online; accessed 26-February-2018].

Wikipedia. Mv yara birkeland — wikipedia, the free encyclopedia. `https://en.wikipedia.org/w/index.php?title=MV_Yara_Birkeland&oldid=822492776`, 2018b. [Online; accessed 6-February-2018].

This page is intentionally left blank.

A

Vessel Information

A.1 Main Particulars

Due to ethical aspects and the agreement with DNV GL, the full vessel information is not public to ensure the anonymous of the vessel owner, charter, crew etc. The information available for the vessel can be seen in Table A.1 below.

Max. TEU	2800
L_{PP} (m)	232
L_{OA} (m)	245
Beam, moulded (m)	32.2
Depth, moulded (m)	19.0
Scantling/design draught (m)	10.78
Scantling block coefficient (-)	0.685
Deadweight (tonnes)	40900
Typical transit draught (m)	9.5
Typical transit stern trim (m)	0.5-1.0
Speed at design draught (kn)	21.3
Engine Power MCR at 104.7/93 rpm (kW)	25786
Vertical 2-node frequency (Hz)	0.76
Built	1998

Table A.1: Main particulars of the DNV GL-classed vessel used in the project (Storhaug and Heggelund, 2008)

This page is intentionally left blank.

B

Closed Form Expression Transfer Functions

B.1 Heave and Pitch Transfer Functions

In the following section of this paper, the formulas for the closed form calculation of ships in motion are gathered from (Jensen et al., 2004).

We want to find the pitch and heave response and they are given by Eqs. (B.1) and (B.2).

$$\Phi_w = \eta F \tag{B.1}$$

$$\Phi_\theta = \eta G \tag{B.2}$$

To calculate these, a couple of formulas that is based on the given input variables is needed. These will be stated below. For further explanation of the formulas, see (Jensen et al., 2004).

$$F = \kappa f \frac{2}{k_e L} \sin\left(\frac{k_e L}{2}\right) \tag{B.3}$$

$$G = \kappa f \frac{24}{(k_e L)^2 L}\left[\sin\left(\frac{k_e L}{2}\right) - \frac{k_e L}{2} cos\left(\frac{k_e L}{2}\right)\right] \tag{B.4}$$

$$k_e = |k\cos(\beta)| \tag{B.5}$$

$$f = \sqrt{(1-kT)^2 + \left(\frac{A^2}{kB\alpha^3}\right)^2} \tag{B.6}$$

$$\kappa = \exp(-kT) \tag{B.7}$$

$$\alpha = 1 - Fn\sqrt{kL}\cos(\beta) \tag{B.8}$$

$$A = 2\sin\left(\frac{\overline{\omega}^2 B}{2g}\right)\exp\left(-\frac{\overline{\omega}^2 T}{g}\right) = 2\sin\left(\frac{1}{2}kB\alpha^2\right)\exp(-kT\alpha^2) \tag{B.9}$$

$$k = \omega^2/g \tag{B.10}$$

$$\overline{\omega} = \omega - kV\cos(\beta) = \alpha\omega \tag{B.11}$$

$$\eta = \left(\sqrt{(1 - 2kT\alpha^2)^2 + \left(\frac{A^2}{kB\alpha^2}\right)^2} \right)^{-1} \tag{B.12}$$

It can be seen from equations above that the only input needed to carry out this closed form expression is in fact L,B, T, β, Fn, ω, V, g. The only ones not given is Fn, ω and g. The calculation can be assumed to regard a vessel on earth hence g (gravitational constant) will be $9.81[m/s^2]$. ω is a set of frequencies that are based on the discretized frequencies f_0. Fn stands for the Froude number which is defined as $Fn = \frac{V}{\sqrt{gL}}$.

B.2 Roll Transfer Functions

The closed form expressions for the roll motion transfer functions is gathered from Jensen et al. (2004) and a summary of the procedure is given below, for every detail, please see the paper.

By assuming that the roll motion is decoupled from the other transverse motions, the roll motion in regular waves can be given according to Eq. (B.13).

$$\left(\frac{T_{\mathrm{N}}}{2\pi}\right)^2 C_{44}\ddot{\varphi} + B_{44}\dot{\varphi} + C_{44}\varphi = M \tag{B.13}$$

where φ is the roll angle, T_{N} is the natural roll period and are parameters that is taken directly from the vessel input information. $C_{44} = g\Delta GM_{\mathrm{T}}$ is the restoring moment coefficient and Δ represent the displacement while GM_{T} is the transverse metacentric height. B_{44} is the damping coefficient which can be calculated using Eq. (B.28). Finally, M is the roll excitation moment which is calculated using the Haskind relation according to Eq. (B.35).

By solving Eq. (B.13), you get the transfer function for roll according to Eq. (B.14) where $\overline{\omega}$ is the encounter frequency and $|M|$ is the amplitude of the excitation moment.

$$\Phi_\varphi = \frac{|M|}{\left(\left[-\overline{\omega}^2 \left(T_{\mathrm{N}}/2\pi\right)^2 + 1 \right]^2 C_{44}^2 + \overline{\omega}^2 B_{44}^2 \right)^{1/2}} \tag{B.14}$$

In the simplified calculations carried out here, the ship is assumed to be made out of two prismatic beams that both have the same draft T but with different breadths B_0 and B_1 and cross sectional areas A_0 and A_1, please see Fig. B.1. To decide the ratio between the two breadths, the real water plane area C_{WP} is used and then the model vessel should have the same water plane area giving Eqs. (B.15) and (B.16).

$$C_{\mathrm{WP}} = \frac{B_0 L(\delta + \gamma(1 - \delta))}{LB_0} \tag{B.15}$$

$$\gamma \equiv \frac{B_1}{B_0} = \frac{C_{\mathrm{WP}} - \delta}{1 - \delta} \tag{B.16}$$

Further, the area A_0 is chosen so the block coefficient is the same for the model and the ship, giving Eq. (B.18)

$$C_b = \frac{L(A_0\delta + A_1(1-\delta))}{LB_0T} = \frac{A_0(\delta + \gamma(1-\delta))}{B_0T} \tag{B.17}$$

$$A_0 = \frac{C_bB_0T}{\delta + \gamma(1-\delta)} \qquad \text{and} \qquad A_1 = \gamma A_0 \tag{B.18}$$

The sectional damping coefficient will be represented by a simplified experimental expression achieved from parametric curve fitting to different shapes etc. The function is then described by Eq. (B.19) where A is the cross sectional area of the submerged part and a, b and d is described by Eqs. (B.20) to (B.22) which is valid for $3 \leq B/T \leq 6$.

$$\frac{b_44}{\rho AB^2}\sqrt{\frac{B}{2g}} = a(B/T)\exp\left(b\,(B/T)\,\overline{\omega}^{-1.3}\right)\overline{\omega}^{d(B/T)} \tag{B.19}$$

$$a(B/T) = 0.256B/T - 0.286 \tag{B.20}$$

$$b(B/T) = -0.11B/T - 2.55 \tag{B.21}$$

$$d(B/T) = 0.033B/T - 1.419 \tag{B.22}$$

For vessels with fuller lines, i.e. $1 \leq B/T \leq 3$, the expressions in Eqs. (B.23) to (B.25) is valid.

$$a(B/T) = -3.94B/T + 13.69 \tag{B.23}$$

$$b(B/T) = -2.12B/T - 1.89 \tag{B.24}$$

$$d(B/T) = 1.16B/T - 7.97 \tag{B.25}$$

The total hydrodynamic damping coefficient B_{44} is thereby given as Eq. (B.26) where $\kappa^2 = b_{44,1}/b_{44,0}$ is the ratio of the sectional damping coefficient for the two beams described

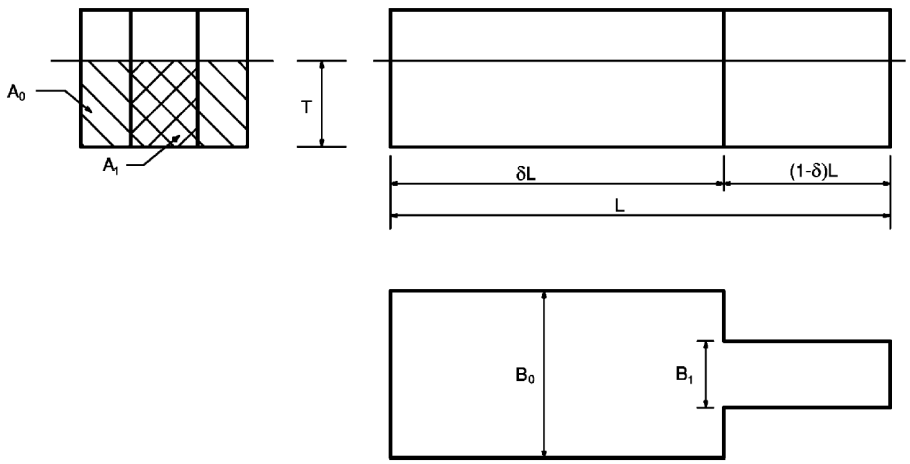

Figure B.1: Schematic view on the simplified vessel model used in the closed form expression of the roll motion transfer functions. (Jensen et al., 2004, page 73)

in Fig. B.1.

$$B_{44} = Lb_{44,0}\left[\delta + \kappa^2\left(1-\delta\right)\right] \tag{B.26}$$

Eq. (B.26) only takes the inviscid damping in to account, and to include the viscous effect, a percentage is added to the critical damping, B_{44}^*, which then results in a total damping according to Eq. (B.28) where μ is the specified percentage of the critical damping.

$$B_{44}^* = \frac{C_{44}T_N}{\pi} \tag{B.27}$$

$$B_{44}^{tot} = B_{44} + \mu B_{44}^* \tag{B.28}$$

By using the Haskind relation, the sectional excitation moment m can be described by the use of the sectional hydrodynamic damping b_{44}. The sectional exciting moment in 2-dimensions can be described by Eq. (B.29) where ϕ_0 is the potential for the incoming waves with unit amplitude given by Eq. (B.30) where ϕ_4 is the potential for the radiated waves for forced roll motions. The radiated waves potential can be assumed to be equal to the asymptotic potential far from the body which enables to define φ_4 as Eq. (B.31) where $P_4^{\pm}$ depends on the wave number and the body shape which in cases of symmetric bodies around the x-axis becomes $P_4^+ = -P_4^- \cdot P_4^+$ which then is related to the hydrodynamic damping in Eq. (B.32)

$$m(x) = i\omega\rho\exp(i\omega t)\int_{-\infty}^{0}\left[\varphi_0\frac{\partial\varphi_4}{\partial y} - \varphi_4\frac{\partial\varphi_0}{\partial y}\right]_{y=-\infty}^{y=\infty} dz \tag{B.29}$$

$$\varphi_0 = \frac{g}{\omega}\exp\left(kz - ixk\cos\beta + iyk\sin\beta\right) \tag{B.30}$$

$$\varphi_4 = P_4^{\pm}\exp\left(kz - i|yk\sin\beta|\right) \qquad \text{for } y \to \pm\infty \tag{B.31}$$

$$b_{44} = \rho\omega\left|P_4^+\right|^2 \tag{B.32}$$

By carrying out the integration of Eq. (B.29) you get the following expression for the sectional excitation moment.

$$\begin{aligned} m(x) &= i\omega\rho\exp\left(i\omega t\right)\frac{g}{\omega}\exp\left(-ixk\cos\beta\right)\int_{-\infty}^{0}\exp\left(2kz\right)dz\left[P_4^+\left(-ik\sin\beta - ik\sin\beta\right)\right] \\ &= \rho g\sin\beta P_4^+\exp\left(-ixk\cos\beta\right)\exp\left(i\omega t\right) \\ &= \sin\beta\sqrt{\frac{\rho g^2}{\omega}b_{44}}\exp\left(-ixk\cos\beta\right)\exp\left(i\omega t\right) \end{aligned} \tag{B.33}$$

By integrating Eq. (B.33) over the length of the vessel gives the total excitation moment M, given in Eq. (B.34). Taking the real part of Eq. (B.29) gives the amplitude, $|M|$, that

should be used in Eq. (B.14), the result is given in Eq. (B.35).

$$
\begin{aligned}
M =& \sin\beta\sqrt{\frac{\rho g^2}{\omega}}e^{i\omega t}\left\{\int_0^{\delta L}\sqrt{b_{44,0}}e^{ixk\cos\beta}+\int_{\delta L}^{L}\sqrt{b_{44,1}}e^{-ixk\cos\beta}dx\right\}\\
=& \sin\beta\sqrt{\frac{\rho g^2}{\omega}}\frac{1}{k\cos\beta}e^{i\omega t}\times\left\{\sqrt{b_{44,0}}\sin(\delta LK\cos\beta)\right.\\
&+2\sqrt{b_{44,1}}\cos(0.5(1+\delta)Lk\cos\beta)\sin(0.5(1-\delta)Lk\cos\beta)\\
&+i\Big[\sqrt{b_{44,0}}\{\cos(\delta Lk\cos\beta)-1\}+2\sqrt{b_{44,1}}\sin(0.5(1+\delta)Lk\cos\beta)\\
&\left.\times\sin(0.5(\delta-1)Lk\cos\beta\Big]\right\}
\end{aligned}
\tag{B.34}
$$

$$
\begin{aligned}
\Re(M) =& |M|\cos(\omega t+\epsilon)=|\sin\beta|\sqrt{\frac{\rho g^2}{\omega}}\frac{2}{k_e}\\
&\times\sqrt{b_{44,0}}\{\sin^2(0.5\delta Lk_e)+\kappa^2\sin^2(0.5(1-\delta)Lk_e)\\
&+2\kappa\sin(0.5\delta Lk_e)\sin(0.5(1-\delta)Lk_e)\cos 0.5Lk_e)\}^{1/2}\cos(\omega t+\epsilon)
\end{aligned}
\tag{B.35}
$$

This page is intentionally left blank.

C

Results

This chapter consist of results that is not of the same importance in the matter of this master thesis compared to the ones presented in Chapter 4. Anyhow, these results could be of general interest and for that reason the results have been presented in many different coalitions. All figures are divided into sub-values, so it can be possible to see how different parameters influence the outcome results. The figures will be presented without any detailed information or discussion and are included for the readers own interpretation and interest.

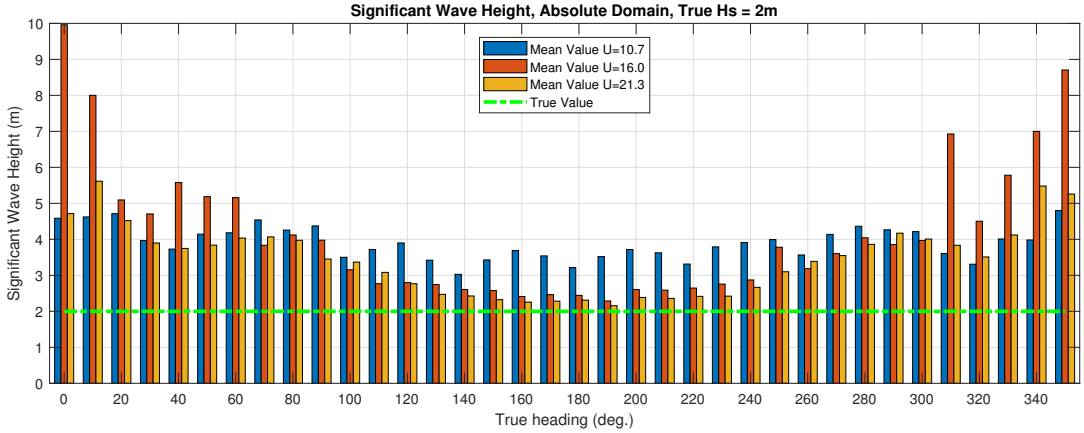

(a) True significant wave height is 2 m

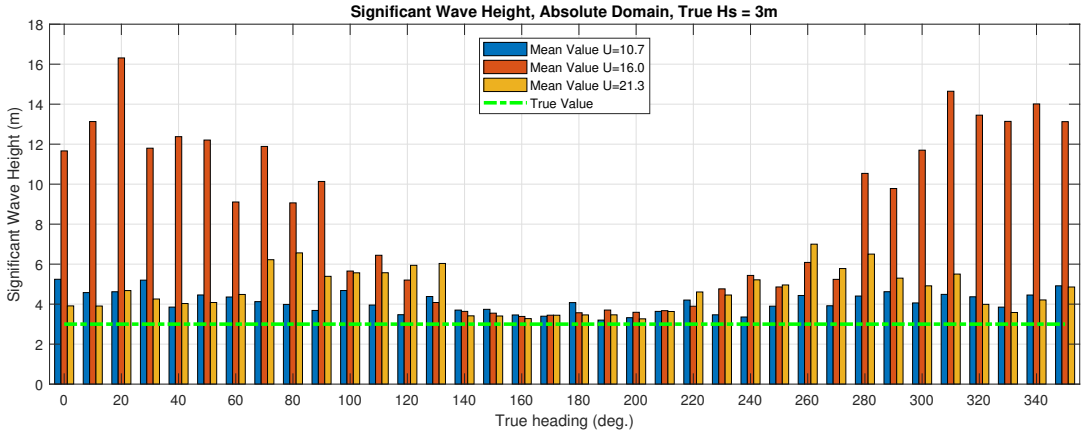

(b) True significant wave height is 3 m

Figure C.1: Estimated significant wave height in absolute domain for each true significant wave height. Each plot is divided by vessel speed

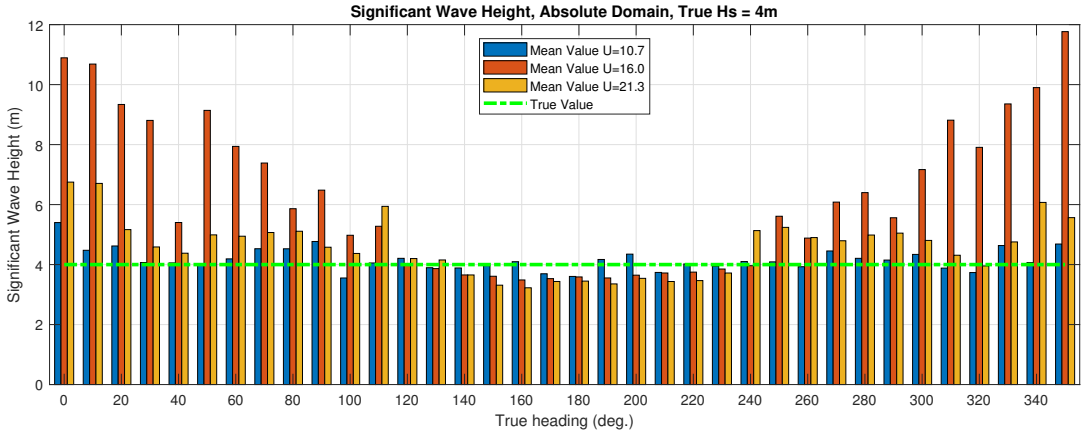

(a) True significant wave height is 4 m

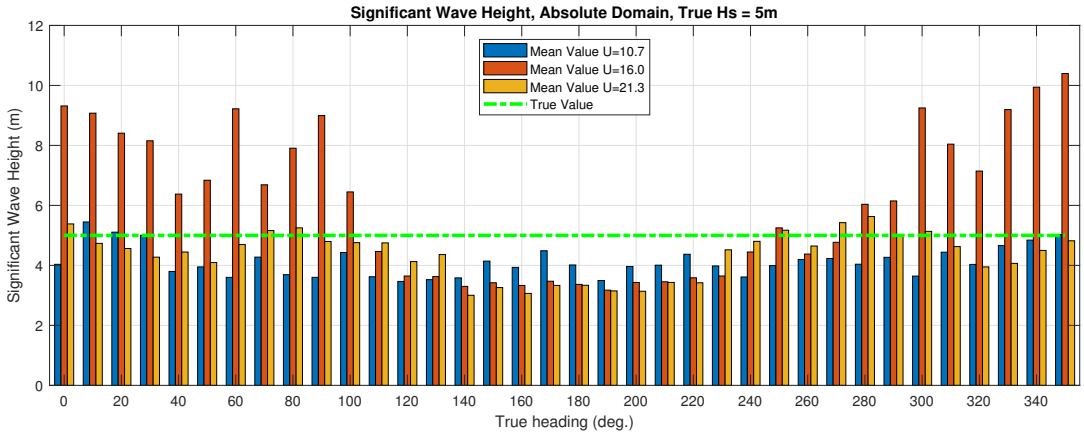

(b) True significant wave height is 5 m

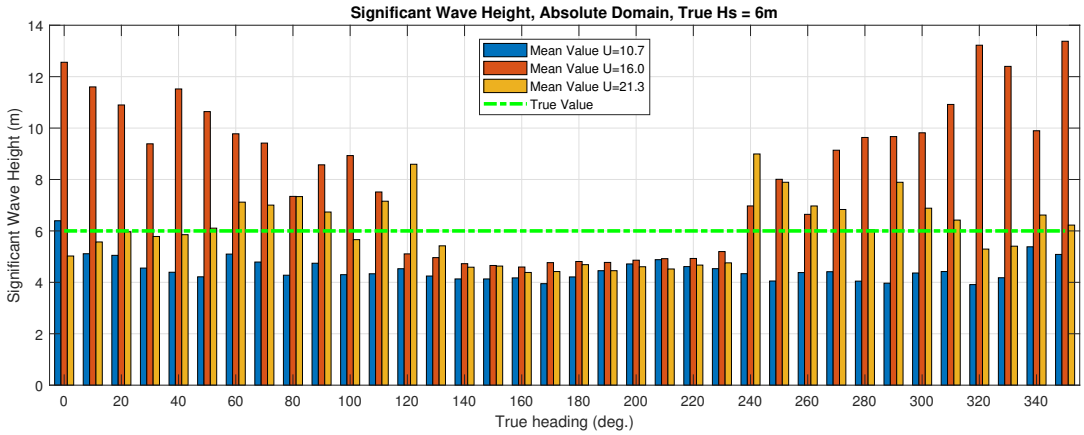

(c) True significant wave height is 6 m

Figure C.2: Estimated significant wave height in absolute domain for each true significant wave height. Each plot is divided by vessel speed

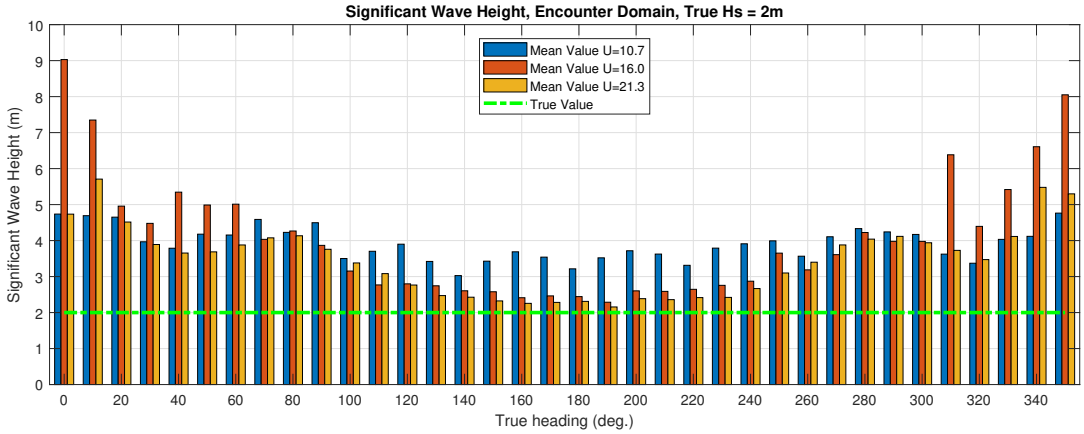

(a) True significant wave height is 2 m

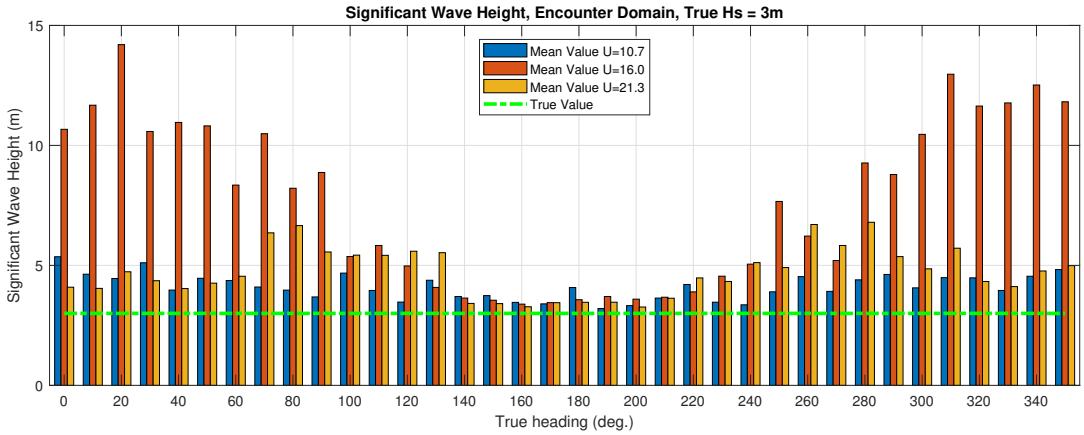

(b) True significant wave height is 3 m

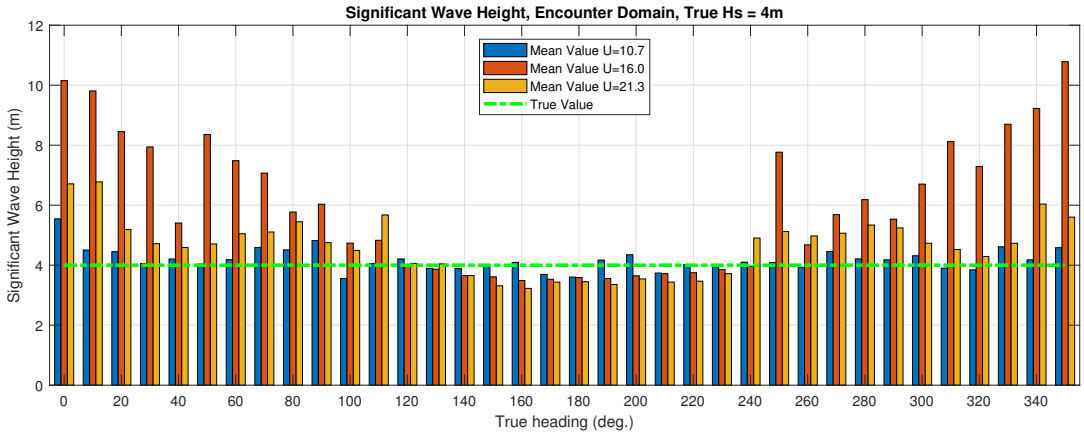

(c) True significant wave height is 4 m

Figure C.3: Estimated significant wave height in encounter domain for each true significant wave height. Each plot is divided by vessel speed

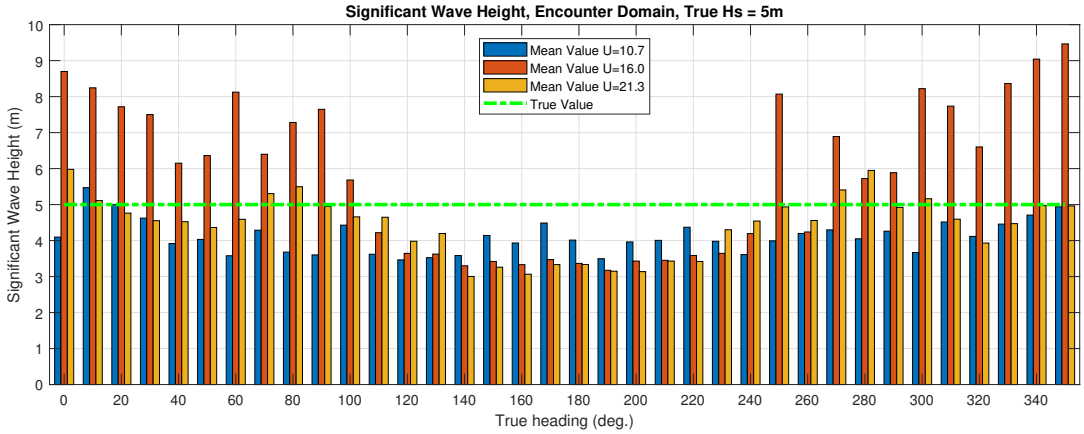

(a) True significant wave height is 5 m

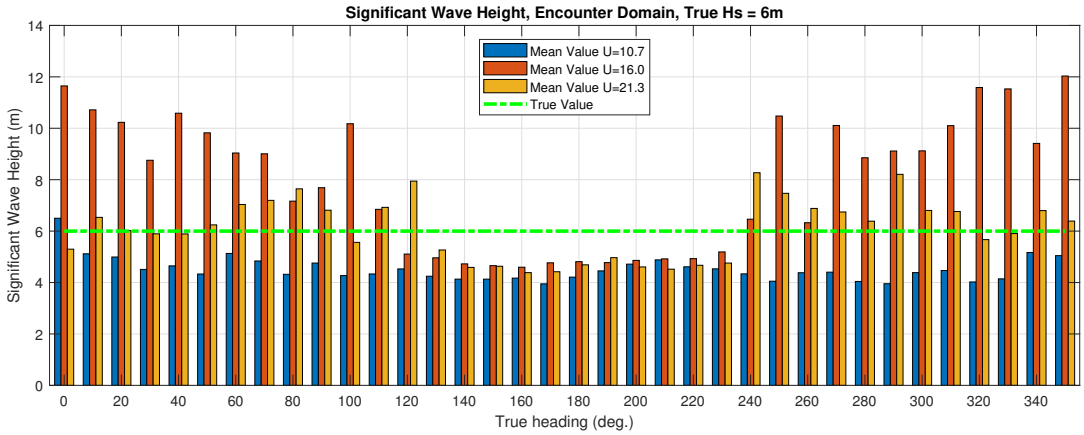

(b) True significant wave height is 6 m

Figure C.4: Estimated significant wave height in encounter domain for each true significant wave height. Each plot is divided by vessel speed

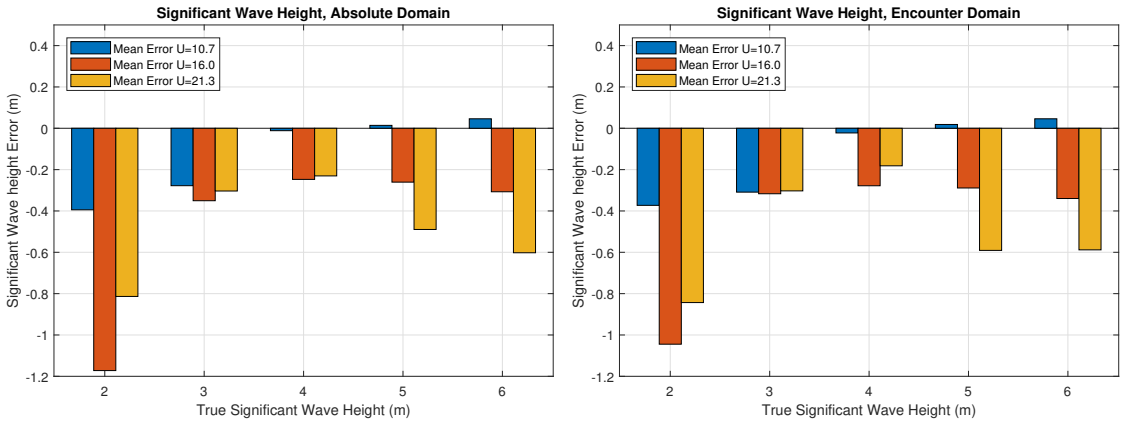

(a) Absolute domain

(b) Encounter domain

Figure C.5: Significant wave height estimation error for each vessel speed and for each true significant wave height.

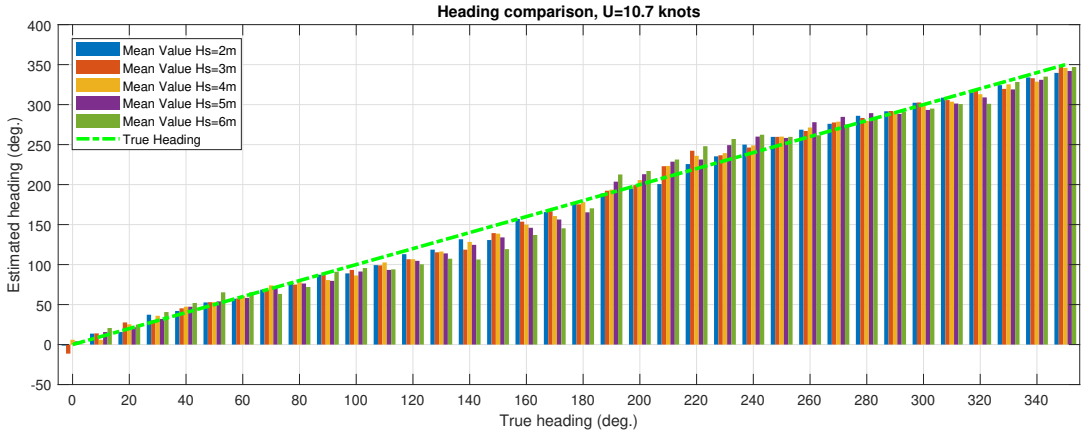

(a) Speed = 10.7 knots

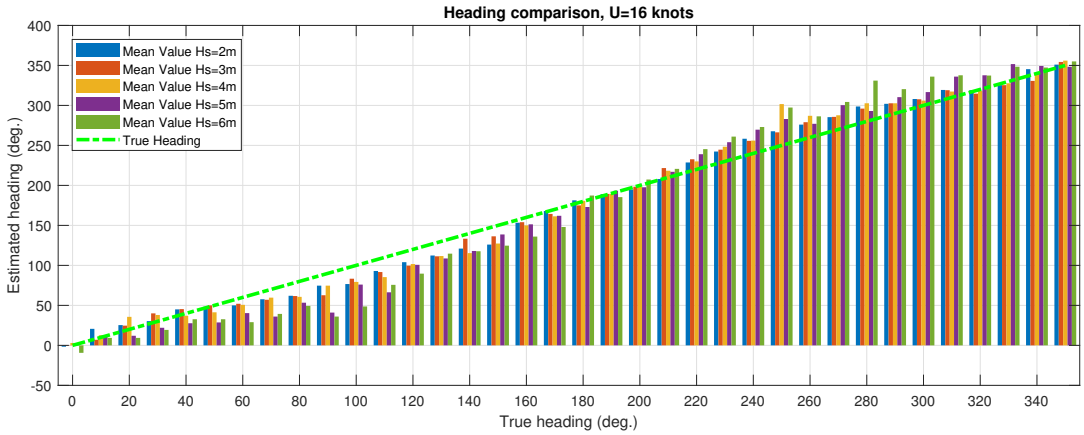

(b) Speed = 16.0 knots

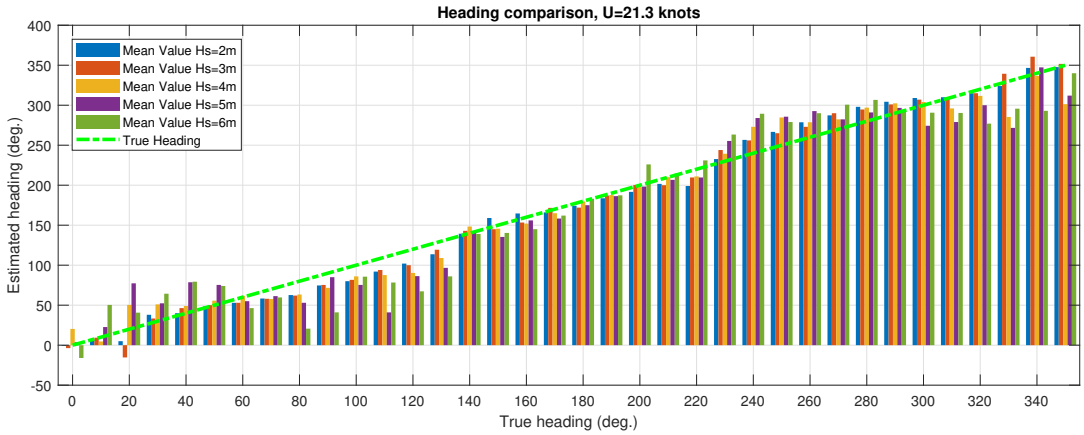

(c) Speed = 21.3 knots

Figure C.6: Wave encounter angle for each vessel speed. Each plot is divided by the true significant wave height.

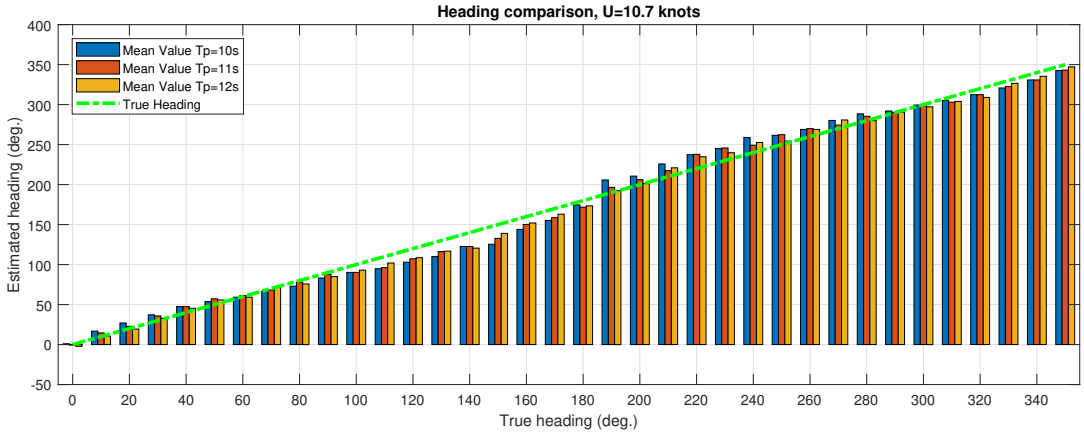

(a) Speed = 10.7 knots

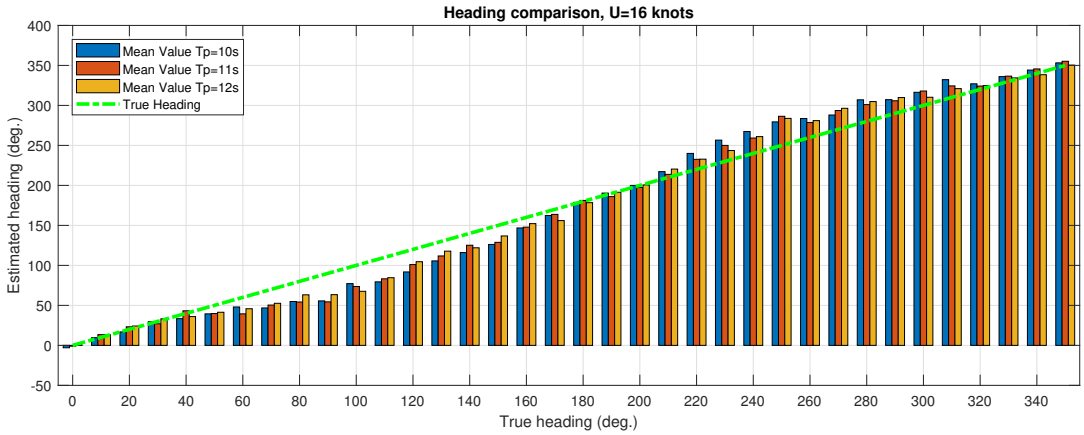

(b) Speed = 16.0 knots

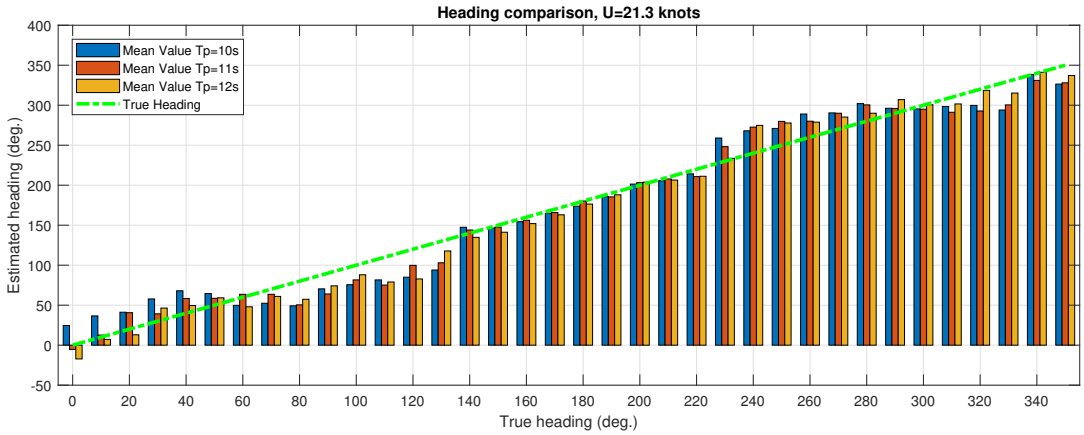

(c) Speed = 21.3 knots

Figure C.7: Wave encounter angle for each vessel speed. Each plot is divided by the true peak period.

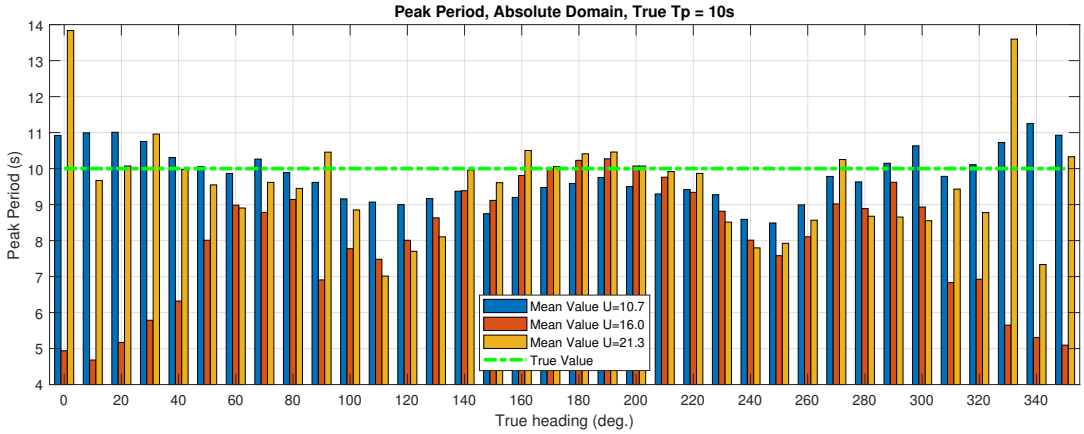

(a) True peak period is 10 s

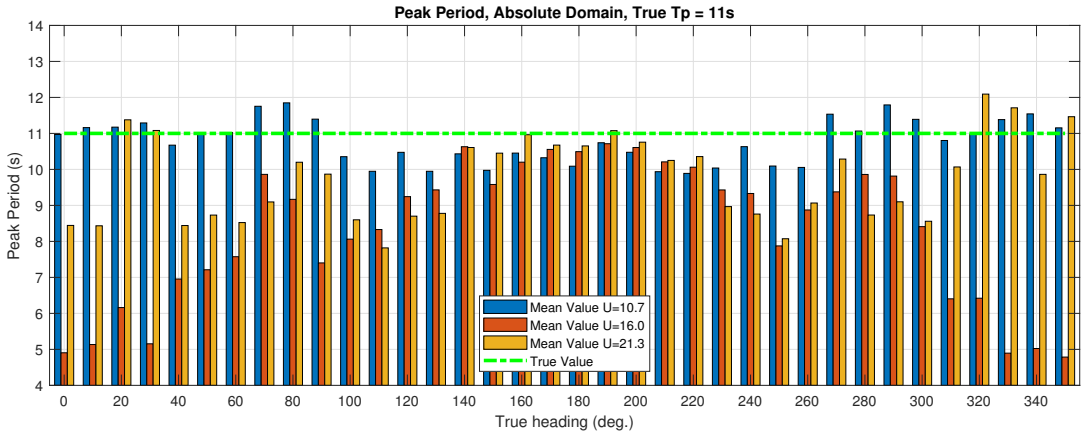

(b) True peak period is 11 s

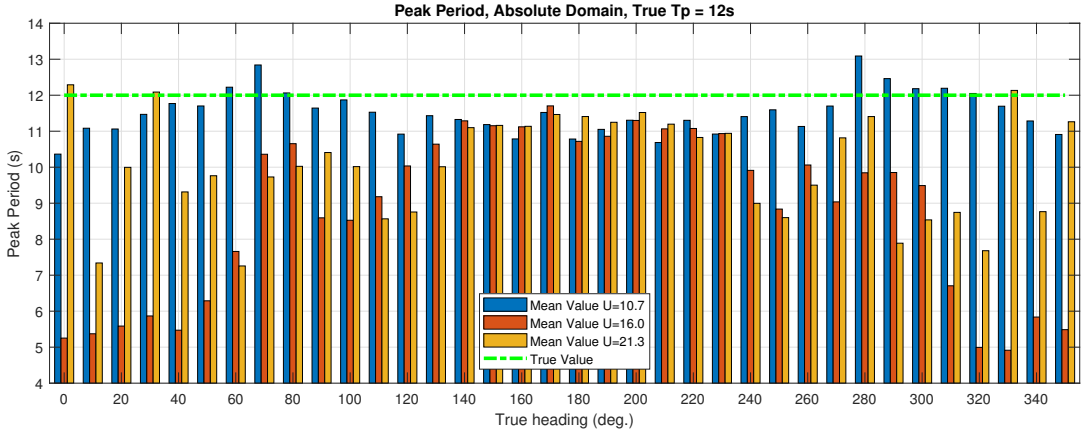

(c) True peak period is 12 s

Figure C.8: Estimated peak period in absolute domain for each true peak period. Each plot is divided by the vessel speed

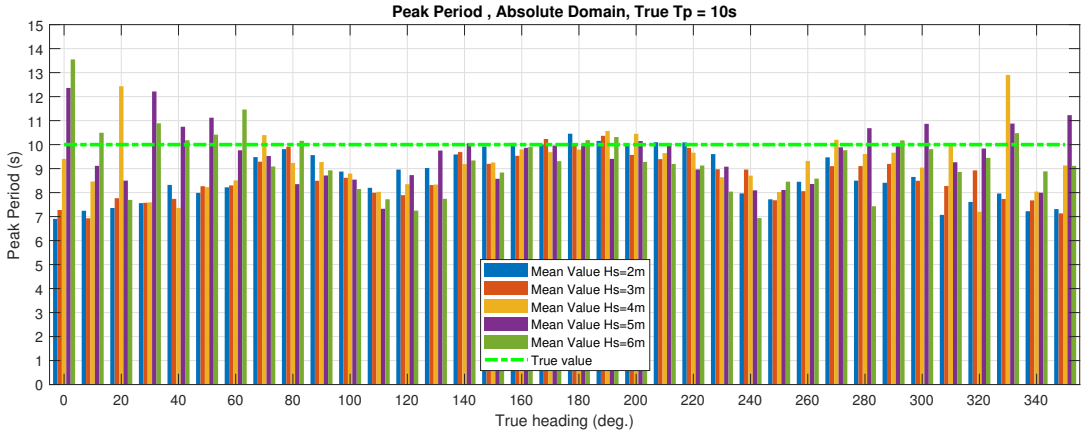

(a) True peak period is 10 s

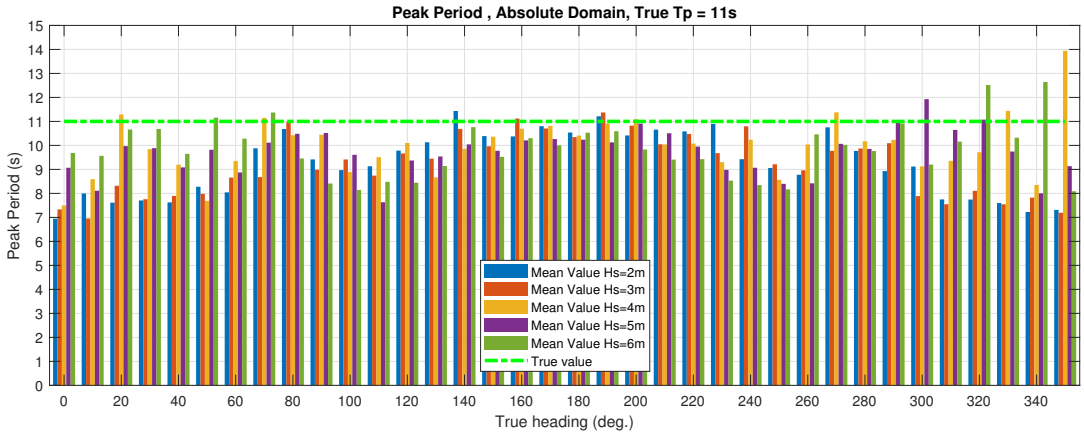

(b) True peak period is 11 s

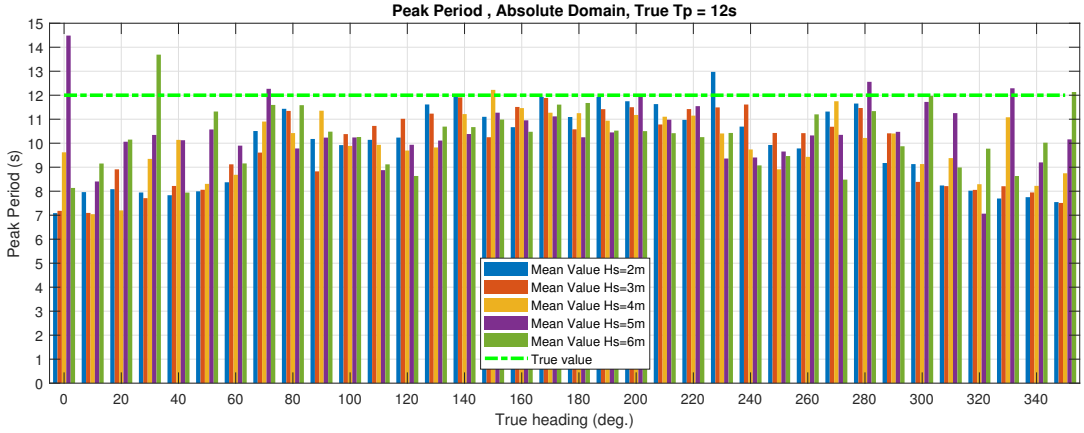

(c) True peak period is 12 s

Figure C.9: Estimated peak period in absolute domain for each true peak period. Each plot is divided by the true significant wave height

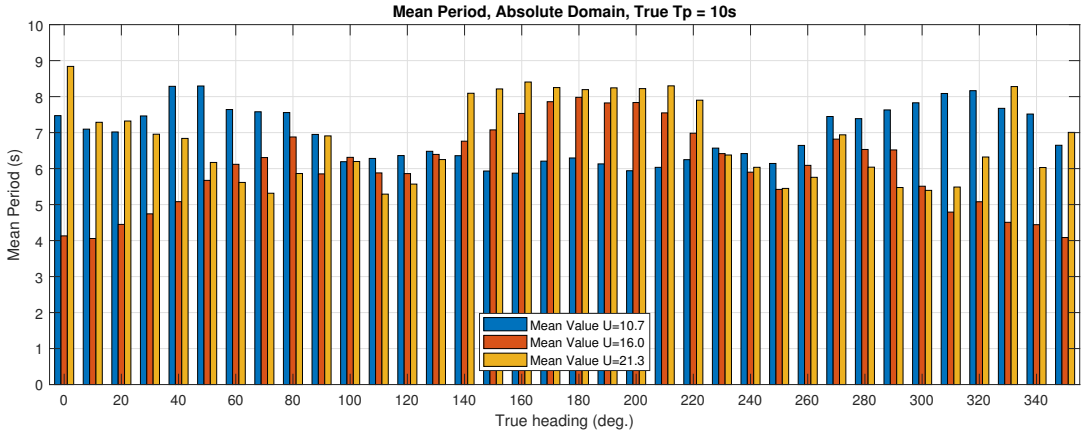

(a) True peak period is 10 s

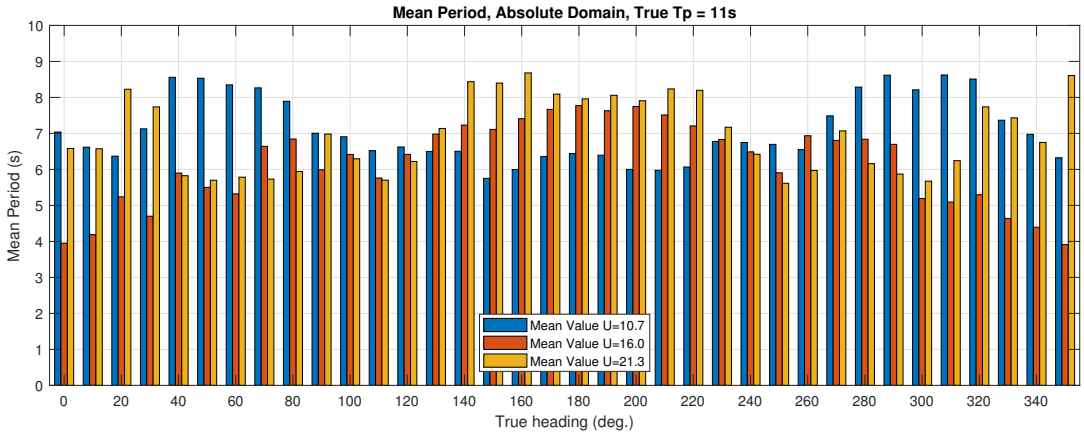

(b) True peak period is 11 s

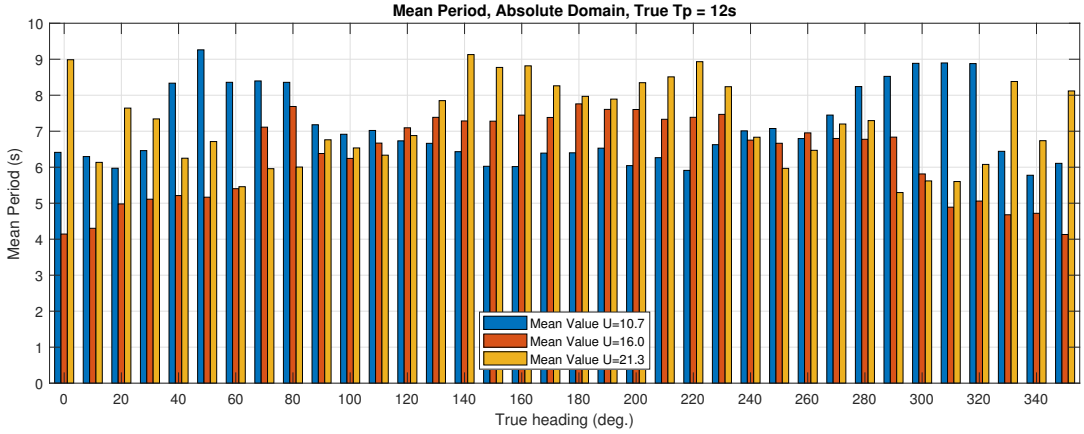

(c) True peak period is 10 s

Figure C.10: Estimated mean period in absolute domain for each true peak period. Each plot is divided by vessel speed

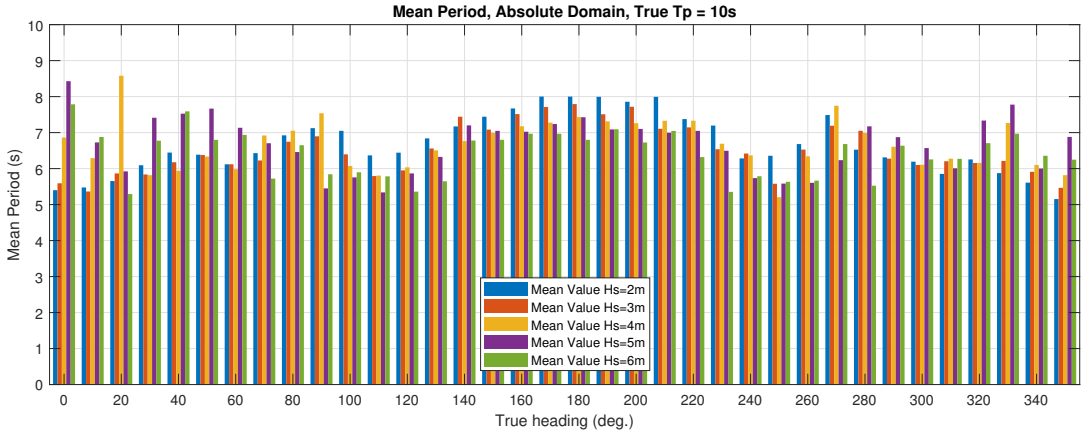

(a) True peak period is 10 s

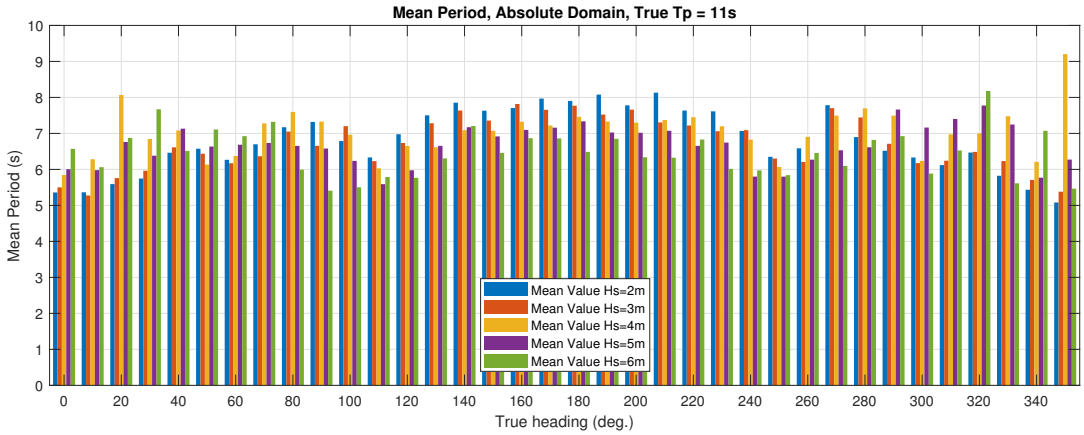

(b) True peak period is 11 s

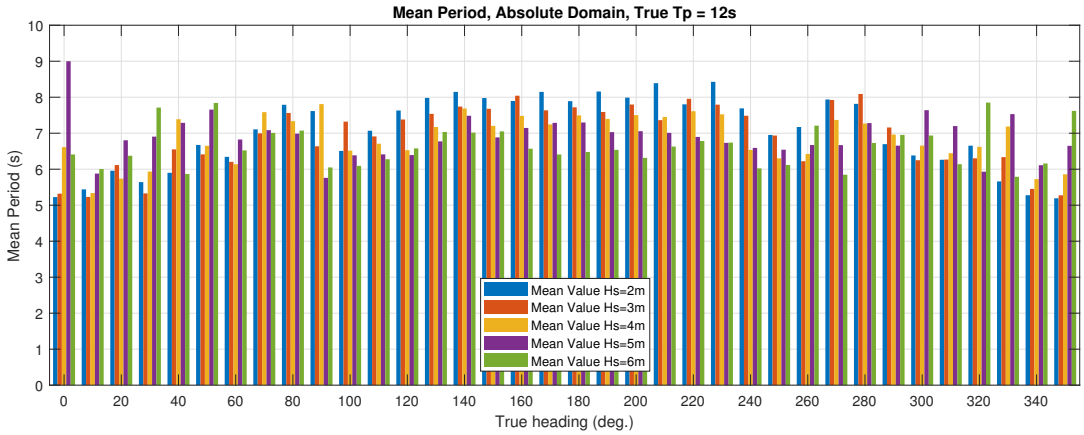

(c) True peak period is 10 s

Figure C.11: Estimated mean period in absolute domain for each true peak period. Each plot is divided by the true significant wave height

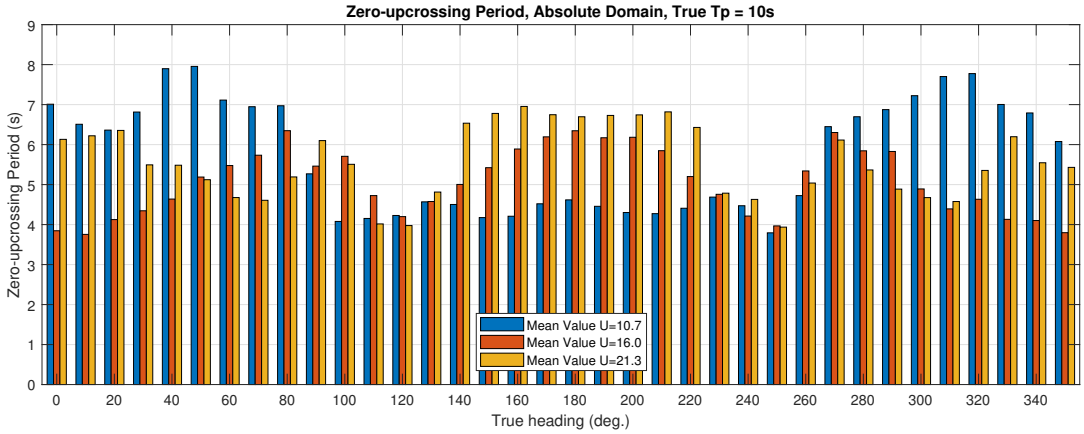

(a) True peak period is 10 s

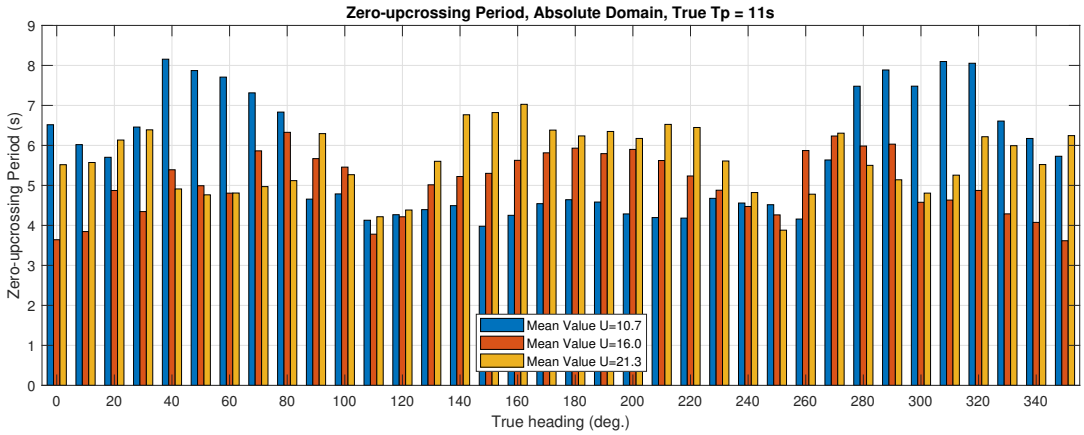

(b) True peak period is 11 s

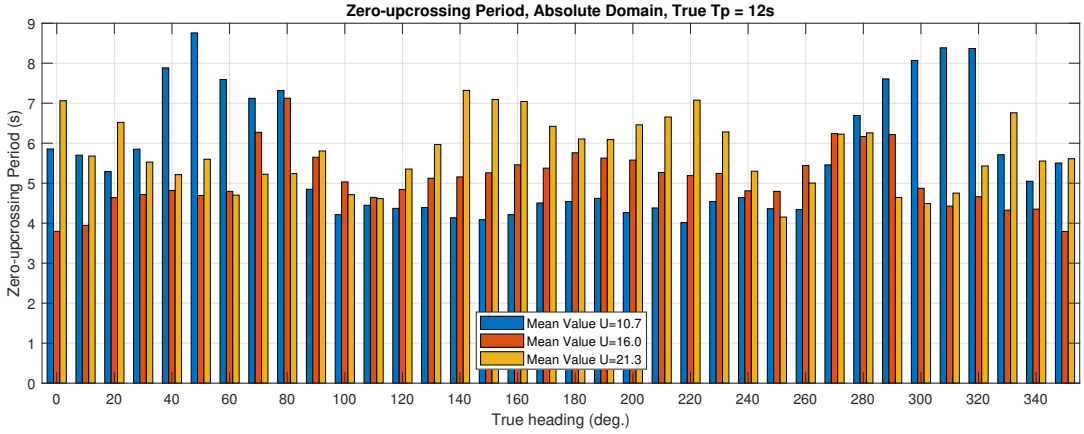

(c) True peak period is 10 s

Figure C.12: Estimated zero-upcrossing period in absolute domain for each true peak period. Each plot is divided by vessel speed

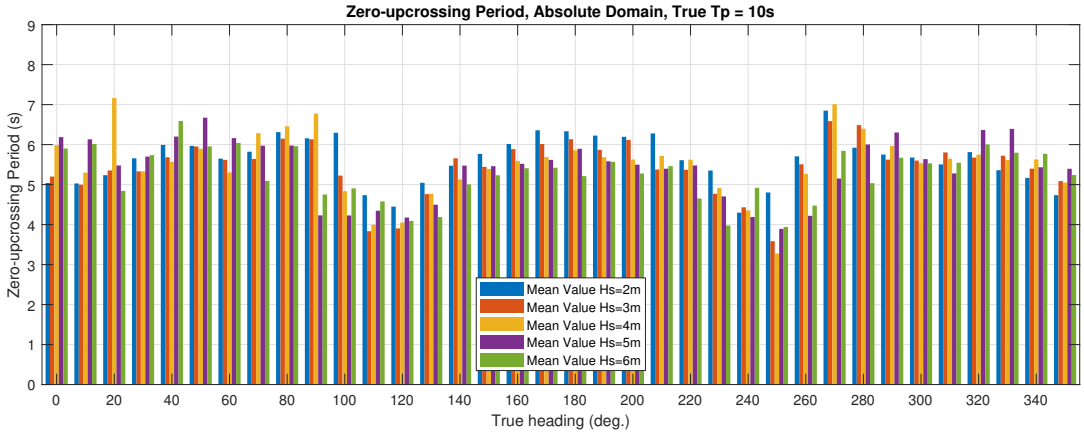

(a) True peak period is 10 s

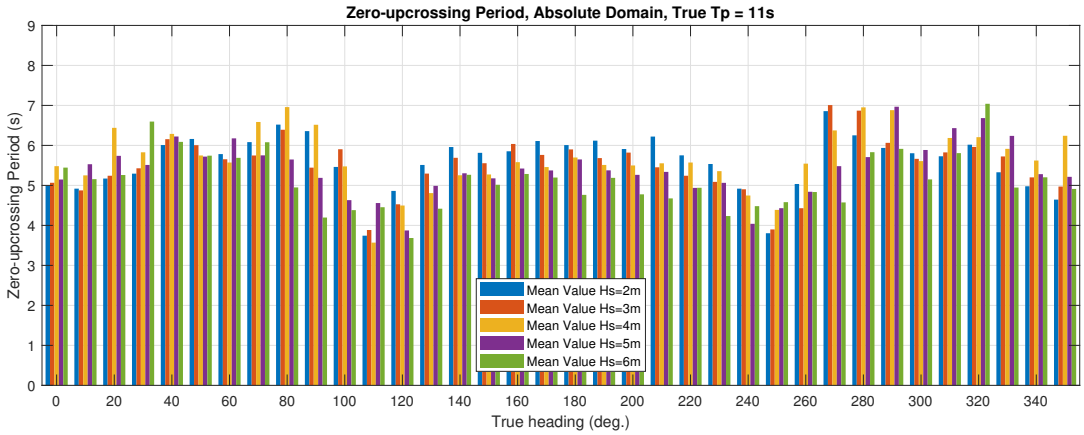

(b) True peak period is 11 s

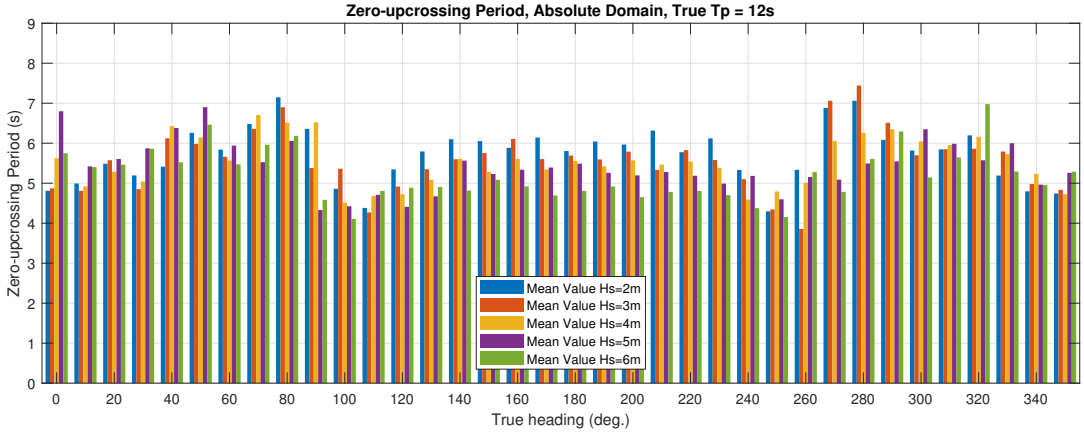

(c) True peak period is 10 s

Figure C.13: Estimated zero-upcrossing period in absolute domain for each true Each plot is divided by the true significant wave height